

# Boundary Values of the Thurston Pullback Map

Russell Lodge  
Indiana University  
Bloomington, Indiana  
rlodge@indiana.edu

July 3, 2012

## Abstract

The Thurston characterization and rigidity theorem gives a beautiful description of when a postcritically finite topological branched cover mapping the 2-sphere to itself is Thurston equivalent to a rational function. Thurston equivalence remains mysterious, but great strides were taken when Bartholdi and Nekrashevych used iterated monodromy groups to solve the “Twisted Rabbit Problem” which sought to identify the Thurston class of the rabbit polynomial composed with an arbitrary Dehn twist. Selinger showed that the Thurston pullback map on Teichmüller space can be extended to the Weil-Petersson boundary. We compute these boundary values for the pullback map associated to  $f(z) = \frac{3z^2}{2z^3+1}$  and demonstrate how the dynamical properties of this map on the boundary can be used as an invariant to solve the twisting problem for  $f$ .

## Contents

<b>1</b>	<b>Introduction</b>	<b>2</b>
1.1	Thurston’s Theorem . . . . .	4
1.2	Boundary Values of the Pullback Map . . . . .	5
1.3	The Twisting Problem . . . . .	6
1.4	Outline . . . . .	7
<b>2</b>	<b>Thurston Maps with <math>n</math> Postcritical Points</b>	<b>8</b>
2.1	Notation, Definitions, and Examples . . . . .	8
2.2	Two definitions of Teichmüller space; Virtual Endomorphisms	12
2.3	Schreier Graphs and the Reidemeister-Schreier Algorithm . .	22
2.4	Iterated Monodromy Groups and Wreath Recursions . . . . .	23

<b>3</b>	<b>General facts in the case <math> P_f  = 4</math></b>	<b>29</b>
<b>4</b>	<b>Analysis of a specific example: <math>f(z) = \frac{3z^2}{2z^3+1}</math></b>	<b>37</b>
4.1	The Dynamical Plane of $f$ . . . . .	37
4.2	The Correspondence on Moduli Space . . . . .	41
4.3	The Virtual Endomorphism and Wreath Recursion on Moduli Space . . . . .	43
4.4	The Wreath Recursion on the Dynamical Plane; Covering and Hurwitz Equivalence . . . . .	49
<b>5</b>	<b>Boundary Values of <math>\sigma_f</math></b>	<b>52</b>
5.1	The Boundary Maps to the Boundary . . . . .	52
5.2	Dynamical behavior of $\phi_f$ . . . . .	53
<b>6</b>	<b>Properties of <math>\sigma_f : \overline{\mathbb{Q}} \rightarrow \overline{\mathbb{Q}}</math></b>	<b>61</b>
<b>7</b>	<b>Slopes of Curves in <math>\widehat{\mathbb{C}} \setminus P</math> when <math> P  = 4</math></b>	<b>66</b>
7.1	Slopes in $\widehat{\mathbb{C}} \setminus P$ when $ P  = 4$ . . . . .	66
7.2	Slopes in $\widehat{\mathbb{C}} \setminus P$ when $P = \{0, 1, \omega, \bar{\omega}\}$ . . . . .	69
<b>8</b>	<b>The Twisting Problem for <math>f</math></b>	<b>71</b>
8.1	Limiting behavior of the Extended Virtual Endomorphism . . . . .	71
8.2	Solution to the Twisting Problem . . . . .	78
<b>9</b>	<b>Future Work</b>	<b>83</b>

## 1 Introduction

Broadly speaking, this dissertation deals with the interplay between geometry, topology, algebra and complex dynamics; the primary focus of this work is Teichmüller space and Thurston’s characterization theorem for rational maps.

In the early 1980’s, John Hubbard and Adrien Douady highlighted a close relationship between combinatorics and complex dynamics when they created combinatorial models for the Julia sets of critically finite polynomials using Hubbard trees [7]. Critically finite quadratic polynomials are highly significant because they could be used to prove the famous conjecture that hyperbolicity is dense—this conjecture was shown by McMullen to be equivalent to the statement that certain quadratics can be approximated by a sequence of critically finite quadratics obtained by a procedure

called renormalization [20]. Douady and Hubbard also present an algorithm that in principle finds the formula for a polynomial realizing any admissible Hubbard tree. These results are very illuminating, and there are a number of other combinatorial invariants that can faithfully encode polynomials, allowing much to be said about the relationship between combinatorics and Julia sets in the case of polynomials. Complex rational functions are another matter, however, and it is not known how to extend results for polynomials to the rational case.

This sets the stage for Thurston’s theorem. Complex rational functions are a very rigid class of functions (e.g. they are conformal outside of a finite set), and finding explicit formulas for one that realizes particular combinatorial data can be challenging. Thus, we focus our attention on a more flexible class of functions. A Thurston map is a critically finite orientation-preserving branched cover from the two-sphere to itself. To pursue the agenda of relating combinatorics to dynamics, one can create a combinatorial model of a dynamical system using Thurston maps, and then Thurston’s theorem characterizes when the Thurston map is equivalent to a rational function. Furthermore, the theorem asserts a rigidity result—if the Thurston map is equivalent to a rational function, this rational function is essentially unique (ignoring a family of well-understood Euclidean examples). Thurston’s theorem for rational functions is proven in [12] using iteration of an analytic map on Teichmüller space called Thurston’s pullback map. The proof parallels the proof of Thurston’s theorem on the hyperbolization of 3-manifolds, which studies dynamics of the skinning map on Teichmüller space.

Thurston’s pullback map is very mysterious, and one goal of my research has been to understand its dynamics on the Weil-Petersson completion of Teichmüller space using the fact of Selinger that the pullback map extends to the boundary [30]. I did this for the Thurston pullback map associated to the rational function  $f(z) = \frac{3z^2}{2z^3+1}$  because  $f$  was investigated in [8]. This paper showed that the Thurston pullback map associated to  $f$  is surjective, and up to some nondynamical equivalence it is essentially the only pullback function where this property has been observed. A second major focus of my work has been to better understand the notion of equivalence used in Thurston’s theorem. Pilgrim described the lack of solution to the Twisted Rabbit Problem a “humbling reminder” of the lack of suitable invariants for Thurston equivalence [27], and though the problem has been solved, the need for invariants remains. The following study of the Thurston pullback map and Thurston equivalence exploit some rich connections between the

Thurston pullback map, combinatorics, Weil-Petersson geometry, hyperbolic geometry, group theory, and arithmetic dynamics.

## 1.1 Thurston's Theorem

Let  $F$  be an orientation-preserving branched cover which maps the two-sphere to itself by degree greater than one. Denote by  $P_F$  the postcritical set as defined in Section 2.1. If  $P_F$  is finite,  $F$  is called a Thurston map. There are several valuable sources for producing examples of Thurston maps: an obvious example would be any post-critically finite rational maps with degree greater than two. Finite subdivision rules of the two-sphere are a convenient way to produce combinatorial models of Thurston maps, and they have been studied extensively in the recent past [9]. A third way to produce examples of Thurston maps is by mating two critically finite polynomials of the same degree [23]. Having shown that a wealth of examples of Thurston maps exist, we define Thurston equivalence and then state Thurston's theorem:

**Definition:** Let  $F$  and  $G$  be Thurston maps with postcritical sets  $P_F$  and  $P_G$  respectively. Then  $F$  is *Thurston equivalent* to  $G$  if there are orientation preserving homeomorphisms  $h_0, h_1 : (S^2, P_F) \rightarrow (S^2, P_G)$  with  $h_0$  homotopic to  $h_1$  rel  $P_F$ , so that the following commutes:

$$\begin{array}{ccc} (S^2, P_F) & \xrightarrow{h_1} & (S^2, P_G) \\ F \downarrow & & \downarrow G \\ (S^2, P_F) & \xrightarrow{h_0} & (S^2, P_G) \end{array}$$

**Thurston's Theorem:** Let  $F$  be a Thurston map which is not a Lattès example. Then  $F$  is Thurston equivalent to a rational map if and only if the Thurston pullback map has a fixed point. Furthermore, if  $F$  is equivalent to a rational map, this rational map is unique up to Möbius conjugation.

Thurston maps are called obstructed if they are not equivalent to a rational function. A different formulation of Thurston's theorem from the one above gives a better sense for why certain Thurston maps are or are not obstructed; having a fixed point of the pullback map is equivalent to the Thurston map not having a special family of simple closed curves in the two-sphere that behave a certain way under preimage. The mapping properties of curves under preimage of a Thurston map have deep implications for the pullback map on Teichmüller space, and we will pursue this theme in both

of the following sections. It is also worth noting that mapping properties of simple closed curves play an important role in the three other groundbreaking theorems proved by Thurston relating geometry and topology, as noted by John Hubbard [15].

Recently there has also been interest in non-dynamical problems involving branched covers of the sphere by higher genus surfaces. See for example the discussion of the Birman-Hilden property in [5, 13]. As was the case in the dynamical setting just described, the preimages of essential curves seem to be significant actors.

## 1.2 Boundary Values of the Pullback Map

Thurston’s pullback map is very complicated—it is transcendental, and in all known examples it is infinite-to-one. It may be surprising, then, that the pullback map associated to  $f(z) = \frac{3z^2}{2z^3+1}$  has boundary values that can be computed by transforming the even continued fraction expansions of rational numbers by a prescribed algorithm (see [8] for an image of the Thurston pullback map studied here).

We call a simple closed curve  $\gamma \subset \widehat{\mathbb{C}} \setminus P_F$  essential if both components bounded by  $\gamma$  contain at least two post-critical points. The collection of homotopy classes of essential curves in  $\widehat{\mathbb{C}} \setminus P_F$  can be put in correspondence with the rational numbers when there are four post-critical points. Furthermore, when  $|P_F| = 4$ , it is a standard fact that Teichmüller space can be identified with the upper half-plane in such a way that the Weil-Petersson completion is obtained by adding the rational points  $\frac{p}{q} + 0i$  along with the point  $\frac{1}{0}$  to the boundary of the upper half-plane where each point corresponds to collapsing the sphere with four marked points along the curve corresponding to  $\frac{p}{q}$ .

In Nikita Selinger’s 2010 paper [30], the observation was made that Thurston’s pullback map extends under the Weil-Petersson completion, and it maps the boundary point corresponding to  $\frac{p}{q}$  to the boundary point corresponding to the preimage of the curve corresponding to  $\frac{p}{q}$  under  $f$ , where only the essential component of the preimage is considered. Thus, if one can fully understand the essential preimages of curves under  $f$ , one can understand the boundary values of the pullback map under the Weil-Petersson completion. Recently, this sort of curve preimage computation was made in [27], where Pilgrim analyzed the fate of essential curves under preimage for some quadratics. In the spirit of [10], we define the *slope function*  $\sigma_f : \mathbb{Q} \rightarrow \mathbb{Q}$  by saying that  $\sigma_f(\frac{p}{q}) = \frac{p'}{q'}$  if the curve corresponding to  $\frac{p}{q}$  has

an essential component of its preimage that corresponds to  $\frac{p'}{q'}$ . The main result about the dynamics of this slope function is the following

**Theorem** Let  $f(z) = \frac{3z^2}{2z^3+1}$ , and let  $\frac{p}{q}$  be an essential curve. Then under iteration of  $\sigma_f$ ,  $\frac{p}{q}$  lands in the set  $\{\frac{0}{1}, \frac{1}{0}, -\frac{1}{1}\}$ . Furthermore,  $\sigma_f(\frac{0}{1}) = \frac{1}{0}$ ,  $\sigma_f(\frac{1}{0}) = \frac{0}{1}$ , and  $\sigma_f(-\frac{1}{1}) = -\frac{1}{1}$ . Under iteration of  $\sigma_f$ ,  $\frac{p}{q}$  lands on  $-\frac{1}{1}$  if and only if  $p$  and  $q$  are odd.

We say that a slope function  $\sigma_f$  has a finite global attractor if there exists a finite set so that under iteration of  $\sigma_f$ , every point  $\frac{p}{q}$  lands in this finite set or under iteration corresponds to a peripheral curve. As mentioned before, this result translates immediately into a fact about the boundary values of the pullback map, and it was also easy to prove that on the boundary, the pullback map is infinite-to-one and surjective.

### 1.3 The Twisting Problem

Despite the intense effort focused on understanding Thurston's theorem, Thurston equivalence remained mysterious. One measure of this is the two decades it took to solve the "Twisted Rabbit Problem" which sought to identify the Thurston class of the rabbit polynomial composed with an arbitrary Dehn twist. Finally, however, the solution came in the work of Bartholdi and Nekrashevych [1], which introduced the permutational biset and the iterated monodromy group as invariants of Thurston equivalence for quadratic polynomials. The machinery introduced in this paper effectively reduced the topological question of determining Thurston class to the algebraic question of determining nuclei of iterated monodromy groups. Though these methods worked well in the setting of quadratic polynomials, it was unclear how to generalize them to the case of rational functions having higher degree.

This sets the context for the solution to the twisting problem when  $f(z) = \frac{3z^2}{2z^3+1}$  presented in this paper. The solution makes use of the first result about the boundary values of the pullback map to produce an invariant not used before to solve twisting problems. Denote by  $\text{PMCG}(\widehat{\mathbb{C}}, P_f)$  the set of homeomorphisms that fix each point in  $P_f$  modulo isotopy; since  $|P_f| = 4$ , this group has two generators  $\alpha$  and  $\beta$  which are chosen explicitly. In the spirit of [1], a function  $\bar{\psi} : \text{PMCG}(\widehat{\mathbb{C}}, P_f) \rightarrow \text{PMCG}(\widehat{\mathbb{C}}, P_f)$  is created so that  $g \circ f$  is Thurston equivalent to  $\bar{\psi}(g) \circ f$ . Coupled with the following theorem, this fact reduces the twisting problem to identifying the Thurston class of each twist in  $\mathfrak{M}$  applied to  $f$ .

**Theorem:** For any  $g \in \text{PMCG}(\widehat{\mathbb{C}}, P_f)$  there is a positive number  $N$  so that  $\overline{\psi}^{\circ n}(g) \in \mathfrak{M}$  for all  $n > N$  where

$$\mathfrak{M} = \{e, \beta, \alpha^{-1}, \alpha^2\beta^{-1}, \alpha^{-1}\beta\alpha^{-1}, \alpha\beta^{-1}, \beta^2\} \cup \{\alpha(\beta\alpha)^k : k \in \mathbb{Z}\}$$

It was possible to show that composing each element of  $\{\alpha(\beta\alpha)^k : k \in \mathbb{Z}\}$  with  $f$  produces a one-parameter family of obstructed and pairwise inequivalent maps. However, in the case where  $h \in \{e, \beta, \alpha^{-1}, \alpha^2\beta^{-1}, \alpha^{-1}\beta\alpha^{-1}, \alpha\beta^{-1}, \beta^2\}$ , it was not immediately clear what the Thurston class of  $h \circ f$  was, though it was easy to show that  $h \circ f$  is unobstructed and that it must by Thurston's characterization theorem be equivalent to  $f$  itself or to a second rational function  $g$ . After repeated attempts to apply known methods, it was still unclear whether  $h \circ f$  was equivalent to  $f$  or  $g$ . Fortunately, a nice finite subdivision rule description of  $g$  exists, and this model allows one to exhibit two distinct two-cycles in the pullback of essential curves. Therefore, if the pullback of  $h \circ f$  on curves has two two-cycles, it must be equivalent to  $g$ . This fact allowed for a complete solution to the "twisted  $f$ " problem as well as highlighting a potentially valuable invariant of Thurston equivalence.

## 1.4 Outline

Section 2 begins with a discussion of Thurston theory for the sphere with an arbitrary finite number of marked points. Point pushing is used to show the equivalence of two standard definitions of Teichmüller space, and a general discussion of virtual endomorphisms is presented. Practically speaking, one can compute virtual endomorphisms using the Reidemeister-Schreier algorithm. The section concludes with a brief summary of known results about the pullback on curves and solutions to twisted polynomial problems.

Section 3 specializes the previous discussion to the case of four marked points. An explicit procedure is described to create an identification between parabolic elements of  $\text{P}\Gamma(2)$ , parabolic elements of the fundamental group of the thrice-punctured sphere, points in the Weil-Petersson boundary, essential curves in the sphere with four punctures, right Dehn twists, and the extended rational numbers  $\mathbb{Q} \cup \{\frac{1}{0}\}$ .

Section 4 presents a study of the critically finite rational function  $f(z) = \frac{3z^2}{2z^3+1}$  studied in [8]. A convenient combinatorial model for this  $f$  is presented, and the virtual endomorphisms on the dynamical plane and moduli space are computed. Finally an enumeration is made of the covering and Hurwitz classes of the branched coverings having the same branch data as  $f$ . Section 5 proves that the boundary values of the Thurston pullback map

have a finite global attractor. Section 6 presents further dynamical and non-dynamical properties of this boundary map.

Section 7 defines the notion of slope for essential curves in the four-punctured sphere by lifting to the torus double cover. This method of assigning slope is related to the assignment of extended rationals to essential curves discussed in Section 3.

Section 8 closes the study of  $f(z) = \frac{3z^2}{2z^3+1}$  with an outline of the solution to the twisting problem for this particular rational function. The pullback on curves is effectively used as an invariant for Thurston maps. A series of future research directions are presented in Section 9.

## 2 Thurston Maps with $n$ Postcritical Points

Though later sections will only require the case of four postcritical points, we present Thurston theory in the more general case.

### 2.1 Notation, Definitions, and Examples

We denote the standard oriented two-sphere by  $S^2$  and the Riemann sphere by  $\widehat{\mathbb{C}}$ . Recall that a *branched covering*  $F : S^2 \rightarrow S^2$  is a continuous, surjective map so that outside of a finite set  $V_F$  (chosen to be minimal), the restricted map  $F : S^2 \setminus F^{-1}(V_F) \rightarrow S^2 \setminus V_F$  is a degree  $d$  covering map. Denote by  $\deg(F, x)$  the local degree of  $F$  at the point  $x \in S^2$ . The set  $C_F$  will denote the set of points  $x$  with  $\deg(F, x) > 1$ , and is called the set of *branched* or *critical points*, and the set  $V_F$  is called the set of *branched values*. The *postcritical set* of a degree  $d$  branched cover  $F : S^2 \rightarrow S^2$  is denoted as follows:

$$P_F = \bigcup_{i>0} F^i(C_F)$$

If  $|P_F|$  is finite, we say  $F$  is *critically finite*. A *Thurston map* is a critically finite orientation-preserving branched cover  $F : S^2 \rightarrow S^2$  where  $\deg(F) \geq 2$ .

To state Thurston's theorem in full generality, we must also define the notion of a Thurston obstruction, but to define this, we need a series of other definitions. A simple closed curve  $\gamma$  in  $S^2 \setminus P_F$  is *essential* if each component of  $S^2 \setminus \gamma$  intersects  $P_F$  in at least two points. In other words  $\gamma$  fails to be essential if it is nullhomotopic or peripheral (this second condition is equivalent to saying  $\gamma$  bounds a disk containing a single point of  $P_F$ ). A *multicurve* is a collection  $\Gamma = \{\gamma_1, \dots, \gamma_k\}$  of disjoint essential, simple closed



curves where the elements of the collection are pairwise non-homotopic. We use  $\mathcal{C}_F$  to denote the set of homotopy classes of simple closed curves in  $S^2 \setminus P_F$ . Denote by  $\mathbb{R}[\mathcal{C}_F]$  the free  $\mathbb{R}$ -module over  $\mathcal{C}_F$ . The Thurston linear map  $\lambda_F : \mathbb{R}[\mathcal{C}_F] \rightarrow \mathbb{R}[\mathcal{C}_F]$  is defined by

$$\lambda_F(\gamma) = \sum_{\gamma'} \sum_{\gamma' \simeq \delta \subset F^{-1}(\gamma)} \frac{1}{\deg(F : \delta \rightarrow \gamma)} \cdot \gamma'$$

where  $\gamma$  and  $\gamma'$  are single components of multicurves and the outer sum is over all  $\gamma'$  homotopic to preimages of  $\gamma$ . A *Thurston obstruction* is a nonempty multicurve  $\Gamma$  so that

- $\mathbb{R}[\Gamma]$  is invariant under  $\lambda_F$
- the spectral radius of  $\lambda_F$  is greater than or equal to 1

We are finally in a position to state Thurston's theorem, referring the reader to [24] for a thorough treatment of Lattès maps and [12] for a proof of Thurston's theorem.

**Theorem 2.1** *Let  $F$  be a Thurston map not equivalent to a Lattès map. Then  $F$  is Thurston equivalent to a rational function if and only if there are no obstructions. If this rational function exists, it is unique up to Möbius conjugation.*

A crucial tool in the proof of Thurston's theorem is the Thurston pull-back map on Teichmüller space. It can be shown that a Thurston map is equivalent to a rational function if and only if its associated pullback map has a fixed point.

**Definition** The Teichmüller space for a Thurston map  $F$  is defined to be

$$\mathcal{T}_F = \{\phi : (S^2, P_F) \rightarrow \widehat{\mathbb{C}}\} / \sim$$

where  $\phi_1 \sim \phi_2$  if and only if there is a Möbius transformation  $M$  so that  $\phi_2$  is isotopic to  $M \circ \phi_1$  rel  $P_F$ .

It is not uncommon to define  $\mathcal{T}_F$  as the universal cover of the moduli space  $\mathcal{M}_F$ , which is defined as follows:

$$\mathcal{M}_F = \{\iota : P_F \hookrightarrow \widehat{\mathbb{C}}\} / \approx$$

where each  $\iota$  is an injection and  $\iota_1 \approx \iota_2$  if there is a Möbius transformation  $M$  so that  $M \circ \iota_1 = \iota_2$ . There is an obvious projection  $\pi_F : \mathcal{T}_F \rightarrow \mathcal{M}_F$

defined by  $\pi([\phi]) = [\phi|_{P_F}]$ . We will see later that this second definition is equivalent to the original.

We describe here the deck group of the universal cover  $\pi_F$ , namely the pure mapping class group acting by precomposition on representing homeomorphisms of points in  $\mathcal{T}_F$ . Denote by  $\text{Homeo}(S^2)$  the group of orientation-preserving homeomorphisms from  $S^2$  to itself (by convention, all homeomorphisms discussed from here on will be orientation preserving). Denote by  $\text{Homeo}(S^2, P_F)$  the subgroup of  $\text{Homeo}(S^2)$  that fixes  $P_F$  pointwise, and let  $\text{Homeo}_0(S^2, P_F)$  be the path component of the identity in  $\text{Homeo}(S^2, P_F)$ . We define *the pure mapping class group* of  $S^2$  with respect to  $P_F$  to be

$$\text{PMCG}(S^2, P_F) = \text{Homeo}(S^2, P_F) / \text{Homeo}_0(S^2, P_F)$$

where  $\text{Homeo}_0(S^2, P_F)$  acts on the right by post-composition.

To define the Thurston pullback map for a Thurston map  $F$ , choose a representative  $\phi$  of  $\tau \in \mathcal{T}_F$ . Pull back the complex structure on  $\widehat{\mathbb{C}}$  by the Thurston map  $F \circ \phi : (S^2, P_F) \rightarrow (\widehat{\mathbb{C}}, \phi(P_F))$ , and use the uniformization theorem to conclude that  $S^2$  with this new complex structure is holomorphically isomorphic to  $\widehat{\mathbb{C}}$  by some  $\tilde{\phi}$ , unique up to postcomposition by elements of  $\text{Aut}(\widehat{\mathbb{C}})$ . We then have the following commutative diagram where  $F_\tau$  is defined to be the holomorphic composition  $\phi \circ F \circ \tilde{\phi}^{-1}$  where some elementary topological considerations show that  $F_\tau$  is a rational function with  $\deg F = \deg F_\tau$ .

$$\begin{array}{ccc} (S^2, P_F) & \xrightarrow{\tilde{\phi}} & (\widehat{\mathbb{C}}, \tilde{\phi}(P_F)) \\ F \downarrow & & \downarrow F_\tau \\ (S^2, P_F) & \xrightarrow{\phi} & (\widehat{\mathbb{C}}, \phi(P_F)) \end{array}$$

**Definition** The *Thurston pullback map*  $\sigma_F : \mathcal{T}_F \rightarrow \mathcal{T}_F$  is defined by  $\sigma_F(\tau) = [\tilde{\phi}]$ . This is well-defined by homotopy-lifting.

An exciting development over the past decade has been the use of correspondences on moduli space to better understand Thurston's pullback map [1, 27, 8, 17]. In many of these sources, one of the functions in the correspondence is an inclusion, which means that the correspondence can be thought of as a function. Bartholdi and Nekrashevych exploit properties of such a function repeatedly in [1]. It is our goal here to catalog a number of results related to correspondences on moduli space. Also included is a brief discussion of two known examples with four postcritical points where images of the Thurston pullback map have been produced.

In Section 5.1 of [1], one finds a discussion of the Thurston map  $F$  with the same critical portrait as the rabbit:

$$0 \xrightarrow{\times 2} 1 \mapsto p_4 \mapsto 0; \infty \mapsto \infty$$

Local degree considerations and a little algebra produce a map  $g(z) = 1 - \frac{1}{z^2}$  so that the following commutes ( $\mathcal{M}_F$  has been identified with  $\widehat{\mathbb{C}} \setminus \{0, 1, \infty\}$  in the obvious way).

$$\begin{array}{ccc} \mathcal{T}_F & \xrightarrow{\sigma_F} & \mathcal{T}_F \setminus \{\pi^{-1}(-1)\} \\ \downarrow \pi & & \downarrow \pi \\ \mathcal{M}_F & \xleftarrow{g} & \mathcal{M}_F \setminus \{-1\} \end{array}$$

This commutative diagram can be used to calculate the image of  $\sigma_F : \mathcal{T}_F \rightarrow \mathcal{T}_F$  in the following way: let  $z_0$  be a fixed point of  $g$  which we choose to be the basepoint, and consider the lifts under  $g$  of paths in  $\mathcal{M}_F$  that start at  $z_0$ . Since the universal cover is defined to be the space of homotopy classes of paths in  $\mathcal{M}_F$  that begin at  $z_0$ , one only needs to identify  $\mathcal{T}_F$  with  $\mathbb{D}$  to generate the image of  $\sigma_F : \mathbb{D} \rightarrow \mathbb{D}$ . Bartholdi and Nekrashevych [1, p.29] also indicate a second use of the map on moduli space when they determine the combinatorial equivalence class of the rabbit twisted by  $T$  and  $T^{-1}$ . This is done by drawing paths in moduli space that correspond to these twists using the ideas from Section 3, and examining longterm behavior of successive lifts of this path.

In general, one should not expect the correspondence on moduli space to be a function on moduli space: for example, the Thurston map for  $f(z) = \frac{3z^2}{2z^3+1}$  in [8] covers a correspondence, not a function. Following the discussion of [8], we produce this correspondence and then describe how to generate the image of  $\sigma_f$  using ideas similar to those just discussed for  $g$ . This correspondence will be the central object of our study in future sections. Let  $\omega = -\frac{1}{2} + \frac{\sqrt{3}}{2}i$ . Denote by  $F_0 = \frac{P_0}{Q_0}$  and  $F_\infty = \frac{P_\infty}{Q_\infty}$  two degree 3 rational functions with three simple critical points at  $1, \omega, \bar{\omega}$ , where  $P_0, Q_0, P_\infty$ , and  $Q_\infty$  are polynomials and both  $F_0$  and  $F_\infty$  have the same mapping properties as  $f$  on  $1, \omega, \bar{\omega}$ . Also assume that  $F_0$  has its fourth critical point at 0, and  $F_\infty$  has its fourth critical point at  $\infty$ . Let  $F = \frac{P}{Q}$  be a degree three rational map with simple critical points  $1, \omega, \bar{\omega}$  where  $F$  has the same mapping properties as  $f$ . Since the numerators of  $F - F_0 = \frac{PQ_0 - QP_0}{QQ_0}$  and  $F - F_\infty = \frac{PQ_\infty - QP_\infty}{QQ_\infty}$  are both scalar multiples of  $(z^3 - 1)^2$ , there exist  $[a, b] \in \mathbb{P}^1$  so that

$$a \cdot (PQ_\infty - QP_\infty) + b \cdot (PQ_0 - QP_0) = 0.$$

One can solve this equation for  $\frac{P}{Q}$ , yielding

$$F_\alpha = \frac{aP_\infty + bP_0}{aQ_\infty + bQ_0}.$$

Finding the fourth critical point and critical value of this function allows one to produce the following commutative diagram where

$$X(z) = z^2, Y(z) = \frac{z(z^3 + 2)}{2z^3 + 1}, A(\tau) = \frac{x^2 - y}{2xy - 2}$$

where

$$y = \pi(\tau), x = \pi \circ \sigma_f(\tau)$$

and  $\Theta$  is the set of cube roots of unity,  $\Theta'$  is the set of sixth roots of unity.

$$\begin{array}{ccc}
 \mathcal{T}_f & \xrightarrow{\sigma_f} & \mathcal{T}_f \\
 \pi \downarrow & \searrow A & \downarrow \pi \\
 & \widehat{\mathbb{C}} - \Theta' & \\
 \pi \downarrow & \swarrow Y & \searrow X \\
 \widehat{\mathbb{C}} - \Theta & & \widehat{\mathbb{C}} - \Theta
 \end{array}$$

To produce a picture of  $\sigma_f : \mathbb{D} \rightarrow \mathbb{D}$  similar to the one exhibited in [8], follow the procedure described above for  $g$ , except do the path lifting step in the following way: take a path based at 0 in  $\widehat{\mathbb{C}} \setminus \Theta$ , chose the unique lift under  $Y$  based at 0, and push down to  $\widehat{\mathbb{C}} \setminus \Theta$  using  $X$ .

## 2.2 Two definitions of Teichmüller space; Virtual Endomorphisms

We prove that point-pushing establishes an equivalence between two common formulations of Teichmüller space. Though this equivalence can be shown non-constructively using some deep results from Teichmüller theory, we prefer to construct an explicit bijective correspondence between the sets described in the two formulations. Having done this, we use these tools to establish a foundational fact about virtual endomorphisms that is used in later sections, namely that the virtual endomorphism on the fundamental group of moduli space and the virtual endomorphism on the pure mapping class of the dynamical plane respect the equivalence just described.

First we establish some conventions and notation. Use the stereographic projection to fix an identification between  $S^2$  and  $\widehat{\mathbb{C}}$ . This allows us to view the group of Möbius transformations  $\text{Möb}$  as a subgroup of  $\text{Homeo}(S^2)$ . Let  $P := \{p_1, p_2, p_3, \dots, p_n\} \subset S^2$  be a set of  $n > 3$  distinct points with  $\Theta := \{p_1, p_2, p_3\} \subset P$ . In the following definition,  $\text{Möb}$  acts on the left by postcomposition, and  $\text{Homeo}_0(S^2, P)$  acts on the right by precomposition.

**Definition 1:**  $\mathcal{T}(S^2, P) := \text{Möb} \backslash \text{Homeo}(S^2) / \text{Homeo}_0(S^2, P)$  with basepoint given by the class of the identity map  $id$ .

Since  $|P| > 3$ , we can make a choice of double coset representative that lies in  $\text{Homeo}(S^2, \Theta)$  by triple transitivity of Möbius transformations. Then such  $\phi_1$  and  $\phi_2$  are in the same double coset if  $\phi_1$  and  $\phi_2$  are isotopic rel  $P$ . We denote such an equivalence by  $\phi_1 \sim \phi_2$ . There is an obvious identification between  $\mathcal{T}(S^2, P)$  and  $\text{Homeo}(S^2, \Theta) / \text{Homeo}_0(S^2, P)$ , a fact frequently used in the proof of Theorem 2.4.

The second definition will require some more notation. Define moduli space with the obvious topology by  $\mathcal{M}(S^2, P) = \{\iota : P \hookrightarrow S^2\} / \approx$  where  $\iota_1 \approx \iota_2$  if there is a Möbius transformation  $M$  so that  $M \circ \iota_1 = \iota_2$ . We fix  $id : P \hookrightarrow S^2$  to be the basepoint of  $\mathcal{M}(S^2, P)$ , and fix the constant path  $const$  to be the basepoint of Teichmüller space in our second definition.

**Definition 2:**  $(\mathcal{T}(S^2, P), const)$  is defined to be the universal cover of the space  $(\mathcal{M}(S^2, P), id)$ .

The usual construction of the universal cover comes from taking the set of paths from the prescribed basepoint  $id : P \hookrightarrow S^2$  in  $\mathcal{M}(S^2, P)$  modulo homotopy rel endpoints. More explicitly, define  $\mathcal{T}(S^2, P) := \{\tau : ([0, 1], 0) \rightarrow (\mathcal{M}(S^2, P), id)\} / \approx$  where  $\tau_0 \approx \tau_1$  if  $\tau_0(1) = \tau_1(1)$  and  $\tau_0$  is homotopic to  $\tau_1$  rel endpoints. The important connection between moduli and configuration space described in the lemma below will be exploited in our proof of Theorem 2.4 since it will allow us to make a substantial reduction from the very start. Define the configuration space on  $n$  points to be  $C(S^2, P) := (S^2)^n \setminus \Delta$  where  $\Delta = \{(x_1, \dots, x_n) \mid x_i \neq x_j \text{ when } i \neq j\}$ . The configuration space is homeomorphic in an obvious way to  $\{\iota : P \hookrightarrow S^2\}$ . We also use a second configuration space  $C(S^2 \setminus \Theta, P \setminus \Theta) := (S^2 \setminus \Theta)^{n-3} \setminus \Delta'$  where  $\Delta' = \{(x_1, \dots, x_{n-3}) \mid x_i \neq x_j \text{ when } i \neq j\}$

**Lemma 2.2** *There is a homeomorphism:*

$$C(S^2 \setminus \Theta, P \setminus \Theta) \xrightarrow{\bar{h}} \mathcal{M}(S^2, P)$$

**Proof** In order to produce  $\bar{h}$  in the theorem statement, we produce a function

$$\text{Möb} \times C(S^2 \setminus \Theta, P \setminus \Theta) \xrightarrow{h} C(S^2, P)$$

defined by the formula

$$h(M, (x_4, \dots, x_n)) = (M(p_1), M(p_2), M(p_3), M(x_4), \dots, M(x_n)).$$

We first prove that  $h$  is a homeomorphism, and then we will quotient by an action of the Möbius group to produce  $\bar{h}$ .

Injectivity of  $h$  follows from triple transitivity of Möb, and surjectivity of  $h$  is also obvious. Since both the domain and range are manifolds, we only need to show  $h$  is continuous and then the classical theorem on invariance of domain allows us to conclude that  $h$  is a homeomorphism. We use the spherical metric  $\rho$  on  $S^2$  and the sup metric  $\sigma$  on Möb where

$$\sigma(M, M') = \sup_{x \in S^2} [\rho(M(x), M'(x))].$$

In order to show that  $h$  is continuous, we work directly from the sequential formulation of continuity. Suppose that in the product metric,

$$\{(M_i, (y_{4,i}, \dots, y_{n,i}))\}_{i=1}^{\infty} \rightarrow (M, (y_4, \dots, y_n)).$$

We must show  $\{(M_i(p_1), M_i(p_2), M_i(p_3), M_i(y_{4,i}), \dots, M_i(y_{n,i}))\}_{i=1}^{\infty}$  converges to  $(M(p_1), M(p_2), M(p_3), M(y_4), \dots, M(y_n))$  in the product metric to establish continuity of  $h$ .

First we just prove the  $j$ th component converges for  $4 \leq j \leq n$ , and observe that convergence is trivial if  $j < 4$ . By assumption,  $M_i \rightarrow M \in \text{Möb}$  and  $y_{j,i} \rightarrow y_j \in S^2$ . Then we immediately see that  $M_i(y_{j,i}) \rightarrow M(y_j)$  since

$$\begin{aligned} \rho(M_i(y_{j,i}), M(y_j)) &\leq \rho(M_i(y_{j,i}), M(y_{j,i})) + \rho(M(y_{j,i}), M(y_j)) \\ &\leq \sigma(M_i, M) + \rho(M(y_{j,i}), M(y_j)) \rightarrow 0 \end{aligned}$$

Having dealt with a single component, we conclude that  $h$  is continuous by observing that Möb acting on  $S^2$  is continuous as an action, implying that the diagonal action of Möb on  $(S^2)^n$  is continuous as well.

The second step in proving the lemma is to note that  $h$  is equivariant with respect to two actions of Möb on the domain and range of the homeomorphism  $h$ . The action  $\cdot$  of Möb on  $\text{Möb} \times C(S^2 \setminus \Theta, P \setminus \Theta)$  is defined by:

$$M \cdot (\hat{M}, (x_4, \dots, x_n)) = (M \circ \hat{M}, (x_4, \dots, x_n))$$

and the action  $*$  of Möb on  $C(S^2, P)$  is defined by:

$$M * (x_1, \dots, x_n) = (M(x_1), \dots, M(x_n))$$

We show equivariance by a straightforward computation:

$$\begin{aligned} h(M \cdot (\hat{M}, (x_4, \dots, x_n))) &= h((M \circ \hat{M}, (x_4, \dots, x_n))) \\ &= (M\hat{M}(p_1), \dots, M\hat{M}(p_3), M\hat{M}(x_4), \dots, M\hat{M}(x_n)) \\ &= M * (\hat{M}(p_1), \dots, \hat{M}(p_3), \hat{M}(x_4), \dots, \hat{M}(x_n)) \\ &= M * h(\hat{M}, (x_4, \dots, x_n)) \end{aligned}$$

Then taking the quotient on the domain and range of  $h$  by the action of Möb, we have:

$$\text{Möb} \backslash (\text{Möb} \times C(S^2 \setminus \Theta, P \setminus \Theta)) \cong \text{Möb} \backslash C(S^2, P)$$

Since the left side is clearly homeomorphic to  $C(S^2 \setminus \Theta, P \setminus \Theta)$  and the right side can be identified with  $\mathcal{M}(S^2, P)$ , the result is proven.  $\square$

We present another lemma to be used in the proof of Theorem 2.4, where this one is necessary for an injectivity result.

**Lemma 2.3** *The evaluation map*

$$\text{Homeo}(S^2, \Theta) \xrightarrow{\epsilon} C(S^2 \setminus \Theta, P \setminus \Theta)$$

defined by  $\epsilon(\phi) = (\phi(p_4), \dots, \phi(p_n))$  is a fibration.

**Proof** To establish the homotopy lifting property for  $\epsilon$ , we need to produce  $\tilde{H}$  in the following diagram for any  $Y, \tilde{h}, H$ :

$$\begin{array}{ccc} Y \times \{0\} & \xrightarrow{\tilde{h}} & \text{Homeo}(S^2, \Theta) \\ \downarrow & \nearrow \tilde{H} & \downarrow \epsilon \\ Y \times I & \xrightarrow{H} & C(S^2 \setminus \Theta, P \setminus \Theta) \end{array}$$

It is a well-known fact that the following is a fibration [4]:

$$\begin{array}{ccc} \text{Homeo}(S^2, P) & \longrightarrow & \text{Homeo}(S^2) \\ & & \downarrow \epsilon_n \\ & & C(S^2, P) \end{array}$$

where  $\epsilon_n$  is the evaluation map at all  $n$  points in  $P$ . There is an obvious inclusion of our given homotopy  $H$  into  $C(S^2, P)$  which comes from tacking

on appropriate constant coordinates. As a point of notation, we call this new homotopy  $H_n$  because it corresponds to the fibration  $\epsilon_n$  and it has  $n$  space variables. Explicitly,  $H_n : Y \times I \rightarrow C(S^2, P)$  is defined by  $H_n(y, t) = (p_1, p_2, p_3, \pi_1(H(y, t)), \dots, \pi_{n-3}(H(y, t)))$  where  $\pi_i$  is the projection to the  $i$ th coordinate. The homotopy lifting property for the fibration map  $\epsilon_n$  guarantees that we can find some  $\tilde{H}_n : Y \times I \rightarrow \text{Homeo}(S^2)$  with  $H_n = \epsilon_n \circ \tilde{H}_n$  and  $\tilde{H}_n(y, 0) = \tilde{h}(y)$ . Note that for all  $t$ ,  $\epsilon_n \circ \tilde{H}_n|_{\Theta}$  fixes  $\Theta$ , which means that the range of  $\tilde{H}_n$  is actually contained in the subspace  $\text{Homeo}(S^2, P) \subset \text{Homeo}(S^2)$ . We then note that  $\tilde{H}(y, t) := \tilde{H}_n(y, t)$  solves the homotopy lifting problem for our fibration.  $\square$

We are now ready to begin the discussion of the main theorem about the equivalence between the two definitions of Teichmüller space. Recall that the pure mapping class group of the sphere with three marked points is trivial, which is a simple consequence of the statement on mapping class group given in [13, p.63]. Thus given any  $\phi \in \text{Homeo}(S^2, \Theta)$ , we can produce a one parameter family  $\phi_t$  with  $\phi_0 = id$ ,  $\phi_1 = \phi$ , and  $\phi_t \in \text{Homeo}(S^2, \Theta)$  for all  $t$ . This will be an essential ingredient in the theorem which claims that the two definitions of Teichmüller space coincide.

**Theorem 2.4** *There is a bijection*

$$\{ \phi \in \text{Homeo}(S^2, \Theta) \} / \sim \xrightarrow{\Phi} \{ \tau : ([0, 1], 0) \rightarrow (\mathcal{M}(S^2, P), id|_P) \} / \approx$$

using the equivalence relations from Definitions 1 and 2.

**Proof** We prove the theorem by showing that there are bijections from both of the sets in the theorem to the set  $\{ \tau : ([0, 1], 0) \rightarrow (C(S^2 \setminus \Theta, P \setminus \Theta), (p_4, \dots, p_n)) \} / \approx$

One of the bijections is easy; since Lemma 2.2 proved that  $\mathcal{M}(S^2, P)$  and  $C(S^2 \setminus \Theta, P \setminus \Theta)$  are homeomorphic, they must have bijective path spaces. Thus, there is a bijection between the right hand side in the theorem  $\{ \tau : ([0, 1], 0) \rightarrow (\mathcal{M}(S^2, P), id|_P) \} / \approx$  and  $\{ \tau : ([0, 1], 0) \rightarrow (C(S^2 \setminus \Theta, P \setminus \Theta), (p_4, \dots, p_n)) \} / \approx$  where the equivalence relation  $\approx$  is homotopy rel endpoint.

A second bijection comes from taking the quotient of the map

$$\Phi : \left\{ \begin{array}{l} \phi \in \text{Homeo}(S^2, \Theta) \\ \phi_t \text{ chosen as above} \end{array} \right\} \longrightarrow \{ \tau : ([0, 1], 0) \rightarrow (C(S^2 \setminus \Theta, P \setminus \Theta), (p_4, \dots, p_n)) \}$$

defined by  $\Phi(\phi) = (t \mapsto (\phi_t(p_4), \dots, \phi_t(p_n))) = (t \mapsto \epsilon(\phi_t))$  where we quotient by  $\sim$  on the left and  $\approx$  on the right. We must show that the quotient



map  $\bar{\Phi}$  is well-defined, surjective, and injective. Our convention for path multiplication is that  $\alpha * \beta$  means follow  $\alpha$  in the positive direction and then follow  $\beta$  in the positive direction. Denote by  $\bar{\alpha}$  the reverse of the path  $\alpha$ .

*Proof that  $\bar{\Phi}$  is well-defined:* Fix  $\phi \in \text{Homeo}(S^2, \Theta)$  and an isotopy  $\phi_t$  to the identity that fixes  $\Theta$  for all  $t$ . If we choose a different isotopy  $\phi'_t$  from  $\phi$  to the identity, we need to show that  $\epsilon(\phi_t)$  is homotopic to  $\epsilon(\phi'_t)$  with respect to endpoints  $(p_4, \dots, p_n)$  and  $(\phi(p_4), \dots, \phi(p_n))$ . This is the case because the path in  $\text{Homeo}(S^2, \Theta)$  given by  $\phi_t * \bar{\phi'_t}$  is an element of the homeotopy group  $\pi_1(\text{Homeo}(S^2, \Theta), id)$  which has been shown to be the trivial group [21, 28]. Thus, there is a nullhomotopy for  $\phi_t * \bar{\phi'_t}$  which can be pushed down by  $\epsilon$  to a nullhomotopy of  $(\phi_t(p_4), \dots, \phi_t(p_n)) * (\phi'_t(p_4), \dots, \phi'_t(p_n))$  in  $C(S^2 \setminus \Theta, P \setminus \Theta)$ . Clearly  $\epsilon(\phi_t)$  is homotopic to  $\epsilon(\phi'_t)$  rel endpoints.

Now suppose that  $\psi \sim \phi$ . By what we just proved, we can fix a specific  $\psi_t$  and  $\phi_t$  as our isotopies to  $id$ . Since  $\phi \sim \psi$ , there exists an isotopy  $\alpha_t$  between  $\psi$  and  $\phi$  where  $\alpha_0 = \psi$ ,  $\alpha_1 = \phi$ , and for all  $t$ , the homeomorphism  $\alpha_t$  fixes  $\Theta$ . Then  $\psi_t * \alpha_t * \bar{\phi_t}$  is a loop in  $\text{Homeo}(S^2, \Theta)$ , and triviality of the homeotopy group allows us again to push down a nullhomotopy via  $\epsilon$ .

*Proof that  $\bar{\Phi}$  is surjective:* Let  $\tau = (\tau_4, \dots, \tau_n)$  be a path in  $C(S^2 \setminus \Theta, P \setminus \Theta)$  starting at  $(p_4, \dots, p_n)$  and ending at  $(x_4, \dots, x_n)$ . We use  $\tau$  to produce a motion of  $n$  points in  $S^2$ , namely:

$$t \mapsto (p_1, p_2, p_3, \tau_4(t), \dots, \tau_n(t))$$

The isotopy extension theorem on p.181 in [14] guarantees existence of an ambient isotopy

$$\phi : S^2 \times I \longrightarrow S^2$$

where  $\phi$  fixes small neighborhoods of  $\Theta$  for all  $t$ , and  $\phi(\tau_i(t), t) = \tau_i(t)$ ,  $4 < i < n$ . Then  $\phi(\cdot, 1) \in \text{Homeo}(S^2, \Theta)$  is a homeomorphism with a choice  $\phi$  of isotopy to the identity that evaluates to  $\tau$  under  $\epsilon$ . This homeomorphism is called the point push of  $(p_4, \dots, p_n)$  along  $\tau$ .

*Proof that  $\bar{\Phi}$  is injective:* Let  $\phi, \psi \in \text{Homeo}(S^2, \Theta)$ . Define  $\phi_t, \psi_t$  to be paths in  $\text{Homeo}(S^2, \Theta)$  to the identity. Assume that  $\tau_0(t) := \epsilon(\phi_t)$  and  $\tau_1(t) := \epsilon(\psi_t)$  are two paths in  $C(S^2 \setminus \Theta, P \setminus \Theta)$  that are homotopic relative to their two endpoints  $(p_4, \dots, p_n)$  and  $(\phi(p_4), \dots, \phi(p_n))$ . Using homotopy lifting, we will show that without loss of generality, we may assume  $\tau_0$  and  $\tau_1$  are equal. By assumption we have  $H : I \times I \rightarrow C(S^2 \setminus \Theta, P \setminus \Theta)$  where

for all  $t, s \in [0, 1]$ ,

$$\begin{aligned} H(t, 0) &= \tau_0(t) \\ H(t, 1) &= \tau_1(t) \\ H(0, s) &= (p_4, \dots, p_n) \\ H(1, s) &= (\phi(p_4), \dots, \phi(p_n)) \end{aligned}$$

and then using the fibration in Lemma 2.3, we lift to a homotopy  $\tilde{H} : I \times I \rightarrow \text{Homeo}(S^2, \Theta)$  defined as follows:

$$\begin{aligned} \tilde{H}(t, 0) &= \phi_t \\ \tilde{H}(t, 1) &= \alpha_t \\ \tilde{H}(0, s) &\subset \epsilon^{-1}(p_4, \dots, p_n) \\ \tilde{H}(1, s) &\subset \epsilon^{-1}(\phi(p_4), \dots, \phi(p_n)) \end{aligned}$$

where  $\alpha_t$  is some path in  $\text{Homeo}(S^2, \Theta)$  with the property that  $\epsilon(\alpha_t) = \tau_1(t)$ . The following chain of isotopies rel  $P$  demonstrate that  $\psi \simeq \phi$  rel  $P$ . First follow  $\phi \simeq \alpha_1$  rel  $P$ , observing that the path  $\tilde{H}(1, s)$  lies in a single fiber of  $\epsilon$ . Next follow  $\alpha_1 \simeq \psi \circ \alpha_0$  rel  $P$ : the isotopy  $\alpha_1 \circ \alpha_1 \circ \psi_t \circ \alpha_0$  is constant on  $P$  (recall that  $\alpha_t$  and  $\psi_t$  evaluate to  $\tau_1$ ). Finally follow  $\psi \circ \alpha_0 \simeq \psi$  rel  $P$ : the map  $\tilde{H}(0, s)$  is a path from  $\alpha_0$  to the identity that remains in a single fiber of  $\epsilon$ .  $\square$

Now our goal is to understand the relationship between two virtual endomorphisms, one defined on the fundamental group of moduli space, and the other on the pure mapping class group of the dynamical plane. In general, a virtual endomorphism is a homomorphism  $\phi : H \rightarrow G$  where  $H$  is a finite index subgroup of  $G$ . We define two virtual endomorphisms that will be relevant to our future study, and use the construction of  $\bar{\Phi}$  to show that they are conjugate. Suppose that the following diagram commutes for some rational Thurston map  $f$  where  $\otimes$  is the unique fixed point of  $\sigma_f$ , and  $z_0 := \pi(\otimes)$ ,  $w_0 = A(\otimes)$ , and the maps  $X, Y$ , and  $A$  are defined according to

the discussion in [17]:

$$\begin{array}{ccc}
(\mathcal{T}_f, \otimes) & \xrightarrow{\sigma_f} & (\mathcal{T}_f, \otimes) \\
\downarrow \pi & \searrow A & \downarrow \pi \\
& (\mathcal{W}_f, w_0) & \\
& \swarrow Y & \searrow X \\
(\mathcal{M}_f, z_0) & & (\mathcal{M}_f, z_0).
\end{array}$$

*Example 1:* Let  $H = \{[\gamma] \in \pi_1(\mathcal{M}_f, z_0) \mid \gamma \text{ lifts to a loop } \tilde{\gamma} \text{ based at } w_0 \text{ under } Y\}$  where  $H$  is evidently a subgroup of  $\pi_1(\mathcal{M}_f, z_0)$ . It is further apparent that this subgroup has finite index since it is the stabilizer of the action of  $\pi_1(\mathcal{M}_f, z_0)$  on  $Y^{-1}(z_0)$ . Define the virtual endomorphism  $\phi_f : H \rightarrow \pi_1(\mathcal{M}_f, z_0)$  by  $\phi_f([\gamma]) = X_*([\tilde{\gamma}])$ .

*Example 2:* Let  $H_f = \{[h] \in \text{PMCG}(\widehat{\mathbb{C}}, P_f) \mid \text{there exists } \tilde{h} \text{ where } \tilde{h} \text{ is a homeomorphism that fixes } P_f \text{ and makes the following diagram commute:}$

$$\begin{array}{ccc}
(\widehat{\mathbb{C}}, P_f) & \xrightarrow{\tilde{h}} & (\widehat{\mathbb{C}}, P_f) \\
f \downarrow & & \downarrow f \\
(\widehat{\mathbb{C}}, P_f) & \xrightarrow{h} & (\widehat{\mathbb{C}}, P_f)
\end{array}$$

The virtual endomorphism  $\psi : H_f \rightarrow \text{PMCG}(\widehat{\mathbb{C}}, P_f)$  is defined by  $\psi(h) = \tilde{h}$ . To see that  $H_f$  is a finite index subgroup, we first define an action of  $\text{Homeo}(\widehat{\mathbb{C}}, P_f)$  on a certain kind of covering class. Let  $p : \widehat{\mathbb{C}} \rightarrow \widehat{\mathbb{C}}$  be a branched cover that preserves its critical locus  $P$  setwise. Two such covers  $p_1$  and  $p_2$  are said to be isomorphic if there exists a homeomorphism  $g$  so that  $g \circ p_1 = p_2$  where  $g$  restricts to the identity on  $P$ . Using postcomposition on the level of representatives, the group  $\text{Homeo}(\widehat{\mathbb{C}}, P_f)$  acts on the set of isomorphism classes of branched covering maps from  $\widehat{\mathbb{C}}$  to  $\widehat{\mathbb{C}}$  that preserve  $P_f$  setwise. This induces a left action of the pure mapping class group on covering classes as follows, where  $[\phi] \in \text{PMCG}(\widehat{\mathbb{C}}, P_f)$ :

$$[\phi].[p] = [\phi \circ p]$$

This action induces an action of the group of outer automorphisms  $\text{Out}(\pi_1(\widehat{\mathbb{C}} \setminus P_f))$  on the set of conjugacy classes of finite index subgroups of  $\pi_1(\widehat{\mathbb{C}} \setminus P_f)$

where the index is equal to the degree of the cover  $p$  which we denote by  $d$ . The action is as follows where  $[\phi] \in \text{Out}(G)$  and  $[H]$  is the conjugacy class of an index  $d$  subgroup:

$$[\phi] \cdot [H] = [\phi(H)]$$

In [19] we find that  $a_d(G)$ , the number of subgroups of index  $d$  of any finitely generated group  $G$  with  $r$  generators, has the following bound where  $h_d(G) = \#\{\text{homomorphisms } \phi : G \rightarrow S_d, \phi \text{ transitive}\}$  :

$$\begin{aligned} a_d(G) &\leq \frac{1}{(d-1)!} \cdot h_d(G) \\ &\leq \frac{1}{(d-1)!} \cdot d!^r \\ &= d \cdot d!^{r-1} \end{aligned}$$

Thus, there is a finite number of conjugacy classes of index  $d$  subgroups contained in  $\pi_1(\widehat{\mathbb{C}} \setminus P_f)$ . There is a natural homomorphism:

$$\text{PMCG}(\widehat{\mathbb{C}}, P_f) \rightarrow \text{Out}(\pi_1(\widehat{\mathbb{C}} \setminus P_f))$$

and this induces an action of the pure mapping class group on the set of conjugacy classes of index  $d$  subgroups of  $\pi_1(\widehat{\mathbb{C}} \setminus P_f)$ . The stabilizer of the subgroup corresponding to  $f$  is the set of all pure mapping classes that lift as in the definition of  $H_f$ , and this stabilizer has finite index in  $\text{PMCG}(\widehat{\mathbb{C}}, P_f)$ . Not everything in this stabilizer lifts to a pure mapping class, but  $H_f$  has finite index in this stabilizer, and so  $H_f$  has finite index in the pure mapping class group.

**Lemma 2.5** *The map  $\Psi$  is a bijection where we have suppressed the bracket notation for the equivalence on Teichmüller space*

$$\{\phi' | \sigma_f(\phi) = \phi'\} \xrightarrow{\Psi} \left\{ \begin{array}{l} [t \mapsto X(\tilde{\alpha}(t))] \text{ where } \alpha : [0, 1] \rightarrow \mathcal{M}_f, \alpha(0) = z_0 \\ \text{and } \tilde{\alpha} \text{ is the unique lift under } Y \text{ with } \tilde{\alpha}(0) = w_0 \end{array} \right\}$$

**Proof** Define  $\Psi$  as follows, where  $\tilde{\alpha}(t) = \widetilde{\epsilon(\phi_t)}$  is the unique lift under  $Y$  of the path class  $\epsilon(\phi_t)$  and the square brackets represent the homotopy class of paths rel endpoint:

$$\Psi(\phi') := [X(\widetilde{\epsilon(\phi_t)})]$$

*Proof that  $\Psi$  is well-defined:* Suppose we choose  $\psi$  in the same class as  $\phi$ . Then since  $A$  maps the basepoint of  $\mathcal{T}_F$  to  $z_0$ , we know that  $[A(\phi_t)] = [\widetilde{\epsilon(\phi_t)}]$ . Then since  $\epsilon \circ \sigma_f = X \circ A$  and by assumption  $[\sigma_f(\phi_t)] = [\sigma_f(\psi_t)]$  we get the following chain of equalities that demonstrate  $\Psi$  is well-defined:

$$\begin{aligned} [X(\widetilde{\epsilon(\phi_t)})] &= [X \circ A(\phi_t)] \\ &= [\epsilon(\sigma_f(\phi_t))] \\ &= [\epsilon(\sigma_f(\psi_t))] \\ &= [X \circ A(\psi_t)] \\ &= [X(\widetilde{\epsilon(\psi_t)})] \end{aligned}$$

*Proof that  $\Psi$  is injective:* Suppose  $\Psi(\phi') = \Psi(\psi')$  where  $\phi' = \sigma_f(\phi)$ ,  $\psi' = \sigma_f(\psi)$ . Again, since  $\epsilon \circ \sigma_f = X \circ A$ , we know

$$\Psi(\phi') = [X(\widetilde{\epsilon(\phi_t)})] = [X \circ A(\phi_t)] = [\epsilon(\sigma_f(\phi_t))] = [\epsilon(\phi'_t)]$$

and similarly

$$\Psi(\psi') = [\epsilon(\psi'_t)]$$

Thus  $[\epsilon(\phi'_t)] = [\epsilon(\psi'_t)]$  and so  $\bar{\Phi}^{-1}(\epsilon([\phi'_t])) = \bar{\Phi}^{-1}(\epsilon([\psi'_t]))$  which immediately implies that  $\phi' = \psi'$ .

*Proof that  $\Psi$  is surjective:* Consider  $[t \mapsto X(\tilde{\alpha}(t))]$ . Then  $\bar{\Phi}^{-1}([Y(\tilde{\alpha}(t))]) = \phi$  for some  $\phi \in \mathcal{T}_f$ . Now it is apparent that  $\Psi(\sigma_f(\phi)) = [X(\tilde{\alpha}(t))]$ .  $\square$

**Theorem 2.6** *The following equality holds, where  $H_f$  is the domain of the virtual endomorphism defined on the mapping class group defined earlier:*

$$\bar{\Phi}(H_f) = H = \left\{ \begin{array}{l} [\alpha] \in \pi_1(\mathcal{M}_f, z_0) \text{ so that } \alpha \text{ lifts} \\ \text{to a loop under } Y \text{ based at } w_0 \end{array} \right\}$$

Furthermore, on the domain where the virtual endomorphism  $\phi_f$  is defined,

$$\bar{\Phi} \circ \phi_f = \psi \circ \bar{\Phi}.$$

**Proof** Suppose  $\alpha$  lifts to a loop under  $Y$  based at  $w_0$ . From Lemma 2.5, we know that by point pushing,  $[\alpha]$  corresponds to  $[h'] \in \mathcal{T}_f$  which is the image of some  $[h] \in \mathcal{T}_f$  under  $\sigma_f$ . From the fact that  $\alpha$  lifts to a loop, it is evident

that  $[h], [h'] \in \text{PMCG}(\widehat{\mathbb{C}}, P_f)$  since  $\pi([h]) = Y \circ A([h]) = Y(w_0) = z_0$  and  $\pi([h']) = \pi \circ \sigma_f([h]) = X \circ A([h]) = X(w_0) = z_0$ . By definition of  $\sigma_f$ , there is a unique representative of  $[h']$  which we suggestively call  $\phi_f(h)$  so that the following commutes for some rational function  $F$ :

$$\begin{array}{ccc} (\widehat{\mathbb{C}}, P_f) & \xrightarrow{\phi_f(h)} & (\widehat{\mathbb{C}}, P_f) \\ f \downarrow & & \downarrow F \\ (\widehat{\mathbb{C}}, P_f) & \xrightarrow{h} & (\widehat{\mathbb{C}}, P_f) \end{array}$$

By the uniqueness of  $f$ , we immediately have that in fact  $F = f$ , and so by examination of the diagram, we have that  $[h] \in H_f$ .

Next suppose that  $[h] \in H_f$ . By Lemma 2.5,  $h$  corresponds to a class  $[t \mapsto X(\tilde{\alpha}(t))]$  where  $\tilde{\alpha}$  is the unique lift of  $\alpha : ([0, 1], 0) \rightarrow (\mathcal{M}_f, z_0)$  with  $\tilde{\alpha}(0) = w_0$ . Furthermore  $[h] \in H_f$  implies that  $\sigma_f([h]) = [\phi_f(h)]$ . Then

$$z_0 = \pi([\phi_f(h)]) = \pi \circ \sigma_f([h]) = X \circ A([h])$$

but  $X \circ A([h]) = w_0$  implies that  $A([h]) = w_0$ , and so  $\tilde{\alpha}$  is actually a loop which means  $\alpha \in H$ . □

### 2.3 Schreier Graphs and the Reidemeister-Schreier Algorithm

Our discussion of the Reidemeister-Schreier algorithm follows the more general presentation of [6]. Let  $f : \widehat{\mathbb{C}} \rightarrow \widehat{\mathbb{C}}$  be a degree  $d$  connected branched cover with critical values  $V_f$ . Choose a basepoint  $z_0 \in \widehat{\mathbb{C}} \setminus f^{-1}(V_f)$ , and note that the branched cover can be restricted to the complement of  $f^{-1}(V_f)$  to produce a cover, which by abuse of notation we call  $f : (\widehat{\mathbb{C}} \setminus f^{-1}(V_f), z_0) \rightarrow (\widehat{\mathbb{C}} \setminus V_f, f(z_0))$ . It is evident that  $G := \pi_1(\widehat{\mathbb{C}} \setminus V_f, f(z_0))$  is a finitely generated free group on  $|V_f| - 1$  generators; choose the basis set  $S$  of the group to be a bouquet of  $|V_f| - 1$  disjoint oriented loops based at  $f(z_0)$ , each of which bounds a unique point of  $V_f$ . It is known that every subgroup of a free group is free [6, p.66], and so for the induced map  $f_*$  on the fundamental group, the subgroup  $H := f_*(\pi_1(\widehat{\mathbb{C}} \setminus f^{-1}(V_f), z_0)) < G$  must be free. Schreier's formula [6, p.66] determines the rank of  $H$ :

$$\text{rank}(H) - 1 = d \cdot (|S| - 1).$$

Finding explicitly the generators of  $H$  requires a little more work, and an important tool for determining this is a labeled directed graph called the *Schreier graph*. The vertices are simply points in  $f^{-1}(z_0)$ , and for a vertex

$v_0$  denote by  $f^{-1}(s)[v_0]$  the endpoint of the unique lift of  $s$  starting at  $v_0$ . Two vertices  $v_0$  and  $v_1$  are joined by a directed edge  $e$  if there is an element  $s \in S$  so that  $f^{-1}(s)[v_0] = v_1$ . Call  $v_0$  the *initial vertex* of edge  $e$  denoted by  $i(e)$  and call  $v_1$  the *terminal vertex* of  $e$  denoted by  $t(e)$ . If  $e$  is an edge in the Schreier graph, the *label* of  $e$  is defined to be  $\ell(e) = s$  where  $s$  is the unique element so that  $f^{-1}(s)[i(e)] = t(e)$ . Denote by the formal symbol  $e^{-1}$  the reverse of the edge  $e$ , and extend to reverse edges the notion of initial and terminal vertex by the following:  $i(e^{-1}) := t(e)$  and  $t(e^{-1}) := i(e)$ . Define a finite path in the Schreier graph to be a finite list of edges or reversed edges  $e_1 e_2 \dots e_n$ , where for all  $j$ ,  $t(e_j) = i(e_{j+1})$ ,  $1 \leq j < n$ . The notion of label can easily be extended to finite paths in the Schreier graph by declaring that  $\ell(\text{empty path}) = 1$ ,  $\ell(e^{-1}) = \ell(e)^{-1}$  for any edge  $e$ , and for any paths  $p, q$  in the Schreier graph with  $t(p) = i(q)$ , we define  $\ell(pq) := \ell(p)\ell(q)$ . Choose a maximal subtree  $\Delta$  of the Schreier graph, and for some vertex  $v$  in the Schreier graph, denote by  $p_v$  the unique shortest path from  $z_0$  to  $v$  contained in  $\Delta$ . Then for every edge  $e$  so that neither  $e$  nor  $e^{-1}$  is contained in  $\Delta$ , define the path  $p_e = p_{i(e)} e p_{t(e)}$  which clearly forms a loop in the Schreier graph based at  $z_0$ . A classical theorem [6, p.67] asserts that  $H$  is generated by the following:

$$\{\ell(p_e) | e \text{ is an edge where neither } e \text{ nor } e^{-1} \text{ are contained in } \Delta\}.$$

Having discussed how to find generators for  $H$ , we describe the Reidemeister-Schreier algorithm which rewrites an element of  $H$  written in terms of  $S \cup S^{-1}$  as a product of the basis elements  $\ell(p_e)$  for  $H$  (and their inverses). Define the *Schreier transversal* of the Schreier graph with specified maximal subtree  $\Delta$  to be the finite set of  $d$  elements:

$$T = \{\ell(p_v^{-1}) | v \text{ is a vertex in the Schreier graph}\}.$$

Let  $g$  be a word in the generators  $\alpha, \beta$  and their inverses. Let  $p$  be the corresponding path in the Schreier graph starting at  $z_0$  with  $\ell(p) = g$ ; define  $\bar{g} = \ell(t)$  where  $t$  is the unique element of  $T$  having the same endpoint as  $p$ . If  $t \in T$  and  $s \in S$ , define  $\gamma(t, s) = ts(\overline{ts})^{-1}$  which is clearly an element in  $H$ . Suppose we wish to rewrite  $h \in H$  in terms of the basis of  $H$  where  $h = s_1 s_2 \dots s_k$ ,  $s_j \in S \cup S^{-1}$ . Then the rewriting of  $h$  is given by

$$h = \gamma(1, s_1) \gamma(\overline{s_1}, s_2) \dots \gamma(\overline{s_1 s_2 \dots s_{k-2}}, s_{k-1}) \gamma(\overline{s_1 s_2 \dots s_{k-1}}, s_k).$$

## 2.4 Iterated Monodromy Groups and Wreath Recursions

We now turn to the machinery that solved the twisted rabbit problem. In [1] these tools are developed in the more general setting of partial self-coverings,

but we restrict our attention to the case where  $f : \widehat{\mathbb{C}} \rightarrow \widehat{\mathbb{C}}$  is a finite branched cover.

First, fix a basepoint  $z_0 \in \widehat{\mathbb{C}} \setminus P_f$ , and note that for a fixed  $n$ ,  $\pi_1(\widehat{\mathbb{C}} \setminus P_f, z_0)$  acts on the set  $f^{-n}(z_0)$  in the following way: if  $z \in f^{-n}(z_0)$  and  $[\gamma] \in \pi_1(\widehat{\mathbb{C}} \setminus P_f, z_0)$ , then  $z \cdot \gamma$  is the endpoint of the unique lift of  $\gamma$  under  $f^n$  that begins at  $z$ . Denote the lift of  $\gamma$  under  $f^n$  beginning at  $z$  by  $f^{-n}(\gamma)[z]$ . The action on the disjoint union  $\coprod_{n \geq 0} f^{-n}(z_0)$  is called the *iterated monodromy action*. We now construct the tree of preimages and describe the iterated monodromy action on this tree. Let  $z_0$  be the root of the tree and each element of  $\coprod_{n > 0} f^{-n}(z_0)$  a vertex. Join each vertex  $z \in f^{-n}(z_0)$  to each of the vertices in  $f^{-1}(z) \subset f^{-n-1}(z_0)$ . It is easily shown that the iterated monodromy action (extended to the edges in the obvious way) acts by automorphisms of this tree, but this action is not necessarily faithful. Thus we define the *iterated monodromy group*  $\text{IMG}(f)$  as follows:

$$\text{IMG}(f) = \pi_1(\widehat{\mathbb{C}} \setminus P_f, z_0) / \ker$$

where  $\ker$  is the kernel of the iterated monodromy action.

We now present a convenient way to index these trees along with their automorphisms. Let  $X = \{1, \dots, d\}$  and denote the set of strings of length  $n$  in the letters  $1, \dots, d$  by  $X^n$ , and the set of infinite strings in these  $d$  letters by  $X^*$ . Identify the tree of preimages of  $z_0$  with the set  $X^*$  as follows:

- Identify  $z_0$  with the empty word
- Choose a bijection between  $z \in f^{-1}(z_0)$  and  $x \in X$ . For each  $x \in X$ , choose paths  $\ell_x$  between  $z_0$  and the point in  $f^{-1}(z_0)$  corresponding to  $x \in X$ .
- If  $v$  is a word in  $X$  and  $x \in X$ , we identify  $vx$  with the endpoint of the path  $f^{-n}(\ell_x)[z]$  where  $z$  is the  $n$ th preimage corresponding to  $v$ .

The iterated monodromy action can be conjugated by this bijection to yield an action of  $\pi_1(\widehat{\mathbb{C}} \setminus P_f, z_0)$  on  $X^*$ . See the next section for a discussion of how the iterated monodromy group solved the twisted rabbit problem.

Another important tool in [1] for understanding the action of the fundamental group on  $X^*$  are wreath recursions. Denote by  $S_d$  the symmetric group on  $d$  letters. We multiply elements of  $S_d$  in the following way:

$$(1 \ 4 \ 2)(1 \ 3 \ 4) = (2 \ 3 \ 4).$$

Define the *wreath product*  $G \wr S_d$  for some group  $G$  to be  $G^d \rtimes S_d$  where  $S_d$  acts on the  $d$ -fold product  $G^d$  by permutation of coordinates. Thus,



if  $\langle\langle g_1, \dots, g_d \rangle\rangle\sigma$  and  $\langle\langle h_1, \dots, h_d \rangle\rangle\tau$  are elements of  $G \wr S_d$ , multiplication is defined by:

$$\langle\langle g_1, \dots, g_d \rangle\rangle\sigma \langle\langle h_1, \dots, h_d \rangle\rangle\tau = \langle\langle g_1 h_{\sigma(1)}, \dots, g_d h_{\sigma(d)} \rangle\rangle\sigma\tau$$

For example, if  $G$  is the free group of rank 2 on generators  $\alpha$  and  $\beta$ ,

$$\begin{aligned} &\langle\langle 1, \beta\alpha, \alpha, \beta^{-1} \rangle\rangle(1 \ 4 \ 2) \langle\langle \beta\alpha, \alpha^{-1}, 1, \beta \rangle\rangle(1 \ 3 \ 4) \\ &= \langle\langle \beta, \beta\alpha\beta\alpha, \alpha, \beta^{-1}\alpha^{-1} \rangle\rangle(2 \ 3 \ 4) \end{aligned}$$

A *wreath recursion* is a homomorphism  $\Phi : G \rightarrow G \wr S_d$ . We denote the restriction to the  $x$ th coordinate of  $\Phi(g)$  by  $g|_x$ , and if  $v \in X^*$ , we define  $g|_{xv} = (g|_x)|_v$ ,  $x \in X$ . We let  $G$  act on  $X$  by projecting to the second factor  $G \wr S_d \rightarrow S_d$  and this extends to the associated action of  $G$  on  $X^*$  by the formula  $(vx)^g = v^g x^{g|_v}$ . We then have the following proposition coming from [1, p.7] where as always in this paper, path multiplication is defined by following the leftmost path in the positive direction and ending with the rightmost. The bar denotes the reverse path.

**Theorem 2.7** *The action of  $\pi_1(\widehat{\mathbb{C}} \setminus P_f, z_0)$  on  $X^*$  is the action associated with  $\Phi : \pi_1(\widehat{\mathbb{C}} \setminus P_f, z_0) \rightarrow \pi_1(\widehat{\mathbb{C}} \setminus P_f, z_0) \wr S_d$  given by*

$$\Phi(\gamma) = \langle\langle \ell_1 \gamma_1 \bar{\ell}_{k_1}, \ell_2 \gamma_2 \bar{\ell}_{k_2}, \dots, \ell_d \gamma_d \bar{\ell}_{k_d} \rangle\rangle \rho$$

where  $\gamma_i = f^{-1}(\gamma)[z_i]$ ,  $z_i$  is the endpoint of  $\ell_i$ ,  $k_i$  is the element of  $X$  corresponding to  $z_i$ , and  $\rho$  is the permutation defined by  $i \mapsto k_i$  for all  $i \in X$ .

We are interested in producing a virtual endomorphism given a wreath recursion ([1] discusses how one might produce a wreath recursion given a virtual endomorphism). Define the domain of the virtual endomorphism  $\phi_i : H_i \rightarrow G$  to be the subgroup  $H_i < G$  where  $h \in H_i$  if the permutation factor of  $\Phi(h)$  fixes  $i$ . Then  $\phi_i(h)$  is defined to be the projection to the  $i$ th component of  $\Phi(h) \in G \wr S_d$ .

The contracting properties of wreath recursions are important for reducing infinite problems to finite problems. A wreath recursion  $\Phi : G \rightarrow G \wr S_d$  is contracting if there is a finite  $\mathcal{N} \subset G$  so that for every  $g \in G$ , there is a positive number  $n_0$  so that  $g|_v \in \mathcal{N}$  for all words  $v$  of length greater than  $n_0$ . The smallest such  $\mathcal{N}$  is called the nucleus of the action. A useful characterization of the contracting property in [25, p.57] is the following: A wreath recursion defined on a group  $G$  with generating set  $S = S^{-1}, 1 \in S$

is contracting if and only if there exists a finite set  $\mathcal{N}$  and a number  $k \in \mathbb{N}$  so that

$$((S \cup \mathcal{N})^2)|_{X^k} \subset \mathcal{N}$$

There is also a notion of contraction for virtual endomorphisms. Let  $\phi : \text{dom}\phi \rightarrow G$  be a virtual endomorphism. Then the spectral radius  $\rho_\phi$  of the virtual endomorphism is

$$\rho_\phi = \limsup_{n \rightarrow \infty} \sqrt[n]{\limsup_{g \in \text{dom}\phi^n, |g| \rightarrow \infty} \frac{|\phi^n(g)|}{|g|}}$$

where  $|\cdot|$  denotes word length with respect to some fixed generating set of  $G$ . In [1, p.9] we find the following proposition:

**Proposition 2.8** *Let  $\Phi : G \rightarrow G \wr S_d$  be a wreath recursion, and let  $\phi$  be an associated virtual endomorphism. If  $\Phi$  is contracting, then  $\rho_\phi < 1$ . If the action of  $G$  is transitive on every level  $X^n$  and  $\rho_\phi < 1$ , then the wreath recursion  $\Phi$  is contracting.*

We now present two important types of problem that have been studied in the past, and will be dealt with in the present work. First we discuss twisting problems, and it is appropriate to begin by discussing the only known solution to such a problem which is found in [1].

Thurston's theorem has a valuable refinement when the Thurston-map exhibits behavior like that of a polynomial. More precisely, we define a Thurston map  $F$  to be a *topological polynomial* if there is some point  $\infty$  so that  $F^{-1}(\infty) = \infty$ , or in other words,  $F$  has a fixed critical point with local degree equal to the degree of the cover. If  $F$  is a topological polynomial, every obstruction contains a *Levy cycle* which is defined to be a multicurve  $\{\gamma_0, \gamma_1, \dots, \gamma_{n-1}\}$  so that the single nonperipheral component of the preimage of each  $\gamma_i$  under  $F$  is homotopic to  $\gamma_{i-1}$ , and  $F$  maps each  $\gamma_{i-1}$  to  $\gamma_i$  by degree 1 for each  $i$  (indices are considered mod  $n$ ).

Let  $f$  be a quadratic polynomial with three finite post-critical points that are cyclically permuted. To find all such polynomials up to conjugacy, we let  $f_c(z) = z^2 + c$  and solve the equation  $f_c^{\circ 3}(0) = 0$  for  $c$ , where the root  $c = 0$  can be ignored because it doesn't have three distinct finite post-critical points, leaving  $c = -1.7549, -0.1226 + 0.7449i, -0.1226 - 0.7449i$  which correspond to the airplane polynomial  $f_A$ , rabbit polynomial  $f_R$ , and corabbit polynomial  $f_C$  respectively. In each case, applying a Dehn twist along a curve that avoids the postcritical set does not change the critical portrait (i.e. the twisted polynomial is still a topological polynomial of

degree three where the three finite post-critical points are cyclically permuted). Obstructions must contain Levy cycles, but a direct application of the Riemann-Hurwitz formula shows that such a cycle cannot exist because of the periodic critical point. Thus, a twist of any of these three polynomials must be equivalent to one of  $f_A$ ,  $f_R$ , or  $f_C$ . Crucial to the work of Bartholdi and Nekrashevych is their Corollary 3.3, which asserts that two Thurston equivalent quadratic topological polynomials with identical post-critical set will have identical iterated monodromy groups. After identifying the marked spheres for  $f_A$ ,  $f_R$ , and  $f_C$ , the iterated monodromy groups of all three polynomials are shown to be Thurston inequivalent because they have different nuclei. Thus, a twisted rabbit will lie in one of three nonobstructed combinatorial classes, and all that remains is to decide which one.

Bartholdi and Nekrashevych fix two generators of the pure mapping class group of the plane for  $f_R$  which they denote  $S$  and  $T$ . Denote by  $\psi : \text{dom}(\psi) < \text{PMCG}(\widehat{\mathbb{C}}, P_f) \rightarrow \text{PMCG}(\widehat{\mathbb{C}}, P_f)$  the virtual endomorphism on the pure mapping class group. This can be extended to a function (no longer a homomorphism on all of  $\text{PMCG}(\widehat{\mathbb{C}}, P_f)$ ) using the following:

$$\bar{\psi}(h) = \begin{cases} \psi(h) & h \in \text{dom}\psi \\ T\psi(hT^{-1}) & \text{otherwise} \end{cases}$$

It is shown that  $h \circ f_R$  is Thurston equivalent to  $\bar{\psi}(h) \circ f_R$  and so it could be valuable to understand what happens to  $h$  under iteration of  $\bar{\psi}$ . Bartholdi and Nekrashevych show in Proposition 4.2 that in fact  $\bar{\psi}$  is contracting, and any  $h$  lands in the set  $\{id, T, T^{-1}\}$  after finitely many iterations. Then in Theorem 4.8, they show that if the orbit of  $h$  under iteration of  $\bar{\psi}$  lands on  $id, T$ , or  $T^{-1}$ , then  $f_R \circ h$  is equivalent to the rabbit, airplane, or corabbit respectively.

The next case of the twisted  $z^2 + i$  is dealt with by [1] in a similar way. The virtual endomorphism is extended to the pure mapping class group, but this time, the twisted  $z^2 + i$  is equivalent to either  $z^2 + i, z^2 - i$ , or a  $\mathbb{Z}$ -parameter family of obstructed examples that are inequivalent to each other. As before, the class of a twisted  $z^2 + i$  is determined by computing the iterative behavior of  $\bar{\psi}$ , and then using explicit computations of iterated monodromy groups to distinguish between the nonobstructed limiting maps. The obstructed maps must be distinguished using another method since there are infinitely many of them.

The final kind of quadratic with three finite postcritical points is the preperiod 2, period 1 case. They extend the virtual endomorphism as before, and note that under iteration the extended virtual endomorphism lands

in one of three attractors, each of which corresponds to a Thurston map with distinct nuclei. As with the twisted rabbit, it is impossible to have obstructed twistings.

Bartholdi and Nekrashevych partially verify their twisted rabbit results by studying the iterative properties of the moduli space map. This procedure would work for correspondences as well. Suppose  $f$  is a Thurston map and that the following diagram defined in [17] commutes:

$$\begin{array}{ccc}
 (\mathcal{T}_f, \otimes) & \xrightarrow{\sigma_f} & (\mathcal{T}_f, \otimes) \\
 \pi \downarrow & \searrow A & \downarrow \pi \\
 & (\mathcal{W}_f, w_0) & \\
 & \swarrow Y & \searrow X \\
 (\mathcal{M}_f, z_0) & & (\mathcal{M}_f, z_0)
 \end{array}$$

The following is an iterative procedure that determines the combinatorial equivalence class of  $f \circ h$ . The orbit of  $\otimes \in \mathcal{T}_f$  under iteration of  $\sigma_{h \cdot f}$  either converges to some  $\tau \in \mathcal{T}_f$  or it escapes to the boundary. In the first case,  $h \cdot f$  is equivalent to a rational map, and in the latter case,  $h \cdot f$  is equivalent to an obstructed map. In order to find the orbit of  $\tau$  under  $\sigma_{h \cdot f}$  projected by  $\pi$ , one uses the easily proven fact that  $\sigma_{h \cdot f}(\tau) = h \cdot \sigma_f(\tau)$ . Thus  $\sigma_{h \cdot f}(\otimes)$  is represented by the path  $\gamma_h$  which corresponds to  $h$  in  $\mathcal{M}_f$  based at  $z_0$ . The following formula shows how one might find the path corresponding to  $\lim_{n \rightarrow \infty} \sigma_{h \cdot f}^{\circ n}(\otimes)$ . Let  $\ell_h$  represent  $\sigma_{h \cdot f}^{\circ n}(\otimes)$ . The path representing  $\sigma_{h \cdot f}^{\circ n+1}(\otimes)$  is  $\gamma_h \cdot X(Y^{-1}(\ell_h)[A(\otimes)])$ , and thus we need only understand where the endpoints of this path approach as  $n$  gets large. The correspondence has fixed points that correspond to all possible combinatorial equivalence classes, and if the path converges to one of these points as  $n \rightarrow \infty$ , then  $h \cdot f$  is combinatorially equivalent to the corresponding rational map. This is demonstrated in Figure 6 of [1].

This describes the solution to the twisting problem for polynomials having three finite post-critical points. One finds in [26] a description of the combinatorial spider algorithm which is known to always converge in the case of sub-hyperbolic bimodules and thus can be used to solve twisting problems in that case. In [16, p.39] we find a theorem asserting the sub-hyperbolicity of the mega-bimodule associated to a topological quadratic polynomial whose finite critical point has period length four. In [2], Bartholdi and Nekrashevych connect the discussion of twisted kneading automata in [26] to the well-known notion of kneading sequences from complex dynamics.

Having summarized the known results about twisted polynomials, we will present a digest of known results about preimages of multicurves under a Thurston map. This data is useful because the dynamics of the pullback function on multicurves has been used to produce invariants for Thurston equivalence, and will be used in this paper to help solve the twisting problem for a rational function. Let  $\Gamma$  and  $\Gamma'$  be multicurves in  $\widehat{\mathbb{C}} \setminus P_F$  for some Thurston map  $F$ . We say that  $\Gamma$  pulls back to  $\Gamma'$  if the essential nonperipheral components of  $f^{-1}(\Gamma)$  form a multicurve homotopic to  $\Gamma'$ , and we denote this by  $\Gamma' \xrightarrow{f} \Gamma$ . In [27] it is shown that if the virtual endomorphism corresponding to a Thurston map is contracting, then there is a finite global attractor for the pullback function on multicurves. Corollary 7.2 in [27] suggests an analytic method for proving that there is a finite global attractor by looking at contracting properties of the map on moduli space, though it should be noted that these methods won't apply to the example present in this paper because of the mixture of attracting and repelling fixed points. Furthermore, when there are four points or more points in the postcritical set, it is shown that there is a finite number of completely invariant multicurves.

There are relatively few explicit computations identifying the finite global attractors of the pullback function. It is proven in [27] that the pullback function of the rabbit polynomial has a finite global attractor which is a cycle of length 3. The pullback function for  $z^2 \pm i$  is eventually trivial, as is the pullback function for  $z^2 - 0.2282 \pm 1.1151$ .

### 3 General facts in the case $|P_f| = 4$

Up to this point, we have dealt with Thurston maps with any number of points in the postcritical set. The end goal of this thesis is to analyze the specific Thurston map  $f(z) = \frac{3z^2}{2z^3+1}$  having four postcritical points, but in this section we simply assume that  $f$  is a Thurston map with  $|P_f| = 4$ . Recall that a multicurve in  $\widehat{\mathbb{C}} \setminus P_f$  is a finite set of nonperipheral non-nullhomotopic disjoint simple closed curves, and since each component of the multicurve must bound two points of  $P_f$  on either side, every multicurve when  $P_f$  contains four points has only one component. Thus, multicurves in this context are curves, and this whole section is devoted to showing how these curves can be conveniently encoded using a variety of familiar objects such as points in the Weil-Petersson completion of  $\mathcal{T}_f$ , extended rational numbers  $\overline{\mathbb{Q}} := \mathbb{Q} \cup \{1/0\}$ , or certain words in the free group on two generators. As will be shown later, there is a geometrically meaningful way to define the

rational slope of a curve in the four-holed sphere; we leave this discussion for a Section 7 if only to highlight its logical independence from the present discussion and avoid confusing notation.

Suppose that the postcritical set of a Thurston map  $f$  is given by  $P_f = \{z_0, z_1, z_2, z_3\}$  and define the subset  $\Theta \subset P_f$  to be  $\Theta = \{z_1, z_2, z_3\}$ . The standard map  $\mathbb{H} \rightarrow \widehat{\mathbb{C}} \setminus \{1, \omega, \bar{\omega}\}$  on the left side of Figure 1 is produced by first defining it on an ideal triangle in  $\mathbb{H}$  with vertices at  $0, 1$ , and  $\infty$  to the unit disk in  $\mathbb{C}$  so that  $(0, 1, \infty)$  map to  $(\bar{\omega}, 1, \omega)$ . Extend the domain of this map by reflection to all of  $\mathbb{H}$ . This defines a cover

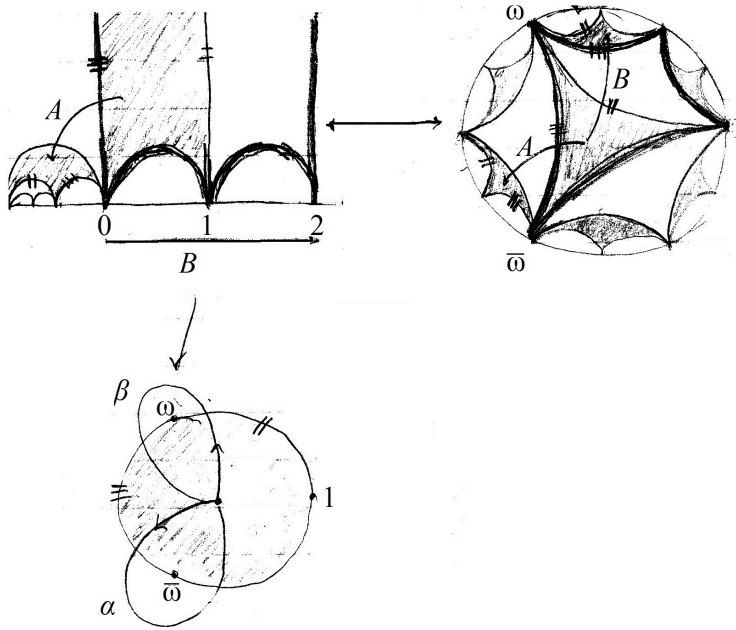


Figure 1: Modular map used to define  $\pi$

$\mathbb{H} \rightarrow \widehat{\mathbb{C}} \setminus \{1, \omega, \bar{\omega}\}$ , so postcompose this projection with the unique Möbius transformation that maps  $(1, \omega, \bar{\omega})$  to  $(z_1, z_2, z_3)$  in an order-preserving way and call the resulting map  $\pi : \mathbb{H} \rightarrow \widehat{\mathbb{C}} \setminus \{z_1, z_2, z_3\}$ . Fix the fundamental domain of the deck group of  $\pi$  to be the ideal quadrilateral with vertices at  $0, 1, 2$  and  $\infty$  where the quadrilateral is half-closed in the sense that it contains the arcs connecting  $0$  to  $1$  and  $\infty$ , but it doesn't contain the arcs connecting  $2$  to  $1$  to  $\infty$ . The set  $\pi^{-1}(z_0)$  intersects this fundamental domain at precisely one point  $\tau_0$ , and we establish this point to be the basepoint of

the cover  $\pi : (\mathbb{H}, \tau_0) \rightarrow (\widehat{\mathbb{C}} \setminus \{z_1, z_2, z_3\}, z_0)$ .

The deck group of  $\pi$  is a well-known subgroup of the modular group, and by fixing a common choice of generators of this group, there is a natural procedure to encode curves in  $\widehat{\mathbb{C}} \setminus P_f$ . The following theory is very classical and discussed in [18]. Denote by  $\mathrm{SL}_2(\mathbb{Z})$  the special linear group of  $2 \times 2$  matrices with integer coefficients, and denote by  $\mathrm{PSL}_2(\mathbb{Z})$  the quotient of  $\mathrm{SL}_2(\mathbb{Z})$  by  $\langle -I \rangle$  where  $I$  denotes the identity matrix. The group  $\mathrm{PSL}_2(\mathbb{Z})$  acts by orientation-preserving isometry on the upper halfplane if we identify the group element  $\begin{bmatrix} a & b \\ c & d \end{bmatrix} \in \mathrm{PSL}_2(\mathbb{Z})$  with the Möbius transformation  $z \mapsto \frac{az+b}{cz+d}$ . The level two congruence subgroup  $\Gamma(2) < \mathrm{SL}_2(\mathbb{Z})$  is defined to be kernel of the obvious projection  $\mathrm{SL}_2(\mathbb{Z}) \rightarrow \mathrm{SL}_2(\mathbb{Z}/2\mathbb{Z})$ , and the projectivized level two congruence subgroup is  $\mathrm{PI}\Gamma(2) := \Gamma(2)/\langle -I \rangle$  where  $I$  denotes the identity matrix. From the definition, it is immediately clear that

$$\Gamma(2) = \left\{ \begin{bmatrix} a & b \\ c & d \end{bmatrix} : a \equiv d \equiv 1, b \equiv c \equiv 0, ad - bc = 1 \right\}.$$

It is also apparent that  $\mathrm{PI}\Gamma(2)$  is the deck group for the universal cover  $\pi$ , and it is known that  $\mathrm{PI}\Gamma(2) = \langle A, B \rangle$  where  $A = \begin{bmatrix} 1 & 0 \\ -2 & 1 \end{bmatrix}$ ,  $B = \begin{bmatrix} 1 & 2 \\ 0 & 1 \end{bmatrix}$ . It should be noted that  $\mathrm{PSL}_2(\mathbb{Z})$  can act on the unit disk by conjugating elements with the unique orientation preserving Möbius transformation that maps the ordered set  $(0, 1, 2)$  to  $(\bar{\omega}, 1, \omega)$ .

Since  $A$  and  $B$  generate the deck group, standard covering space theory gives a natural way to produce generators of the fundamental group  $\pi_1(\widehat{\mathbb{C}} \setminus \{z_1, z_2, z_3\}, z_0)$ . Specifically, choose an arc in the universal cover whose starting point is  $\tau_0$  and whose endpoint is  $A(\tau_0)$ . In like manner, choose oriented arcs connecting  $\tau_0$  to  $B(\tau_0)$  and  $B^{-1}A^{-1}(\tau_0)$  (where  $A^{-1}$  acts first). Pushing these three arcs down by  $\pi$  yield three loops  $\alpha, \beta$ , and  $\gamma$  respectively based at  $z_0$ . Note that  $\alpha$  bounds a singly-punctured disk and a doubly-punctured disk. Orient  $\alpha$  by declaring that the single puncture lies on the left side of  $\alpha$ , and carry out the same procedure for  $\beta$  and  $\gamma$ . Note that  $\alpha, \beta, \gamma$  generate the fundamental group. Since the three-holed sphere is homotopy equivalent to the wedge of two circles, we have

$$\pi_1(\widehat{\mathbb{C}} \setminus \{z_1, z_2, z_3\}, z_0) = \langle \alpha, \beta \rangle = \langle \alpha, \beta, \gamma \mid \beta\alpha\gamma \rangle$$

The point push of  $z_0$  along a curve was defined in the proof of Theorem 2.4. Fact 4.7 of [13] describes precisely how to write a point push along a positively-oriented simple loop as a composition of a left and a right Dehn twist, and in the setting  $|P_f| = 4$ , the left Dehn twist is evidently trivial. One can show that point pushing  $z_0$  along the loops  $\alpha, \beta, \gamma$  in the positive

direction yield three right Dehn twists  $T_\alpha, T_\beta, T_\gamma$  respectively that generate  $\text{PMCG}(\widehat{\mathbb{C}}, P_f)$ .

We are finally in a position to identify rational boundary points of  $\mathbb{H}$  with curves in  $\widehat{\mathbb{C}} \setminus P_f$ . In the special case when  $|P_f| = 4$ , the Weil-Petersson completion is the set  $\mathbb{H} \cup \overline{\mathbb{Q}}$  equipped with the horoball topology [31], and as we will show, the even continued fraction expansions of these rational numbers can be transformed by some algorithm to compute the extended Thurston's pullback map on the boundary. Identify  $\frac{p}{q} \in \overline{\mathbb{Q}}$  with the element  $[\frac{p}{q}]$  of the projective line over the vector space  $\mathbb{Q}^2$  which we denote by  $P\mathbb{Q}^2$ . Then action of  $\text{PG}(2)$  on  $\overline{\mathbb{Q}}$  is simply the induced action of  $\Gamma(2)$  on this projective line. An orbit transversal of the action is the set  $\{\frac{0}{1}, \frac{1}{0}, -\frac{1}{1}\}$ . Note that  $\frac{0}{1}, \frac{1}{0}$ , and  $-\frac{1}{1}$  are fixed by  $A, B$ , and  $B^{-1}A^{-1}$  respectively, again thought of as a left action. The stabilizer of some point  $\frac{p}{q}$  is the set of group elements of the form  $w^{-1}v^n w$  where  $w \in \text{PG}(2)$  with  $w \cdot \frac{p}{q} \in \{\frac{0}{1}, \frac{1}{0}, -\frac{1}{1}\}$ ,  $n$  an integer, and  $v$  the unique element of  $\{A, B, B^{-1}A^{-1}\}$  that fixes  $w \cdot \frac{p}{q}$ . The union

$$\bigcup_{\frac{p}{q} \in \overline{\mathbb{Q}}} \text{Stab}_{\text{PG}(2)}\left(\frac{p}{q}\right)$$

is defined to be the set of *parabolic elements* of  $\text{PG}(2)$ . Equivalently, an element  $C \in \text{PG}(2)$  is parabolic if  $(\text{trace}(C))^2 = 4$ . We define the (unoriented) curve in  $\widehat{\mathbb{C}} \setminus P_f$  that corresponds to  $\frac{p}{q}$  to be the core curve of the Dehn twist that comes from point pushing  $z_0$  in the positive direction along the loop in the fundamental group that corresponds to  $w^{-1}vw$ . For example,  $\frac{9}{5}$  is fixed by the parabolic element  $BA^2(AB)A^{-2}B^{-1} \in \text{PG}(2)$  acting from the left which corresponds to the Dehn twist which arises by pushing  $z_0$  along the path  $\beta^{-1}\alpha^{-2}\beta\alpha\alpha^2\beta$  in the positive direction. Several matters related to this procedure will be discussed soon, but first we examine how one might compute two pieces of data that describe  $\text{Stab}_{\text{PG}(2)}(\frac{p}{q})$ : the element of the orbit transversal  $\frac{r}{s}$  that lies in the orbit of  $\frac{p}{q}$ , and an essentially unique word  $w$  so that  $w \cdot \frac{r}{s} = \frac{p}{q}$ . It is evident that  $\text{Stab}_{\text{PG}(2)}(\frac{p}{q}) = w \text{Stab}_{\text{PG}(2)}(\frac{r}{s}) w^{-1}$  where depending on the circumstances,  $\text{Stab}_{\text{PG}(2)}(\frac{r}{s})$  is the infinite cyclic group generated by  $A, B$ , or  $B^{-1}A^{-1}$ .

We will use an algorithm for finding an even continued fraction expansion of a rational number  $\frac{p}{q}$  which is closely related to the standard development in [18]. To demonstrate that the algorithm has a finite number of steps we define the naive rational height of  $\frac{p}{q}$  to be  $\max(|p|, |q|)$ . Each iteration of the algorithm begins by determining where  $\frac{p}{q}$  lies in relation to  $-1, 0$ , and  $1$ . Depending on this location, the algorithm dictates the application



of the unique element from the list  $A, A^{-1}, B, B^{-1}$  that strictly decreases the naive rational height  $\frac{p}{q}$  (except when  $\frac{p}{q} = \frac{1}{1}$  in which case the height is preserved). This element is recorded in a string as output and the whole procedure is repeated on the fraction with decreased naive rational height until some iterate lands in  $\{\frac{0}{1}, \frac{1}{0}, -\frac{1}{1}\}$ .

The input for the machine is a rational number  $\frac{p}{q}$  and the output is an element of  $\{\frac{0}{1}, \frac{1}{0}, -\frac{1}{1}\}$  and a string written in the symbols  $A, A^{-1}, B, B^{-1}$ . Let  $p_0 := p$ ,  $q_0 := q$  and let  $k = 0$  and  $w$  be the empty string. Start at the beginning state of the machine.

Depending on which interval or singleton contains  $\frac{p_k}{q_k}$ , follow one of the seven outbound arrows to a new state. If this new state has two concentric circles, append the expression inside the circles to the right of  $w$  and terminate the algorithm. If the new state does not have two concentric circles, use the following rules to compute the value of  $\frac{p_{k+1}}{q_{k+1}}$  and determine what character to append to the right of the output string  $w$ :

- If  $\frac{p_k}{q_k} \in (-\infty, -1)$ , set  $\frac{p_{k+1}}{q_{k+1}} := B \cdot \frac{p_k}{q_k}$ , and append  $B^{-1}$ .
- If  $\frac{p_k}{q_k} \in (-1, 0)$ , set  $\frac{p_{k+1}}{q_{k+1}} := A^{-1} \cdot \frac{p_k}{q_k}$ , and append  $A$ .
- If  $\frac{p_k}{q_k} \in (0, 1]$ , set  $\frac{p_{k+1}}{q_{k+1}} := A \cdot \frac{p_k}{q_k}$ , and append  $A^{-1}$ .
- If  $\frac{p_k}{q_k} \in (1, \infty)$ , set  $\frac{p_{k+1}}{q_{k+1}} := B^{-1} \cdot \frac{p_k}{q_k}$ , and append  $B$ .

Increment  $k$  and repeat the process as described above in this paragraph until the process terminates. The algorithm that was just described records the word  $w \in \text{PG}(2)$ , but the machine depicted in Figure 2 records the corresponding continued fraction notation. The continued fraction notation  $[a_0; a_1; a_2; \dots; a_n]$ ,  $a_i \in \mathbb{Z}$  is interpreted differently depending on the value of  $a_n$ . From an examination of Figure 2, one sees that if  $a_n = \frac{0}{1}$  then  $n \neq 1$ . If  $a_n = \frac{0}{1}$  and  $n \geq 2$ , then

$$[a_0; a_1; a_2; \dots; a_n] = a_0 + \frac{1}{a_1 + \frac{1}{a_2 + \frac{1}{\ddots + \frac{1}{a_{n-2}}}}}$$

Next, if  $a_n = \frac{1}{0}$ ,

$$[a_0; a_1; a_2; \dots; a_n] = a_0 + \frac{1}{a_1 + \frac{1}{a_2 + \frac{1}{\ddots + \frac{1}{a_{n-1}}}}}$$

For all other  $a_n$ , one has

$$[a_0; a_1; a_2; \dots; a_n] = a_0 + \frac{1}{a_1 + \frac{1}{a_2 + \frac{1}{\ddots + \frac{1}{a_n}}}}$$

For example,

$$\frac{7}{12} = A^{-1} \cdot -\frac{7}{2} = A^{-1}B^{-1} \cdot -\frac{3}{2} = A^{-1}B^{-1}B^{-1} \cdot \frac{1}{2} = A^{-1}B^{-1}B^{-1}A^{-1} \cdot \frac{1}{0},$$

and the machine yields the following continued fraction expansion:

$$\frac{7}{12} = [0; 2; -2 - 2; 2; \frac{1}{0}] = 0 + \frac{1}{2 + \frac{1}{-4 + \frac{1}{\frac{1}{2}}}}$$

For any fixed  $* \in \overline{\mathbb{Q}}$  there are infinitely many reduced words  $w \in \text{PF}(2)$  so that  $w.* = \frac{p}{q}$ , e.g.  $BA^n \cdot \frac{0}{1} = \frac{2}{1}$  for all integers  $n$ . This is problematic because we would like to uniquely identify an element of  $\overline{\mathbb{Q}}$  with an element of  $\text{PF}(2)$ . Fortunately, the algorithm presented above produces a word  $w$  with the property that any other  $w'$  so that  $w'.* = \frac{p}{q}$  must be less optimal in the sense that it contains  $w$  as a subword (ignoring the trivial differences that arise from the fact that  $A \cdot \frac{1}{1} = B^{-1} \cdot \frac{1}{1}$ ). For example, suppose that  $\frac{p}{q} = w \cdot \frac{0}{1}$  and that  $\frac{p}{q} = w' \cdot \frac{0}{1}$  as well. Then if  $w \cdot \frac{0}{1} = w' \cdot \frac{0}{1}$ , we know  $(w')^{-1}w \cdot \frac{0}{1} = \frac{0}{1}$  which means that  $(w')^{-1}w$  lies in the maximal parabolic subgroup which fixes  $\frac{0}{1}$ . Thus  $(w')^{-1}w = A^n$  for some  $n \in \mathbb{Z}$ , and from a quick examination of the algorithm, one can see that  $w$  is a subword of  $w'$ .

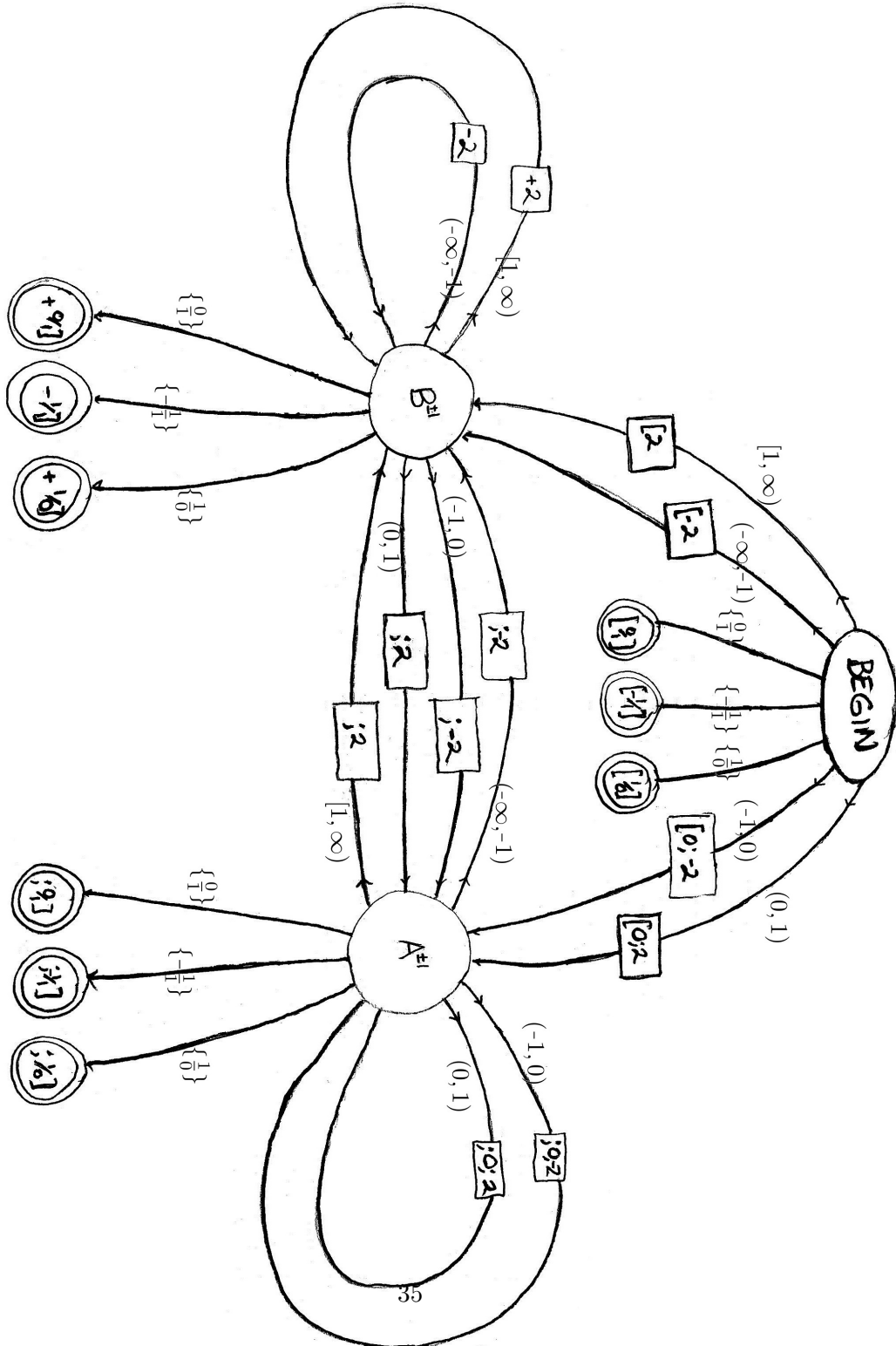


Figure 2: Machine to compute continued fraction expansion

We conclude this section by discussing the actions of  $\text{PMCG}(\widehat{\mathbb{C}}, P_f)$  and  $\pi_1(\widehat{\mathbb{C}} \setminus \Theta, z_0)$  on the set of rational numbers and we also consider some examples. First we summarize the identifications of the groups mentioned above. It is assumed that  $\text{PG}(2)$  is a left action, namely, matrix multiplication. Though one might expect  $\text{PMCG}(\widehat{\mathbb{C}}, P_f)$  to act on the left because of the nature of function composition, we wish to make it a right action because the Birman isomorphism naturally identifies it with the fundamental group which naturally acts on the right. Some notation is then necessary so that  $\text{PMCG}(\widehat{\mathbb{C}}, P_f)$  can be written as a right action. By the notation  $f \cdot g$  we mean  $g \circ f$ . The Birman isomorphism from  $\pi_1(\widehat{\mathbb{C}} \setminus \Theta, z_0)$  to  $\text{PMCG}(\widehat{\mathbb{C}}, P_f)$  is defined on generators as follows:

$$\alpha \mapsto T_\alpha$$

$$\beta \mapsto T_\beta.$$

The relationship between these groups and  $\text{PG}(2)$  involves cumbersome terminology and a little subtlety since these two groups act on the right and  $\text{PG}(2)$  acts on the left. Let  $G$  and  $H$  be groups. An *antihomomorphism* from  $G$  to  $H$  is a function  $\phi : G \rightarrow H$  so that  $\phi(g_1g_2) = \phi(g_2)\phi(g_1)$  for all  $g_1, g_2 \in G$ . The *opposite* of a homomorphism  $\phi : G \rightarrow H$  is the function  $\tilde{\phi} : G \rightarrow H$  defined by  $\tilde{\phi}(g_1g_2) = \phi(g_2)\phi(g_1)$ . This is evidently an antihomomorphism. The composition of two antihomomorphisms is a homomorphism. The anti-isomorphism between  $\text{PG}(2)$  and  $\pi_1(\widehat{\mathbb{C}} \setminus \Theta, z_0)$  is defined by postcomposing the homomorphism defined below by the opposite of the identity homomorphism on the fundamental group:

$$A \mapsto \alpha$$

$$B \mapsto \beta.$$

Thus, the deck group  $\text{PG}(2)$  acts on the left, and the fundamental group and pure mapping class group act on the right. The isomorphisms and anti-isomorphism described above yield isomorphic group actions on  $\overline{\mathbb{Q}}$  in all three cases. One can see that the element of the deck group  $B^{-1}A^2BA^{-1} \in \text{PG}(2)$ , the element of the pure mapping class group  $T_\alpha^{-1} \cdot T_\beta \cdot T_\alpha^2 \cdot T_\beta^{-1} \in \text{PMCG}(\widehat{\mathbb{C}}, P_f)$ , and the element of the fundamental group  $\alpha^{-1}\beta\alpha^2\beta^{-1} \in$

$\pi_1(\widehat{\mathbb{C}} \setminus \Theta, z_0)$  are all identified, and furthermore:

$$\begin{aligned} -\frac{41}{18} &= B^{-1}A^2BA^{-1} \cdot \frac{1}{0} \\ &= \frac{1}{0} \cdot T_\alpha^{-1} \cdot T_\beta \cdot T_\alpha^2 \cdot T_\beta^{-1} \\ &= \frac{1}{0} \cdot \alpha^{-1} \beta \alpha^2 \beta^{-1} \end{aligned}$$

These identifications can be used to produce a very natural right action of  $\pi_1(\widehat{\mathbb{C}} \setminus \Theta, z_0)$  on curves in  $\widehat{\mathbb{C}} \setminus P_f$  that makes it far easier to find curves corresponding to particular  $\frac{p}{q}$ . Let  $[\gamma] \in \mathcal{C}_f$ ,  $[w] \in \pi_1(\widehat{\mathbb{C}} \setminus \Theta, z_0)$ , and let  $[\gamma].[w]$  be the free homotopy class of curves found by observing the effect on  $\gamma$  of pushing the point  $z_0$  along  $w$ . This action on curves respects all the identifications, isomorphisms, and anti-isomorphisms defined before. Practically speaking then, to locate the curve corresponding to  $\frac{p}{q}$ , one should identify the curves in  $\widehat{\mathbb{C}} \setminus P_f$  corresponding to  $\{\frac{0}{1}, \frac{1}{0}, -\frac{1}{1}\}$ , and then observe the effect on the appropriate curve of pushing  $z_0$  along the element of the fundamental group corresponding to  $w$  as found in the continued fraction expansion algorithm above. We demonstrate below how one would find the curve corresponding to  $\frac{2}{1}$  by observing the effect on  $\frac{0}{1}$  of pushing  $z_0$  along  $\beta$ . In Figure 3, the diagram on the left exhibits the three generators of the fundamental group, and the diagram on the right exhibits the three curves corresponding to  $\{\frac{0}{1}, \frac{1}{0}, -\frac{1}{1}\}$ . Figure 3 exhibits the curve corresponding to  $\frac{2}{1}$  which is found by pushing the curve corresponding to  $\frac{0}{1}$  by  $\beta$ .

## 4 Analysis of a specific example: $f(z) = \frac{3z^2}{2z^3+1}$

We now turn our attention to the analysis of a specific Thurston map  $f(z) = \frac{3z^2}{2z^3+1}$ . Properties of  $f$  on the dynamical plane are first studied, and then a study is made of the moduli space map. Finally, the wreath recursions corresponding to both of these maps

### 4.1 The Dynamical Plane of $f$

The postcritical set is  $P_f = \{0, 1, \omega, \bar{\omega}\}$ , and each one of these four points is also a critical point, which means  $f$  is in the class of nearly Euclidean Thurston map studied in [10]. Recalling the notation from earlier sections, let  $\Theta = \{1, \omega, \bar{\omega}\}$ . The function  $f$  has the following critical portrait:

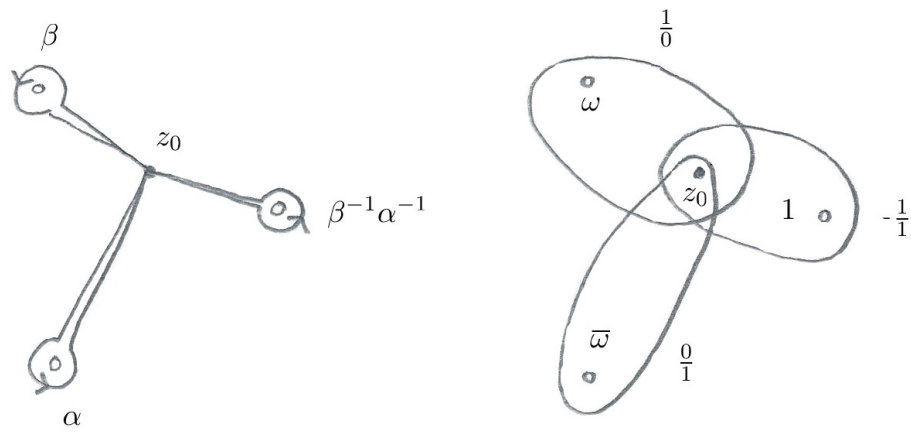


Figure 3: Generators of fundamental group; three curves corresponding to points in orbit transversal

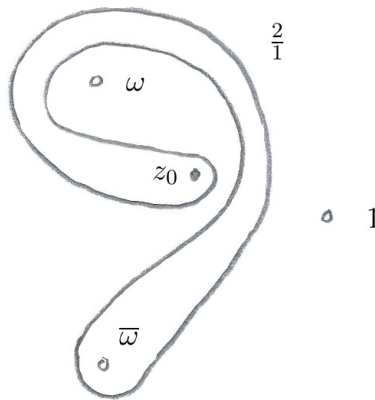


Figure 4: The curve corresponding to  $\frac{2}{1}$  found by pushing the curve corresponding to  $\frac{0}{1}$  by  $\beta$

$$\begin{array}{ccc} \omega & 0 & 1 \\ \times 2 \left( \begin{array}{c} \curvearrowright \\ \curvearrowleft \end{array} \right) \times 2 & \times 2 \curvearrowright & \times 2 \curvearrowright \\ \bar{\omega} & & \end{array}$$

One useful property of  $f$  is that it has a very convenient affine model. Consider the two equilateral triangles in Figure 5 as subsets of  $\mathbb{R}^2$  where both outer equilateral triangles have vertices at  $(0,0)$ ,  $(2,0)$ , and  $(1,\sqrt{3})$ . Identify the marked edges in Figure 5 to form tetrahedra on both left and

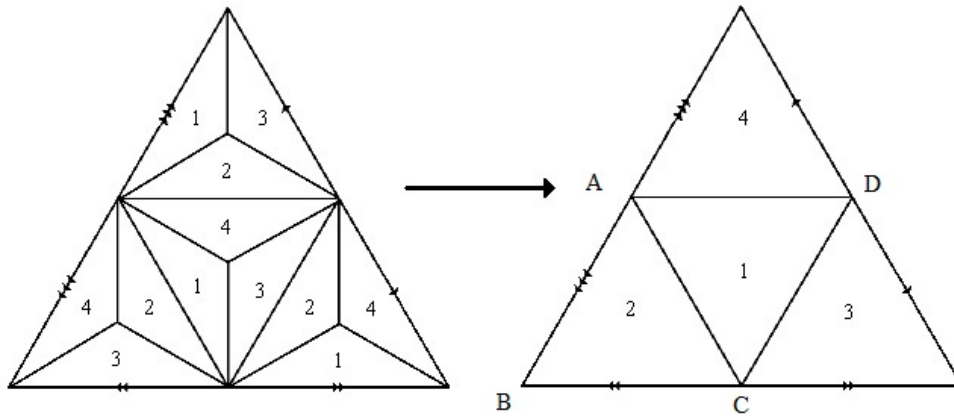


Figure 5: Affine model of  $f$

right. Define the affine model by first mapping the triangle from the domain with vertices  $(1,0)$  and  $(2,0)$  and label 1 to the triangle in the range labeled 1 by the unique affine map that respects the labels of adjacent triangles. Extend this map by reflection over the whole tetrahedron to produce a three to one map from the tetrahedron to itself with four simple critical points. To prove that this is actually a model of  $f$ , explicitly embed this tetrahedron into  $\mathbb{R}^3$  isometrically by mapping:

$$A \mapsto (0, 0, -\frac{\sqrt{18}}{3}).$$

$$B \mapsto (-\frac{1}{2}, \frac{\sqrt{3}}{2}, 0)$$

$$C \mapsto (1, 0, 0)$$

$$D \mapsto \left(-\frac{1}{2}, -\frac{\sqrt{3}}{2}, 0\right)$$

Circumscribe this regular tetrahedron by a sphere of radius  $\sqrt{\frac{9}{8}}$  as in Figure 6. The stereographic projection from this sphere with north pole  $N$  at

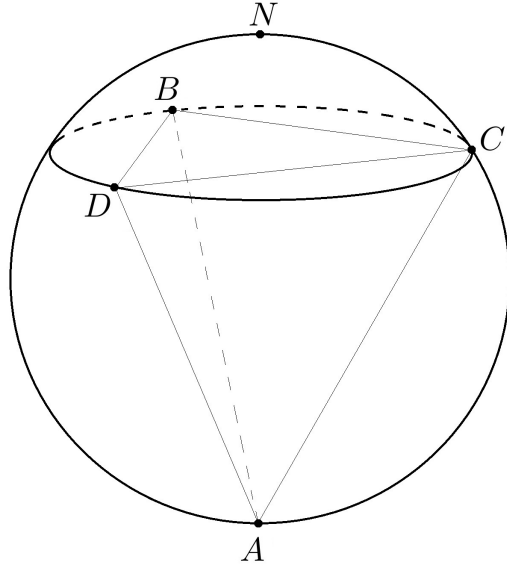


Figure 6: Circumscribed regular tetrahedron

$(0, 0, \frac{1}{\sqrt{2}})$  onto the plane  $\{(x, y, z) : z = 0\}$  is conformal. Identify this plane with the complex plane by the mapping  $(x, y, z) \mapsto x + iy$ . Then one can conformally map the tetrahedron onto  $\mathbb{C}$  by first radially projecting onto the circumsphere and then mapping onto  $\mathbb{C}$  by the stereographic projection. Conjugating the affine model for  $f$  by this composition will up to homotopy yield a rational function  $\mathbb{C} \rightarrow \mathbb{C}$  that is conformal except at  $P_f$  where the map has local degree 2. An argument has already been presented for the uniqueness of degree 3 rational functions with post-critical set  $P_f$  with the same critical portrait as  $f$ . Thus  $f$  arises as a finite subdivision rule of the sphere, though it has unbounded valence.

In [8], it is shown that  $f$  is a very important example. The authors proved that the Thurston pullback map  $\sigma_f$  is surjective and that it has a fixed point of local degree 2. Up to some non-dynamical equivalence, this is the only known example where  $\sigma_f$  is surjective. Xavier Buff generated



an image of this function using the method described in Section 2.4, and from simple observation, it seems that the points on the boundary map to one of three points under iteration of the extended Thurston pullback map. Thus, using ideas from Selinger's work, there is reason to believe that under iterated preimage of  $f$ , all curves eventually land in the homotopy class of one of three curves. This is actually the case, and we will prove this fact and demonstrate its usefulness in distinguishing Thurston classes.

Another feature of  $f$  is that it arises as a mating [23] of the two cubic polynomials  $P$  and  $Q$  where  $P$  has two finite fixed critical points, and  $Q$  has two finite critical points that are interchanged in a two-cycle. This is a consequence of the fact from Section 5 that the curve corresponding to  $-\frac{1}{1}$  in  $\widehat{\mathbb{C}} \setminus P_f$  pulls back to itself in an orientation preserving way, and since  $f$  is hyperbolic, it is a mating with equator given by this invariant curve. Note that the polynomials  $P$  and  $Q$  are unique up to affine conjugacy. This implies that  $P$  and  $Q$  commute with the map that interchanges the two critical points. In general one should expect two ways of identifying the circles at infinity for two cubic polynomials, but the properties just mentioned imply that  $f$  is the only possible mating.

## 4.2 The Correspondence on Moduli Space

A feature of  $f$  that was introduced and exploited in [8] is the existence of the correspondence on moduli space mentioned in Section 2.1. Note that  $Y$  has degree 4, and it has the following portrait since  $Y'(z) = \frac{2(z^3-1)^2}{(2z^3+1)^2}$ . Some elementary considerations prove that  $Y$  is the unique degree 4 rational function that fixes each of  $1, \omega$ , and  $\bar{\omega}$  with local degree 3. Suppose that  $W$  is another such degree 4 rational function. Then  $\deg(Y - W) \leq 8$ , but  $Y - W$  has 9 zeros counted with multiplicity and must therefore be identically 0. It is also worth noting that  $Y$  has some remarkable properties as a dynamical system, though we won't be studying it as such. The critical portrait of  $Y$  is as follows:

$$\omega \curvearrowright \times 3 \quad 1 \curvearrowright \times 3 \quad \bar{\omega} \curvearrowright \times 3$$

It is the map used by McMullen [22] to give a generally convergent iterative algorithm for solving cubic equations. Also, using the uniqueness property described above, one can easily prove that the automorphism group of this function is isomorphic to the symmetric group on three symbols.

We now produce an affine model of  $Y$  using triangles, as depicted in

Figure 7. The upper left object in the diagram is the equilateral triangle with vertices  $-2, 1 + \frac{3}{2}i, 1 - \frac{3}{2}i$  doubled over its boundary. The lower left object is the equilateral triangle with vertices  $1, \omega, \bar{\omega}$  doubled over its boundary. Thus the domain is the union of eight equilateral triangles with disjoint interior, where the three outer triangles on the front face are shaded as well as the central triangle on the back face. The range is the union of two equilateral triangles with disjoint interior, where the back face is shaded. The affine model for  $Y$  which we denote by  $Y^\Delta$  is constructed by mapping the unshaded triangle on the front face of the domain to the front face of the range via the identity. Extend this map by reflection so that it is defined on all eight triangles in the domain. This produces a degree 4 map that is conformal except at the vertices  $1, \omega, \bar{\omega}$  which all map by degree 3.

Though it certainly exists in theory, the unique Riemann map  $(\Delta, \{1, \omega, \bar{\omega}\}) \rightarrow (\mathbb{D}, \{1, \omega, \bar{\omega}\})$  can be defined explicitly for the Euclidean triangle in  $\mathbb{C}$  which has vertices  $1, \omega$ , and  $\bar{\omega}$ . It is defined as a composition of a series of conformal maps. First apply the translation  $z \mapsto z + \frac{1}{2} + \frac{\sqrt{3}}{2}i$ , then rotate by  $z \mapsto e^{-\frac{\pi i}{6}}$ , and then scale by  $z \mapsto \frac{\beta(\frac{1}{3}, \frac{1}{3})}{\sqrt{3}}z$  where  $\beta(\frac{1}{3}, \frac{1}{3}) = \frac{\Gamma(\frac{1}{3})\Gamma(\frac{1}{3})}{\Gamma(\frac{2}{3})}$ . Under these transformations, the original triangle maps to an equilateral triangle in the first quadrant of side length  $\beta(\frac{1}{3}, \frac{1}{3})$  with one vertex at the origin and a second vertex at  $\beta(\frac{1}{3}, \frac{1}{3}) + 0i$ . Then under preimage of the Schwarz-Christoffel transformation  $z \mapsto \int_0^z w^{-2/3}(1-w)^{-2/3}dw$ , this latter triangle is mapped to the upper half plane with vertices  $0, 1$  and  $\infty$ . Then the Möbius transformation  $z \mapsto \frac{z\omega+1}{z\bar{\omega}+1}$  maps the upper halfplane to the unit disk where  $0$  maps to  $1$ ,  $1$  maps to  $\omega$ , and  $\infty$  maps to  $\bar{\omega}$ . This Riemann map is evidently unique, because precomposition by the inverse of any other such Riemann map yields an isomorphism of  $\mathbb{D}$  that fixes three points in the boundary.

Now we define the other maps in Figure 7. The map  $A_{ran}$  is the unique isomorphism defined by applying Schwarz reflection to the Riemann map constructed above, where  $A_{ran}$  evidently fixes the points  $1, \omega, \bar{\omega}$ . With a slight adjustment to the work done above, one constructs the unique Riemann map from the front face of the domain of  $Y^\Delta$  to the unit disk in  $\widehat{\mathbb{C}}$  that fixes the points  $1, \omega, \bar{\omega}$ . The map  $A_{dom}$  is the unique isomorphism defined by applying Schwarz reflection to this Riemann map. It is clear that  $A_{ran}^{-1} \circ Y^\Delta \circ A_{dom}^{-1}$  is a holomorphic map away from the points  $1, \omega, \bar{\omega}$ , and so by application of the removable singularity theorem it is a holomorphic map on  $\widehat{\mathbb{C}}$ . Since it is evidently a rational function, we conclude that  $A_{ran}^{-1} \circ Y^\Delta \circ A_{dom}^{-1} \equiv Y$  by the uniqueness of  $Y$ .

We now specialize the discussion of Section 3 to the case where  $P_f =$

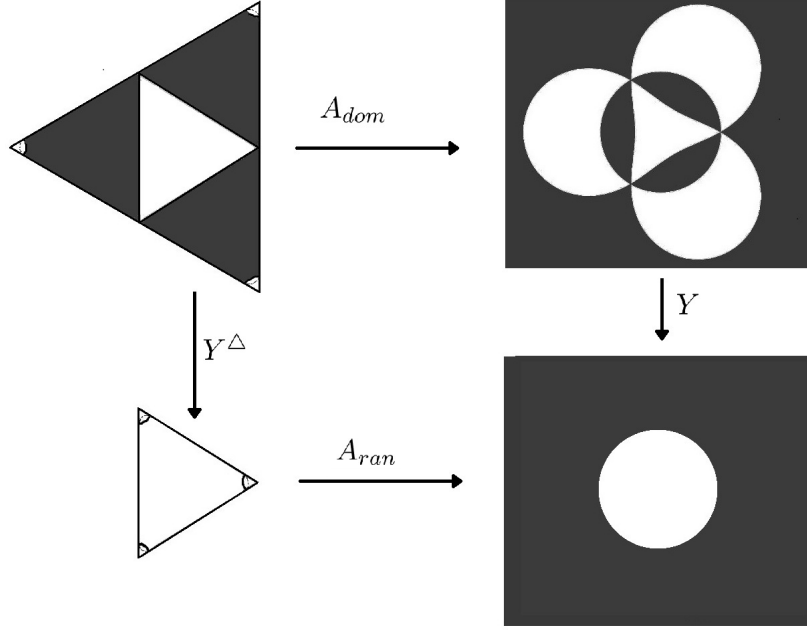


Figure 7: Isomorphisms from domain and range of affine model to  $\widehat{\mathbb{C}}$

$\{0, 1, \omega, \bar{\omega}\}$ . The first step in the process as described in Section 3 is to define a cover of  $\widehat{\mathbb{C}} \setminus \Theta$  and then postcompose by some Möbius transformation. Since the standard modular map used in that section was a cover  $(\mathbb{H}, \frac{1+\sqrt{3}i}{2}) \rightarrow (\widehat{\mathbb{C}} \setminus \Theta, 0)$ , simply use the identity Möbius transformation. Thus we have the map  $\pi$  exhibited in Figure 8 along with the standard identification with  $\mathbb{D}$  from before. The deck group is again  $\text{PG}(2) = \langle A, B \rangle$  where  $A = \begin{bmatrix} 1 & 0 \\ -2 & 1 \end{bmatrix}$ ,  $B = \begin{bmatrix} 1 & 2 \\ 0 & 1 \end{bmatrix}$ , and these generators are identified with the generators  $\alpha$  and  $\beta$  respectively of the fundamental group  $\pi_1(\widehat{\mathbb{C}} \setminus \Theta, 0)$ . These two loops are depicted in Figure 8. Pushing the point 0 in the positive direction along  $\alpha$  and  $\beta$  yield generators of  $\text{PMCG}(\widehat{\mathbb{C}}, P_f)$  which we denote by  $T_\alpha$  and  $T_\beta$  respectively.

### 4.3 The Virtual Endomorphism and Wreath Recursion on Moduli Space

There are two wreath recursions that will be associated to  $f$ : the wreath recursion on the dynamical plane and the wreath recursion on moduli space given specific choices of connecting paths. This section will present formulas

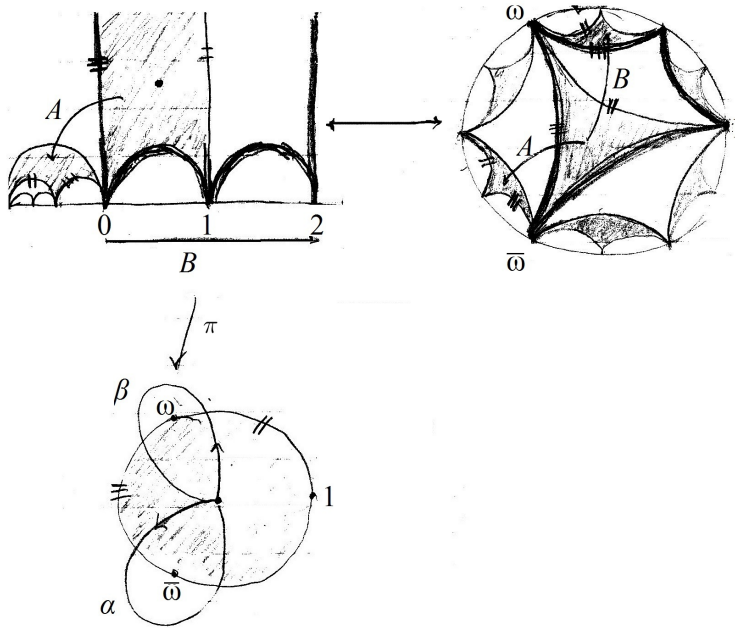


Figure 8: Specific choice of the cover  $\pi$

for the the virtual endomorphism on the fundamental group of moduli space and the wreath recursion on moduli space, as well as a discussion of algebraic contracting properties.

We now use the Reidemeister-Schreier algorithm to compute the virtual endomorphism on moduli space using the methods from Section 2.3. Using the choice of labeling of  $Y^{-1}(0)$  given in Figure 12, one can compute that the monodromy of  $Y$  is isomorphic to the alternating group on four letters. In Figure 9 we exhibit the preimage of the two generators under  $Y$  calculated using the affine model presented earlier. By adding appropriate labels to the graph in the domain of  $Y$ , we produce the Schreier graph of  $Y$  with basepoint  $z_0 = 0$  in the domain and basepoint  $Y(z_0) = 0$  in the range. The maximal subtree we choose will have vertices and edges depicted in Figure 10 by the solid lines, and the corresponding Schreier transversal is  $T = \{1, \alpha, \alpha^{-1}, \beta\}$ . From Figure 10 and the discussion in 2.3 it is evident that

$$H = \langle \beta\alpha\beta^{-1}, \beta^2\alpha^{-1}, \beta^{-1}\alpha^{-1}, \alpha^3, \alpha^{-1}\beta\alpha \rangle.$$

To define our virtual endomorphism, it is necessary to write an arbitrary  $w \in H$  as a word in the five generators of  $H$  and their inverses; the Reidemeister-Schreier rewriting process will be used, where  $S = \{\alpha, \beta\}$ . Table 1 exhibits

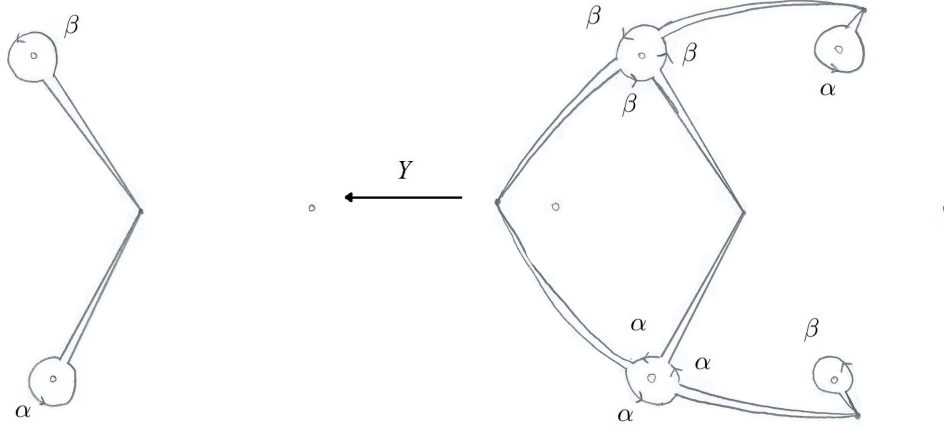


Figure 9: Lift of generators under  $Y$

$\gamma(\text{row}, \text{column})$	$\alpha$	$\alpha^{-1}$	$\beta$	$\beta^{-1}$
1	1	1	1	$\beta^{-1}\alpha^{-1}$
$\beta$	$\beta\alpha\beta^{-1}$	$\beta\alpha^{-1}\beta^{-1}$	$\beta^2\alpha^{-1}$	1
$\alpha$	$\alpha^3$	1	$\alpha\beta$	$\alpha\beta^{-2}$
$\alpha^{-1}$	1	$\alpha^{-3}$	$\alpha^{-1}\beta\alpha$	$\alpha^{-1}\beta^{-1}\alpha$

Table 1: All values of  $\gamma$  in the Reidemeister-Schreier algorithm

all necessary values of  $\gamma$ , where the left column corresponds to the first argument of  $\gamma$ , and the right column corresponds to the second. Also, recall that path multiplication was earlier defined so that for example  $\alpha\beta$  is the path obtained by traversing  $\alpha$  in the positive direction, and then  $\beta$ . The following is a sample computation to show how one would write the word  $\alpha\beta^2\alpha^{-1}\beta^{-1} \in H$  in terms of the generators of  $H$ :

$$\begin{aligned}
\alpha\beta^2\alpha^{-1}\beta^{-1} &= \gamma(1, \alpha) \cdot \gamma(\bar{\alpha}, \beta) \cdot \gamma(\overline{\alpha\beta}, \beta) \cdot \gamma(\overline{\alpha\beta^2}, \alpha^{-1}) \cdot \gamma(\overline{\alpha\beta^2\alpha^{-1}}, \beta^{-1}) \\
&= \gamma(1, \alpha) \cdot \gamma(\alpha, \beta) \cdot \gamma(1, \beta) \cdot \gamma(\beta, \alpha^{-1}) \cdot \gamma(\beta, \beta^{-1}) \\
&= 1 \cdot \alpha\beta \cdot 1 \cdot \beta\alpha^{-1}\beta^{-1} \cdot 1
\end{aligned}$$

This completes the discussion of how to lift elements of the fundamental group under  $Y$  based at 0. We now turn to computing the image of these elements under  $X(z) = z^2$ , namely we would like to compute  $\phi_f : H < \pi_1(\widehat{\mathbb{C}} \setminus \Theta, 0) \rightarrow \pi_1(\widehat{\mathbb{C}} \setminus \Theta, 0)$ , where this virtual endomorphism corresponds

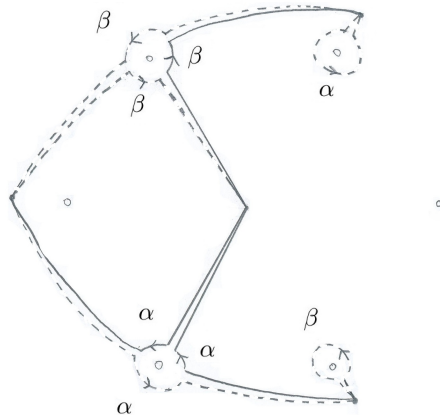


Figure 10: Choice of maximal subtree in the Schreier graph

to the virtual endomorphism on  $\text{PMCG}(\widehat{\mathbb{C}}, P_f)$  as described in Section I. For example, the lift of  $\beta\alpha\beta^{-1}$  under  $Y$  is homotopic to the loop on the left side of Figure 11, and it is actually quite easy to compute the image under  $X$ : Thus  $X(Y^{-1}(\beta\alpha\beta^{-1})[0]) = \beta$ . In fact it is easy to carry out this

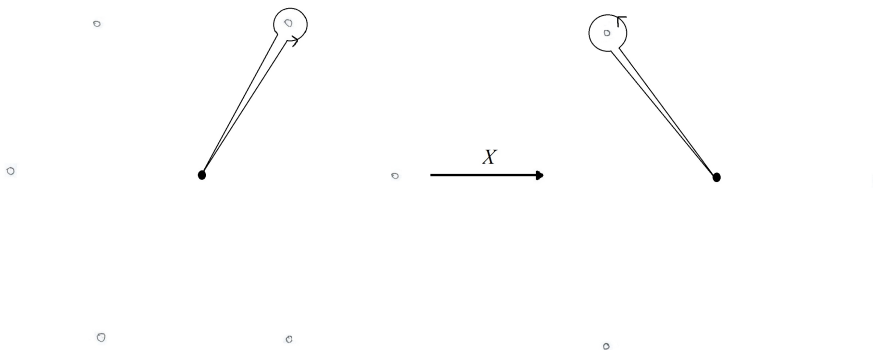


Figure 11: The image of a representative of  $Y^{-1}(\beta\alpha\beta^{-1})[0]$  under  $X$

computation for all generators of  $H$  in a similar fashion, and it can be shown that  $\phi_f$  behaves on generators as follows:

$$\begin{aligned}\beta\alpha\beta^{-1} &\mapsto \beta \\ \beta^2\alpha^{-1} &\mapsto \beta^{-1}\end{aligned}$$

$$\begin{aligned}\beta^{-1}\alpha^{-1} &\mapsto \alpha^{-1}\beta^{-1} \\ \alpha^3 &\mapsto \beta \\ \alpha^{-1}\beta\alpha &\mapsto \alpha.\end{aligned}$$

The whole process of computing  $\phi_f(w)$  for some word  $w = s_1s_2\dots s_k \in H$  where  $s_i \in S \cup S^{-1}$  can be streamlined by the diagram in Figure 12. The starting state is the one at the center of the diagram. Let  $j = 1$ , and let the output string be the empty string.

If  $s_j \in S$ , the new state is determined by following the arrow with the group element  $s_j$  in the first coordinate of the label; append the contents of the second coordinate to the right of the output string. If  $s_j \in S^{-1}$ , the new state is determined by following the arrow with  $s_j^{-1}$  in the first coordinate; append the inverse of the second coordinate to the right of the output string. Repeat the process described in this paragraph until the whole input string  $w$  is consumed. Upon completion, the output string is precisely  $\phi_f(w)$ . For example, the diagram gives that

$$\begin{aligned}\phi_f(\alpha^2\beta^{-1}\alpha^{-1}\beta^{-1}\alpha^2\beta^{-1}) &= 1 \cdot \beta \cdot \alpha^{-1} \cdot \beta^{-1} \cdot \beta \cdot \beta \cdot \beta \cdot 1 \\ &= \beta\alpha^{-1}\beta^2.\end{aligned}$$

There is a close relationship between virtual endomorphisms arising from

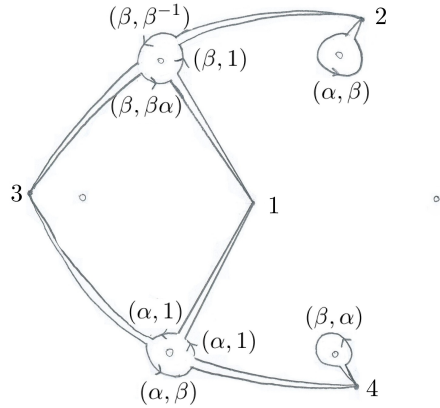


Figure 12: Machine to compute the virtual endomorphism  $\phi_f$  drawn in  $\mathcal{W}_f = \widehat{\mathcal{C}} \setminus \Theta'$

rational maps on moduli space and wreath recursions. In the case that a wreath recursion is contracting, there is a finiteness property that can be

exploited to help understand the virtual endomorphism, and the following is devoted to defining a wreath recursion on  $\pi_1(\widehat{\mathbb{C}} \setminus \Theta)$  and discussing its contracting properties. As mentioned in Section 2.4, we must make a choice of labels for the points in  $X \circ Y^{-1}(0)$  as well as a choice of connecting paths between the basepoints in  $\widehat{\mathbb{C}} \setminus \Theta$ . These paths are exhibited in Figure 13. The three small circles in Figure 13 denote the points in  $\Theta$ , and the four

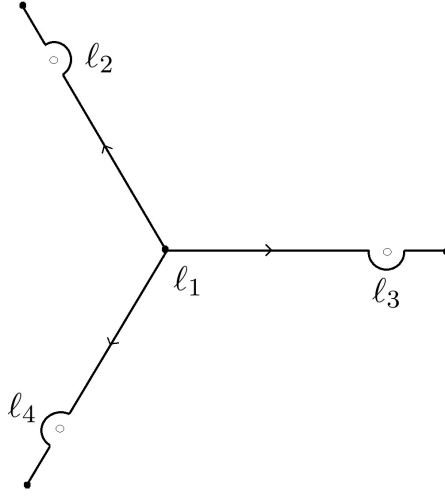


Figure 13: Connecting paths for the wreath recursion  $\Phi$  drawn in  $\widehat{\mathbb{C}} \setminus \Theta$

dots correspond to the points in  $X \circ Y^{-1}(0) = \{0, \sqrt[3]{4}, \sqrt[3]{4}\omega, \sqrt[3]{4}\bar{\omega}\}$  which are labeled 1,3,2, and 4 respectively. The connecting path  $l_1$  is the constant path at 0, and the path  $l_3$  is the path that runs from 0 to  $\sqrt[3]{4}$  along the positive real axis, except at the omitted point  $1 + 0i$  where the path goes into the lower half-plane along a small semi-circular arc. The other paths are defined as follows:  $l_2 = e^{2\pi i/3}l_3$  and  $l_4 = e^{4\pi i/3}l_3$ . Using this choice of connecting paths, we find that

$$\Phi(\beta) = \langle \langle \beta^{-1}, \beta\alpha, 1, \alpha \rangle \rangle (1 \ 2 \ 3)$$

$$\Phi(\alpha) = \langle \langle \beta\alpha, \beta, \alpha^{-1}, 1 \rangle \rangle (1 \ 3 \ 4).$$

Recall that  $(1 \ 3 \ 4)$  denotes the cycle  $1 \mapsto 3 \mapsto 4 \mapsto 1$ . We observe that the wreath recursion  $\Phi$  on  $\pi_1(\widehat{\mathbb{C}} \setminus \Theta)$  is not contracting using a straightforward computation:

$$\Phi(\beta\alpha) = \langle \langle 1, \beta, \beta\alpha, \alpha \rangle \rangle (1 \ 2 \ 4)$$



$$\Phi((\beta\alpha)^3) = \langle\langle\beta\alpha, \beta\alpha, (\beta\alpha)^3, \alpha\beta\rangle\rangle id$$

from which it is clear that

$$\Phi((\beta\alpha)^{3n}) = \langle\langle(\beta\alpha)^n, (\beta\alpha)^n, (\beta\alpha)^{3n}, (\alpha\beta)^n\rangle\rangle id.$$

Lemma 2.11.2 from [25] implies that  $\mathcal{N}$  must contain  $(\beta\alpha)^{3n}$  for all  $n$  since it must be true in this setting that  $((S \cup \mathcal{N})^2)|_{X^k} \subset \mathcal{N}$  for all  $k \in \mathbb{N}$ .

In addition to the fact that the wreath recursion on  $\pi_1(\widehat{\mathbb{C}} \setminus \Theta)$  is not contracting, it is easy to conclude that the action on the tree of preimages is not contracting. A proposition in [25, p.60] states that if a level-transitive action is contracting, then  $\rho_{\phi_f} < 1$ , where

$$\rho_{\phi_f} = \limsup_{n \rightarrow \infty} \sqrt[n]{\limsup_{g \in \text{dom} \phi_f^n, |g| \rightarrow \infty} \frac{|\phi_f^n(g)|}{|g|}}.$$

We construct a sequence  $g_i \in \langle\alpha, \beta\rangle$  to demonstrate that  $\rho_{\phi_f} = 1$ . First define  $h_i$  for  $i > 0$  as follows:  $h_1 = \beta, h_2 = \alpha^3, h_3 = \beta^9, h_4 = \alpha^{27}, \dots$ . Observe that  $\phi_f(h_i) = h_{i-1}$  for  $i > 1$  by inspection of Figure 12. Let  $g_i = (\prod_{j=1}^i h_j)(\beta\alpha)^{i^3}(\prod_{j=1}^i h_j)^{-1}$ . Then  $\phi_f^i(g_i) = (\beta\alpha)^{i^3}$  and

$$\frac{|\phi_f^i(g_i)|}{|g_i|} \approx \frac{i^3}{2i^2 + i^3} \rightarrow 1$$

#### 4.4 The Wreath Recursion on the Dynamical Plane; Covering and Hurwitz Equivalence

To compute the wreath recursion on the dynamical plane, let the basepoint be the unique real fixed point of  $f$  that lies between 0 and 1. The choice of four generators  $\alpha, \beta, \gamma$ , and  $\delta$  of  $\pi_1(\widehat{\mathbb{C}} \setminus P_f)$  is presented in Figure 14 where  $\alpha\gamma\beta\delta = e$ . A choice of connecting paths  $\ell_1, \ell_2, \ell_3$  is also made, where  $\ell_2$  is the constant path at the basepoint. The endpoints of each path  $\ell_1, \ell_2, \ell_3$  is labeled 1, 2, 3 respectively. With these choices, the wreath recursion on the dynamical plane is

$$\begin{aligned} \Phi_f(\alpha) &= \langle\langle e, e, \beta \rangle\rangle(1 \ 3) \\ \Phi_f(\beta) &= \langle\langle \beta^{-1}, e, \gamma^{-1}\delta^{-1} \rangle\rangle(1 \ 3) \\ \Phi_f(\gamma) &= \langle\langle e, \gamma, e \rangle\rangle(2 \ 3) \\ \Phi_f(\delta) &= \langle\langle \delta, e, e \rangle\rangle(1 \ 2) \end{aligned}$$

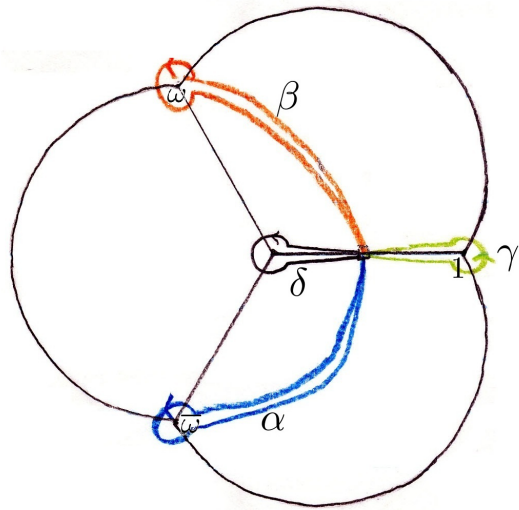
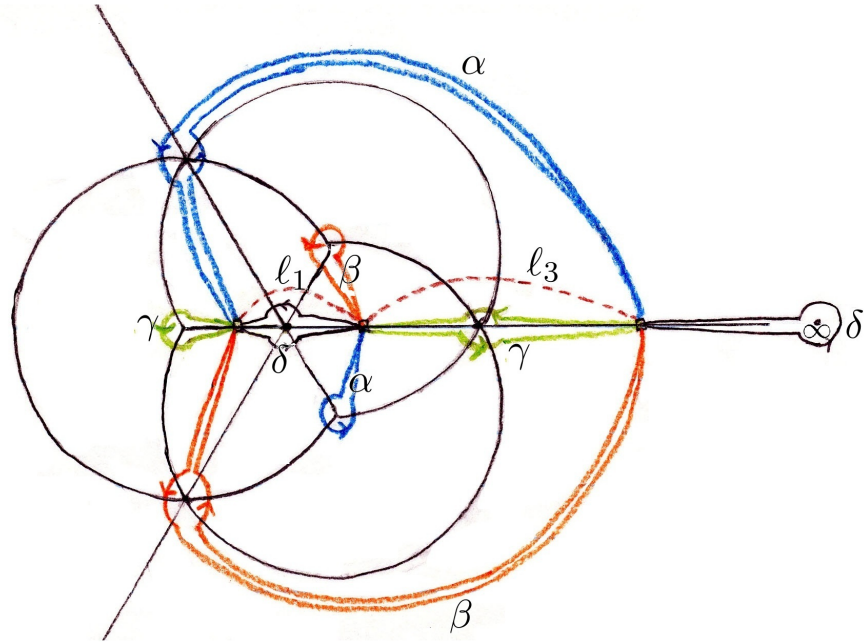


Figure 14: Choice of connecting paths and lift of generators under  $f$

The results of Koch in [17] discuss remarkable connections between the correspondence on moduli space and facts about the covering class and Hurwitz class of  $f$ . We discuss the latter objects here. Let  $f_1, f_2 : S^2 \rightarrow S^2$  be two connected degree three branched covers with critical points  $C_{f_1}, C_{f_2}$  and critical values  $V_{f_1}, V_{f_2}$  where the assumption is made that  $V_{f_1} = V_{f_2}$ . The maps  $f_1, f_2$  are said to be equivalent if there exists a homeomorphism  $h : S^2 \rightarrow S^2$  that satisfies  $f_1 = f_2 \circ h$ . Note that  $h(C_{f_1}) = (C_{f_2})$  by a local degree argument. The Hurwitz classification of such branched covers up to equivalence is given in [3], where the invariant used is the conjugacy class of monodromy representations from  $\pi_1(S^2 \setminus V_{f_1})$  into the symmetric group on three letters. These are encoded by an ordered quadruple of transpositions in the symmetric group on three letters where the product of all four components is the identity and the group generated by the transpositions is transitive. Also, these quadruples are considered up to simultaneous conjugation of all four components. For our work, the consecutive entries of the quadruple correspond to the monodromy about the elements  $\alpha, \gamma, \beta$  and  $\delta$  respectively using the generators from Figure 14. Thus, one can represent the branched covering class of the function  $f(z) = \frac{3z^2}{2z^3+1}$  by the following quadruple considered up to simultaneous conjugation of the four components:

$$((1 \ 3), (2 \ 3), (1 \ 3), (1 \ 2)).$$

One can systematically produce a list of admissible Hurwitz data representatives for all other connected degree three branched covering classes  $S^2 \rightarrow S^2$  with four simple critical points and the same critical values as  $f$ :

$$((1 \ 3), (2 \ 3), (2 \ 3), (1 \ 3))$$

$$((1 \ 3), (2 \ 3), (1 \ 2), (2 \ 3))$$

$$((2 \ 3), (2 \ 3), (1 \ 3), (1 \ 3)).$$

See [11] for formulas that predict the number of covering classes in far more general settings.

Recall the conventions on the action of pure mapping classes on equivalence classes of covers from Section 2.2. By abuse of notation let  $A$  and  $B$  represent the Dehn twist generators of  $\text{PMCG}(\widehat{\mathbb{C}}, P_f)$  coming from the identification with  $\text{PI}(2)$ . The effect of  $A^{-1}$  and  $B^{-1}$  on the generators of  $\pi_1(\widehat{\mathbb{C}} \setminus V_f)$  can be computed by hand to be

$$A^{-1} \cdot (\alpha, \beta, \gamma, \delta) = (\alpha^{-1} \delta^{-1} \alpha \delta \alpha, \beta, \gamma, \alpha^{-1} \delta \alpha)$$

$$B^{-1} \cdot (\alpha, \beta, \gamma, \delta) = (\alpha, \delta^{-1} \beta \delta, \gamma, \delta^{-1} \beta^{-1} \delta \beta \delta).$$

One computes that

$$\begin{aligned}\rho_{A \circ f} &= \rho_f \circ A^{-1} \\ \rho_{B \circ f} &= \rho_f \circ B^{-1}\end{aligned}$$

where  $\rho$  denotes the monodromy representation of its subscript. Identify the set of isomorphism classes of coverings determined by the four maps corresponding to the preimages of the origin under the map  $Y$  with the four quadruples mentioned above respectively where the preimage at the origin is identified with  $f$ . One can verify directly that the monodromy action of  $\pi_1(\widehat{\mathbb{C}} \setminus \Theta, 0)$  on the fiber  $Y^{-1}(0)$  is isomorphic to the action of  $\text{PMCG}(\widehat{\mathbb{C}}, P_f)$  on the four covering classes.

Two branched covers  $f_1, f_2$  as before are said to be Hurwitz equivalent if there exists homeomorphisms  $h$  and  $g$  so that  $g \circ f_1 = f_2 \circ h$ .

$$\begin{array}{ccc} S^2 & \xrightarrow{h} & S^2 \\ f_1 \downarrow & & \downarrow f_2 \\ S^2 & \xrightarrow{g} & S^2 \end{array}$$

Since the pure mapping class group acts transitively on the set of covering classes, it is clear that representatives of the four covering classes mentioned above all lie in one Hurwitz class.

## 5 Boundary Values of $\sigma_f$

In this section, we analyze the behavior of the Thurston pullback map  $\sigma_f$  on the Weil-Petersson boundary of Teichmüller space for  $f(z) = \frac{3z^2}{2z^3+1}$ .

### 5.1 The Boundary Maps to the Boundary

Denote by  $\overline{\mathcal{T}}_f$  the Weil-Petersson completion of Teichmüller space, and let  $\partial\mathcal{T}_f$  denote the Weil-Petersson boundary. We first show that the extended Thurston pullback map  $\overline{\sigma}_f : \overline{\mathcal{T}}_f \rightarrow \overline{\mathcal{T}}_f$  has the property that  $\overline{\sigma}_f(\partial\mathcal{T}_f) \subset \partial\mathcal{T}_f$ . This is accomplished by showing that the preimage under  $f$  of an essential curve in  $\widehat{\mathbb{C}} \setminus P_f$  has an essential component. It will be seen in the next section that actually  $\overline{\sigma}_f(\partial\mathcal{T}_f) = \partial\mathcal{T}_f$ . In general one should not expect the boundary of Teichmüller space to map to itself, as the Thurston pullback map for the rabbit polynomial provides a counterexample.

Recall the definition of the correspondence covered by  $\sigma_f$  in Section 2 and that  $H < \pi_1(\widehat{\mathbb{C}} \setminus \Theta, 0)$  is the subgroup of elements that lift to loops under  $Y$  based at 0. To understand the preimages of essential curves in

$\widehat{\mathbb{C}} \setminus P_f$  under  $f$ , first identify such a curve with an element of  $\pi_1(\widehat{\mathbb{C}} \setminus \Theta, 0)$  by the point-pushing isomorphism. This element may not lie in  $H$ , though, so an appropriate power must be taken. Then to compute the preimage of the essential curve under  $f$ , Theorem 2.6 indicates that one should lift elements of  $H$  under  $Y$  and push them down by  $X$ . All results in this section are devoted to understanding this process. For convenience the notation  $\gamma = \alpha^{-1}\beta^{-1}$  is used.

**Lemma 5.1** *Let  $g \in \{w\alpha^n w^{-1}, w\beta^n w^{-1}, w\gamma^n w^{-1}\} \cap H$  where  $n \in \mathbb{Z}, w \in \pi_1(\widehat{\mathbb{C}} \setminus \Theta, 0)$ . Then  $X_*(Y^{-1}(g)[0]) \neq 1$ .*

**Proof** We give a topological proof of this fact. Note that each such  $g$  is in the free homotopy class of a peripheral curve about some point  $p \in \Theta$ . There exists a simply connected neighborhood  $\mathcal{D}$  about  $p$  so that  $Y$  is a finite-to-one branched cover over  $\mathcal{D}$ . One can then choose a closed curve  $s$  in the free homotopy class of  $g$  with  $s \subset \mathcal{D}$ . As a simple consequence of the mapping properties of  $Y$  on  $\Theta'$ , any component of  $Y^{-1}(s)$  is peripheral about some  $p' \in \Theta'$ , and by homotopy lifting it is apparent that  $Y^{-1}(g)[0]$  is peripheral in  $\widehat{\mathbb{C}} \setminus \Theta'$ . The function  $X(z) = z^2$  maps peripheral curves in  $\widehat{\mathbb{C}} \setminus \Theta'$  to peripheral curves in  $\widehat{\mathbb{C}} \setminus \Theta$  since  $X$  maps  $\Theta'$  to  $\Theta$  and  $X$  is a homeomorphism near  $\Theta'$ . Thus,  $X_*(Y^{-1}(g)[0]) \neq 1$  since  $Y^{-1}(g)[0]$  was peripheral.  $\square$

The fact that  $\bar{\sigma}_f(\partial \mathcal{T}_f) \subset \partial \mathcal{T}_f$  is a consequence of this lemma and the following argument. Selinger showed that  $\sigma_f(S_\gamma) \subset S_{f^{-1}(\gamma)}$  where  $\gamma$  is essential [30, p. 590]. We must then show that every essential simple closed curve in  $\widehat{\mathbb{C}} \setminus P_f$  has an essential preimage. To compute the preimage of a curve  $\Gamma$  under  $f$ , choose a Dehn twist with core curve  $\Gamma$  that is identified with a parabolic element of  $\pi_1(\widehat{\mathbb{C}} \setminus \Theta, 0)$ . The cube of a parabolic element can be lifted under  $Y$  by examination of Figure 9. Lemma 5.1 demonstrates that the correspondence on moduli space maps this parabolic element to another parabolic element, and this second parabolic element is equivalent to a Dehn twist that fixes an essential curve that is precisely  $f^{-1}(\Gamma)$ . It is therefore evident that the Weil-Petersson boundary is mapped to itself by the extended Thurston pullback map.

## 5.2 Dynamical behavior of $\phi_f$

The motivation for the following theorem is that the dynamical behavior of  $\phi_f$  applied to (a power of) parabolic elements describes the iterative behavior of the extended Thurston pullback map. Though every parabolic element

can be written in the form  $w\alpha^n w^{-1}$ ,  $w\beta^n w^{-1}$ , or  $w\gamma^n w^{-1}$ , it becomes useful to consider words of the form  $w\delta^n w^{-1}$  with  $\delta = \beta^{-1}\alpha^{-1}$  to simplify many of the following statements. Note that  $\delta^{\beta^{-1}} = \gamma$ . In this section the subscript on  $\phi_f$  will be suppressed. Recall that  $G$  denotes  $\pi_1(\widehat{\mathbb{C}} \setminus \Theta, 0)$ . The word length of  $g \in G$  with respect to the generating set  $S = \{\alpha, \beta\}$  is denoted by  $|g|$ . For any  $k \in \mathbb{Z}$  and  $g \in G$ , use the standard notation  $g^{k \cdot w} = w^{-1}g^k w$  where one should recall that thought of as a path,  $w^{-1}$  is traversed first. Also recall that  $\gamma = \alpha^{-1}\beta^{-1}$ .

**Theorem 5.2** *Let  $w \in G$  and  $x \in \{\alpha, \beta, \gamma\}$ . Then there is some  $k \in \mathbb{N}$  and an appropriate choice of  $n \in \mathbb{N}$  so that:*

$$\phi^{\circ k}(x^{n \cdot w}) \in \{x^m \mid m \in \mathbb{N}\}.$$

Put informally, iteration of  $\phi$  will always eliminate the conjugator  $w$  of a parabolic element, and under iteration, all parabolics eventually fall into one of three classes depending on what the base of the element was at the beginning.

The first step in the proof is to write formulas that describe the effect of  $\phi$  on parabolic elements. Define the function  $\bar{\phi} : \pi_1(\widehat{\mathbb{C}} \setminus \Theta, 0) \rightarrow \pi_1(\widehat{\mathbb{C}} \setminus \Theta, 0)$  as follows:

$$\bar{\phi}(w) = \begin{cases} \phi(w) & w \in H \\ \phi(\beta w) & w \in \beta^{-1}H \\ \phi(\alpha^{-1}w) & w \in \alpha H \\ \phi(\alpha w) & w \in \alpha^{-1}H \end{cases}$$

**Lemma 5.3** *For any  $w \in G$ , there exists  $k \in \{1, 3\}$  so that for any  $n \in \mathbb{Z}$ :*

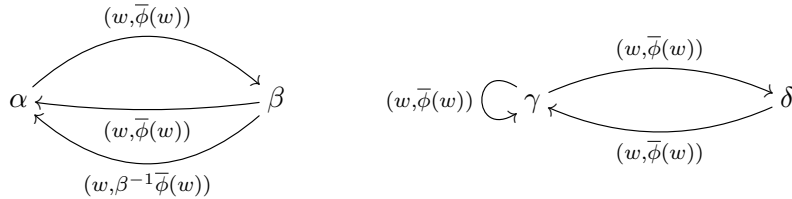
$$\phi(\alpha^{3n \cdot w}) = (\beta^{k \cdot n})\bar{\phi}(w) \quad (1)$$

$$\phi(\beta^{3n \cdot w}) = \begin{cases} (\alpha^{k \cdot n})\bar{\phi}(w) & w \in H \cup \beta^{-1}H \cup \alpha H \\ (\alpha^n)\beta^{-1}\bar{\phi}(w) & w \in \alpha^{-1}H \end{cases} \quad (2)$$

$$\phi(\gamma^{3n \cdot w}) = \begin{cases} (\gamma^{k \cdot n})\bar{\phi}(w) & w \in H \cup \alpha^{-1}H \\ (\delta^n)\bar{\phi}(w) & w \in \beta^{-1}H \cup \alpha H \end{cases} \quad (3)$$

$$\phi(\delta^{3n \cdot w}) = (\gamma^{k \cdot n})\bar{\phi}(w) \quad (4)$$

Schematically this lemma can be summarized by the following directed and labeled graph. The vertices of the graph represent the base of the expressions in the lemma. Directed edges indicate how the base changes under an application of  $\phi$ , and edges are labeled by ordered pairs to indicate the change in exponent under application of  $\phi$ .



**Proof** We prove the third equality and the others are proved analogously.

Case  $w \in H$ :

$$\begin{aligned} \phi((\alpha^{-1}\beta^{-1})^{3n \cdot w}) &= \phi((\alpha^{-1}\beta^{-1})^{3n})\phi(w) \\ &= \phi((\alpha^{-1}\beta^{-1})^3)^n \phi(w) \\ &= (\alpha^{-1}\beta^{-1})^n \phi(w) \end{aligned}$$

Case  $w \in \alpha^{-1}H$ : Let  $w = \alpha^{-1}h, h \in H$ .

$$\begin{aligned}
\phi((\alpha^{-1}\beta^{-1})^{3n \cdot w}) &= \phi((\alpha^{-1}\beta^{-1})^{3n \cdot \alpha^{-1}h}) \\
&= \phi(\alpha(\alpha^{-1}\beta^{-1})^{3n}\alpha^{-1})^{\phi(h)} \\
&= \phi(\beta^{-1}\alpha^{-1})^{3n \cdot \phi(h)} \\
&= (\alpha^{-1}\beta^{-1})^{3n \cdot \bar{\phi}(w)}
\end{aligned}$$

Case  $w \in \beta^{-1}H$ : Let  $w = \beta^{-1}h, h \in H$ .

$$\begin{aligned}
\phi((\alpha^{-1}\beta^{-1})^{3n \cdot w}) &= \phi(\beta(\alpha^{-1}\beta^{-1})^3\beta^{-1})^{n \cdot \phi(h)} \\
&= \phi(\beta^{-1}\alpha^{-1})^{n \cdot \phi(h)} \\
&= (\alpha^{-1}\beta^{-1})^{n \cdot \bar{\phi}(w)}
\end{aligned}$$

Case  $w \in \alpha H$ : Let  $w = \alpha h, h \in H$ .

$$\begin{aligned}
\phi((\alpha^{-1}\beta^{-1})^{3n \cdot w}) &= \phi(\alpha^{-1}(\alpha^{-1}\beta^{-1})^3\alpha)^{n \cdot \bar{\phi}_f(h)} \\
&= (\beta^{-1}\alpha^{-1})^{n \cdot \bar{\phi}(w)}
\end{aligned}$$

□

To prove the theorem, it is enough to show that  $\phi$  has a particular kind of contracting property on the exponents of parabolic elements. A path in the graph in Figure 12 which starts and ends at the vertex labeled 1 and passes through the vertex labeled 3, must immediately continue on to some vertex beside the one labeled 3. Thus, a new directed labeled graph can be produced to condense the sequence of labels encountered along such paths. Such a graph is exhibited in Figure 15, and is obtained from the graph in Figure 12 in the following way. Delete the vertex labeled 3 and the four edges incident to it. Add six new edges which correspond to paths  $e_1e_2$  in the old graph where  $e_1$  and  $e_2$  are either edges or reverse edges, and  $t(e_1)$  is the vertex labelled 3 where  $i(e_1) \neq t(e_2)$ . Each such edge connects  $i(e_1)$  to  $t(e_2)$  and is given the label  $\ell(e_1e_2)$  (the new edges corresponding to  $e_1e_2$  and  $e_2^{-1}e_1^{-1}$  are considered redundant and one of them is omitted). One shows that for elements of  $H$ , this graph yields the same result as the graph in Figure 12 by computing its effect on the generators of  $H$ . In some situations such as the proof of the following lemma, this new graph is the preferred perspective.

**Lemma 5.4** *Let  $w \in H$ . Then either  $|\phi(w)| \leq |w| - 2$  or  $|\phi(w)| = |w|$  in which case  $w = (\alpha\beta)^k, k \in \mathbb{Z}$ .*



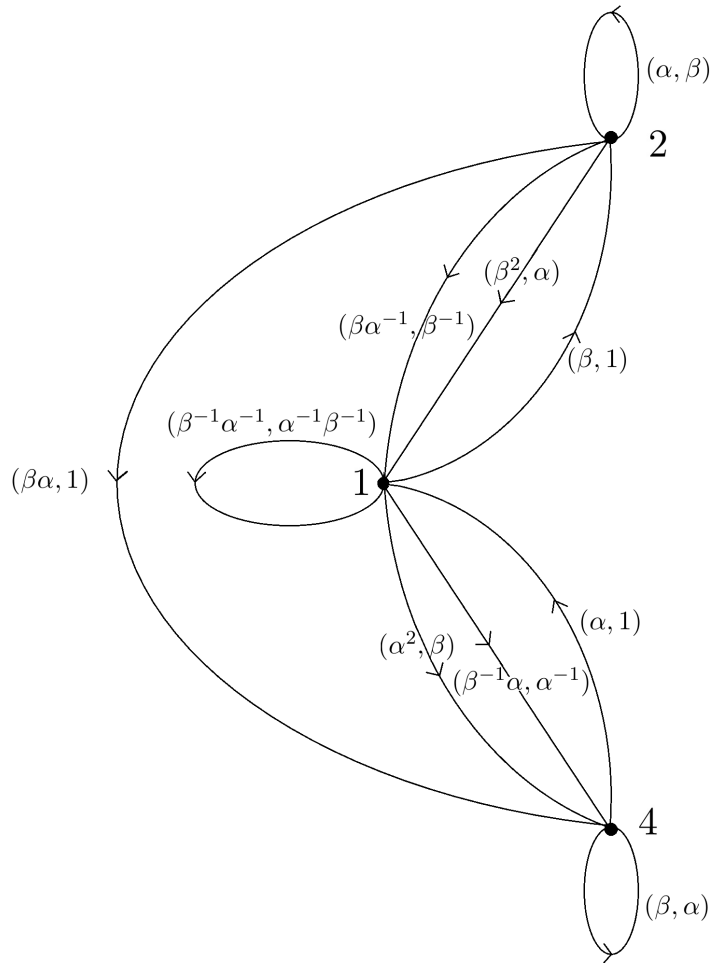


Figure 15: New machine for computing  $\phi_f$

**Proof** Recall that elements of  $H$  can be regarded as paths in the graph in Figure 12 that begin and end at the vertex labeled 1. Write  $w = (\alpha\beta)^m h (\alpha\beta)^n$  where  $h \in H$ ,  $m, n \in \mathbb{Z}$  so that  $|m|$  and  $|n|$  are maximal, and  $|w| = 2|m| + |h| + 2|n|$ . If  $h = 1$ , then evidently  $|\phi(w)| = |w|$ . Otherwise  $h$  corresponds to a path in the Schreier graph that begins and ends at the vertex labeled 1 whose first and last edges traversed are not  $(\beta^{-1}\alpha^{-1}, \alpha^{-1}\beta^{-1})$  in Figure 15. Note from Figure 15 that these first and last edges that  $h$  could pass through decrease word length, and all other edges traversed by  $h$  are nonincreasing on word length.  $\square$

Define the set of “bad” elements  $\mathcal{B}_\phi$  in  $H$  where  $\phi$  is not length-decreasing as follows:

$$\mathcal{B}_\phi = \{(\alpha\beta)^k : k \in \mathbb{Z}\}.$$

**Lemma 5.5** *Let  $w \in G$ . Then precisely one of the following is true:*

- $|\bar{\phi}(w)| \leq |w| - 1$ .
- $|\bar{\phi}(w)| = |w|$  and  $w = (\alpha\beta)^k$ ,  $k \in \mathbb{Z}$ .
- $|\bar{\phi}(w)| = |w| + 1$  and  $w = \beta(\alpha\beta)^k$ ,  $k \geq 0$ .

Using suggestive notation, define  $\mathcal{B}_{\bar{\phi}}$  by

$$\mathcal{B}_{\bar{\phi}} = \mathcal{B}_\phi \cup \{\beta(\alpha\beta)^k, k \geq 0\}.$$

Put differently, the lemma says that  $\bar{\phi}$  contracts word length on the complement of  $\mathcal{B}_{\bar{\phi}}$ , preserves word length on  $\mathcal{B}_\phi$ , and increases word length by one on  $\mathcal{B}_{\bar{\phi}} \setminus \mathcal{B}_\phi$ .

**Proof** It is immediately evident from the definition of  $\bar{\phi}$  and Lemma 5.4 that for any  $w \in G$ ,

$$0 \leq |\bar{\phi}(w)| \leq |w| + 1.$$

First suppose that  $w \in \mathcal{B}_{\bar{\phi}}$ . By direct computation we have

$$\bar{\phi}((\alpha\beta)^k) = (\beta\alpha)^k, k \in \mathbb{Z} \tag{5}$$

$$\bar{\phi}(\beta(\alpha\beta)^k) = (\beta\alpha)^{k+1}, k \geq 0. \tag{6}$$

which proves that one iteration of  $\bar{\phi}$  preserves the length of elements in  $\mathcal{B}_\phi$  and increases the length of the remaining elements in  $\mathcal{B}_{\bar{\phi}}$  by one.

Next suppose that  $w \notin \mathcal{B}_{\bar{\phi}}$ . There are four subcases depending on the coset representative of  $w$ . If  $w \in H$ , it is clear that  $|\bar{\phi}(w)| = |\phi(w)| \leq |w| - 2 \leq |w| - 1$ . To deal with the other three subcases, let  $x \in \{\beta, \alpha, \alpha^{-1}\}$  be the inverse of the coset representative of  $w$ , and we must consider two further cases depending on whether appending the inverse of the coset representative and reducing lengthens or shortens the word. First suppose that the length is shortened, i.e.  $|xw| = |w| - 1$ . Then

$$|\bar{\phi}(w)| = |\phi(xw)| \leq |xw| \leq |w| - 1$$

When the length increases when  $x$  is appended, i.e.  $|xw| = |w| + 1$ , there are two simple cases to consider. If  $xw \notin \mathcal{B}_{\bar{\phi}}$ , then we have

$$|\bar{\phi}(w)| = |\phi(xw)| \leq |xw| - 2 \leq |w| - 1$$

On the other hand, it is impossible for  $xw \in \mathcal{B}_{\bar{\phi}}$ , because then  $x = \alpha$  and so  $w = \beta(\alpha\beta)^{k-1}$  contrary to the assumption that  $w \notin \mathcal{B}_{\bar{\phi}}$ . □

Continuing to the proof of Theorem 5.2, it will be helpful to note the following fact which can easily be verified by examination of the Schreier graph: if  $k \equiv 0 \pmod{3}$  then  $(\beta\alpha)^k \in H$ , if  $k \equiv 1 \pmod{3}$  then  $(\beta\alpha)^k \in \beta^{-1}H$ , and if  $k \equiv 2 \pmod{3}$  then  $(\beta\alpha)^k \in \alpha H$ .

**Proof of Theorem 5.2** To minimize notation in the following computations, denote by  $*$  the presence of some integer that is necessary for each of the following expressions to be in  $H$ , though the precise values is not significant for our present concerns. The value of  $*$  may even vary within a single equation. The directed graph from Lemma 5.3 and the contracting property of Lemma 5.5 make it evident that apart from a single exception, one application of  $\phi$  to a suitable power of a parabolic word with exponent  $w \notin \mathcal{B}_{\bar{\phi}}$  will decrease the length of the exponent. This single exception occurs when the base is  $\beta$  and  $w \in \alpha^{-1}H$  in which case the length of the exponent may be preserved (but may not increase); but if the new exponent  $\beta^{-1}\bar{\phi}(w)$  lies outside of  $\mathcal{B}_{\bar{\phi}}$ , the next iterate of  $\phi$  will decrease its length according to Lemma 5.5. Hence, the single exception causes no problem because the length of the exponent may decrease, or it may fall into the following situation. We consider next  $w \in \mathcal{B}_{\bar{\phi}}$ , which will require four cases depending on the base to show that under iteration of  $\phi$  exponent lengths decrease. For  $x \in \{\alpha, \beta\}$ , it is shown that  $\phi^{\circ 2}(x^{*w}) = x^{*w'}$  where  $w'$  is minimal and  $|w'| < |w|$ . For  $x \in \{\gamma, \delta\}$ , it is shown that  $\phi(x^{*w}) = \gamma^*$ .

**Case when base is  $\alpha$ :** First assume that  $w \in \mathcal{B}_\phi$ , and consider separately the situation when  $k > 0$  and  $k < 0$  where  $w = (\alpha\beta)^k$ . For  $k < 0$ , note that

$$\phi(\alpha^{*w}) \stackrel{(1)}{=} \beta^{*\bar{\phi}((\alpha\beta)^k)} \stackrel{(5)}{=} \beta^{*(\beta\alpha)^k}$$

and upon taking a second iterate we obtain:

$$\phi^2(\alpha^{*w}) = \phi(\beta^{*(\beta\alpha)^k}) \stackrel{(2)}{=} \alpha^{*\bar{\phi}((\beta\alpha)^k)}$$

where  $|\bar{\phi}((\beta\alpha)^k)| < |w|$  because  $(\beta\alpha)^k \notin \mathcal{B}_{\bar{\phi}}$ . When  $k > 0$  one observes that  $\alpha^{*(\alpha\beta)^k} = \alpha^{*\beta(\alpha\beta)^{k-1}}$ , which means that a simple cancellation puts the exponent in  $\mathcal{B}_{\bar{\phi}} \setminus \mathcal{B}_\phi$ .

Finally, suppose  $w \in \mathcal{B}_{\bar{\phi}} \setminus \mathcal{B}_\phi$ . Then

$$\phi(\alpha^{*w}) \stackrel{(1)}{=} \beta^{*\bar{\phi}(\beta(\alpha\beta)^k)} \stackrel{(6)}{=} \beta^{*(\beta\alpha)^{k+1}} = \beta^{*\alpha(\beta\alpha)^k}$$

and taking a second iterate,

$$\phi^2(\alpha^{*w}) = \alpha^{*\bar{\phi}(\alpha(\beta\alpha)^k)}$$

where  $|\bar{\phi}(\alpha(\beta\alpha)^k)| < |w|$  since  $\alpha(\beta\alpha)^k \notin \mathcal{B}_{\bar{\phi}}$ .

**Case when base is  $\beta$ :** If  $w \in \mathcal{B}_\phi$  we can assume that  $k > 0$ , for otherwise a cancellation occurs. So assuming  $w = (\alpha\beta)^k, k > 0$ , it follows from Lemma 5.3 that  $\phi(\beta^{*w}) \stackrel{(5)}{=} \alpha^{*(\beta\alpha)^k}$  and so  $\phi^2(\beta^{*w}) \stackrel{(2)}{=} \beta^{*\bar{\phi}((\beta\alpha)^k)}$ , where one sees that  $|\bar{\phi}((\beta\alpha)^k)| < |w|$  since  $(\beta\alpha)^k \notin \mathcal{B}_{\bar{\phi}}$ . The second case is when  $w \in \mathcal{B}_{\bar{\phi}} \setminus \mathcal{B}_\phi$ , but one immediately sees that a cancellation with the base occurs that puts the exponent in  $\mathcal{B}_\phi$ .

**Case when base is  $\gamma$ :** If  $w \in \mathcal{B}_\phi$ , then from the formulas of Lemma 5.3 and a simple cancellation it is seen that,

$$\phi(\gamma^{*w}) \stackrel{(3)}{=} \gamma^{*(\beta\alpha)^k} = \gamma^*.$$

Finally, if  $w \in \mathcal{B}_{\bar{\phi}} \setminus \mathcal{B}_\phi$ , there is the simple cancellation  $\gamma^{*w} = \delta^*$  and so  $\phi(\gamma^{*w}) = \gamma^*$ .

**Case when base is  $\delta$ :** For  $w \in \mathcal{B}_\phi$ , simple cancellation shows that  $\delta^{*w} = \delta^*$ , and since  $\bar{\phi}(\delta^{*w}) = \gamma^*$  the conclusion immediately follows. If on the other hand  $w \in \mathcal{B}_{\bar{\phi}} \setminus \mathcal{B}_\phi$ , it is seen that

$$\phi(\delta^{*w}) \stackrel{(4)}{=} \gamma^{*\bar{\phi}(w)} \stackrel{(6)}{=} \gamma^{*(\beta\alpha)^{k+1}} = \gamma^*.$$

□

## 6 Properties of $\sigma_f : \overline{\mathbb{Q}} \rightarrow \overline{\mathbb{Q}}$

In Sections 3 and 4, the Weil-Petersson boundary of Teichmüller space was identified with the extended rationals  $\overline{\mathbb{Q}}$ , and the observation was made that the Thurston pullback map extends to the boundary which maps to itself. Denote by  $\sigma_f : \overline{\mathbb{Q}} \rightarrow \overline{\mathbb{Q}}$  the effect of this extended pullback map on the rational numbers associate to points in the Weil-Petersson boundary. The purpose of this section is to exhibit numerical properties of  $\sigma_f$  that are a consequence of earlier sections.

The following functional equation is a crucial computational tool that appears in [1], where  $\frac{p}{q} \in \overline{\mathbb{Q}}$  and  $w \in H$ :

$$\sigma_f\left(\frac{p}{q}.w\right) = \sigma_f\left(\frac{p}{q}\right).\phi(w). \quad (7)$$

This equation is a consequence of the following commutative diagram and the fact that  $\sigma_f$  and the action of  $\text{PMCG}(\widehat{\mathbb{C}}, P_f)$  extend continuously to the Weil-Petersson boundary. Denote by  $T_{p/q}$  the right Dehn twist that fixes the point  $\frac{p}{q}$  in the Weil-Petersson boundary and denote by  $T_w$  the mapping class that comes from pushing 0 along the positive direction of  $w \in H$ .

$$\begin{array}{ccccc} (\widehat{\mathbb{C}}, P_f) & \xrightarrow{T_{\sigma_f(p/q)}} & (\widehat{\mathbb{C}}, P_f) & \xrightarrow{T_{\phi(w)}} & (\widehat{\mathbb{C}}, P_f) \\ f \downarrow & & \downarrow f & & \downarrow f \\ (\widehat{\mathbb{C}}, P_f) & \xrightarrow{T_{p/q}} & (\widehat{\mathbb{C}}, P_f) & \xrightarrow{T_w} & (\widehat{\mathbb{C}}, P_f) \end{array}$$

For future reference it is necessary to state some simple results, the first being that  $\sigma_f\left(\frac{1}{1}\right) = -\frac{1}{1}$ . This is demonstrated as follows:

$$\begin{aligned} \sigma_f\left(\frac{1}{1}\right) &= \sigma_f\left(\frac{1}{1}.\beta^{-1}\alpha^{-1}\right) \\ &= \sigma_f\left(\frac{1}{1}\right).\phi(\beta^{-1}\alpha^{-1}) \\ &= \sigma_f\left(\frac{1}{1}\right).\alpha^{-1}\beta^{-1} \end{aligned}$$

where  $\sigma_f\left(\frac{1}{1}\right) = -\frac{1}{1}$  because it is the fixed point of the action of  $\alpha^{-1}\beta^{-1}$ . One could similarly prove that

$$\begin{aligned} \sigma_f\left(-\frac{2}{1}\right) &= \frac{1}{0} \\ \sigma_f\left(-\frac{1}{2}\right) &= \frac{0}{1} = \sigma_f\left(\frac{1}{2}\right) \end{aligned}$$

$$\sigma_f\left(\frac{1}{1}\right) = -\frac{1}{1} = \sigma_f\left(\frac{1}{3}\right) \quad (8)$$

The following consequence of Theorem 5.2 gives a surprising description of the global dynamics of  $\sigma_f : \overline{\mathbb{Q}} \rightarrow \overline{\mathbb{Q}}$ :

**Theorem 6.1** *Let  $\frac{p}{q} \in \overline{\mathbb{Q}}$  be reduced. Then there exists  $N \in \mathbb{N}$  so that for all  $n \geq N$ ,  $\sigma_f^{\circ n}\left(\frac{p}{q}\right) \in \left\{\frac{0}{1}, \frac{1}{0}, -\frac{1}{1}\right\}$ . If both  $p$  and  $q$  are odd, then for such  $n$ ,  $\sigma_f^{\circ n}\left(\frac{p}{q}\right) = -\frac{1}{1}$ . If either  $p$  or  $q$  is even, then for such  $n$ ,  $\sigma_f^{\circ n}\left(\frac{p}{q}\right)$  lies in the two-cycle  $\frac{0}{1} \longleftrightarrow \frac{1}{0}$ .*

**Proof** Recall that points in the Weil-Petersson boundary are encoded by Dehn twists  $T_{p/q}$ . It is a consequence of Equation 7 that  $\sigma_f\left(\frac{p}{q}\right) = \frac{p'}{q'}$  if and only if  $\frac{p'}{q'} = \text{Fix}(\phi(T_{p/q}^n))$  for some appropriate value of  $n \in \mathbb{N}$  because

$$\sigma_f\left(\frac{p}{q}\right) = \frac{p'}{q'} \iff \sigma_f\left(\frac{p}{q} \cdot T_{p/q}^n\right) = \frac{p'}{q'} \iff \sigma_f\left(\frac{p}{q}\right) \cdot \phi(T_{p/q}^n) = \frac{p'}{q'}.$$

For some choice of power  $n \in \mathbb{N}$ , Theorem 5.2 implies that under iteration of  $\phi$ ,  $T_{p/q}^n$  lands in one of the three maximal parabolic subgroups  $\langle \alpha \rangle$ ,  $\langle \beta \rangle$ , or  $\langle \gamma \rangle$ . Then since  $\phi(\alpha^3) = \beta$ ,  $\phi(\beta^3) = \alpha$  and  $\phi(\gamma^3) = \gamma$ , the mapping properties of  $\sigma_f$  on the finite global attractor are given below.

$$\frac{0}{1} \longleftrightarrow \frac{1}{0} \quad \left. \begin{array}{l} \text{---} \\ \text{---} \end{array} \right\} -\frac{1}{1}$$

The continued fraction algorithm presented before gives a way of writing  $\frac{p}{q} = *.w$  where  $* \in \left\{\frac{0}{1}, \frac{1}{0}, \frac{1}{1}\right\}$  and  $w \in G$ . In the case where  $* = \frac{1}{1}$ , one can use Equation 8 to observe that if:

$$w \in H, \text{ then } \sigma_f\left(\frac{p}{q}\right) = \sigma_f\left(\frac{1}{1}.w\right) = -\frac{1}{1}.\phi(w).$$

$$w \in \alpha H, \text{ then } \sigma_f\left(\frac{p}{q}\right) = \sigma_f\left(-\frac{1}{1}.\alpha^{-1}w\right) = -\frac{1}{1}.\phi(\alpha^{-1}w).$$

$$w \in \alpha^{-1}H, \text{ then } \sigma_f\left(\frac{p}{q}\right) = \sigma_f\left(\frac{1}{3}.\alpha w\right) = -\frac{1}{1}.\phi(\alpha w).$$

$$w \in \beta^{-1}H, \text{ then } \sigma_f\left(\frac{p}{q}\right) = \sigma_f\left(-\frac{1}{1}.\beta w\right) = -\frac{1}{1}.\phi(\beta w).$$

This shows that for all possible  $w \in G$ , it is true that  $\sigma_f\left(\frac{1}{1}.w\right) = -\frac{1}{1}.\overline{\phi}(w)$ . Similar computations apply when  $* = \frac{0}{1}$  and  $* = \frac{1}{0}$ , and so the following hold:

$$\sigma_f\left(\frac{1}{0}.w\right) = \frac{0}{1}.\overline{\phi}(w)$$

$$\begin{aligned}\sigma_f\left(\frac{0}{1}.w\right) &= \frac{1}{0}.\overline{\phi}(w) \\ \sigma_f\left(\frac{1}{1}.w\right) &= -\frac{1}{1}.\overline{\phi}(w).\end{aligned}$$

Since the action of  $\text{PT}(2)$  on  $\overline{\mathbb{Q}}$  preserves the parity of numerator and denominator, these equations make evident that when  $p$  and  $q$  are both odd, then  $\sigma_f(\frac{p}{q})$  will have odd numerator and denominator in reduced form. One can also conclude that when  $p$  is odd and  $q$  is even, then  $\sigma_f(\frac{p}{q})$  will have *even* numerator and *odd* denominator when written in reduced form. An analogous result holds for  $p$  even and  $q$  odd.  $\square$

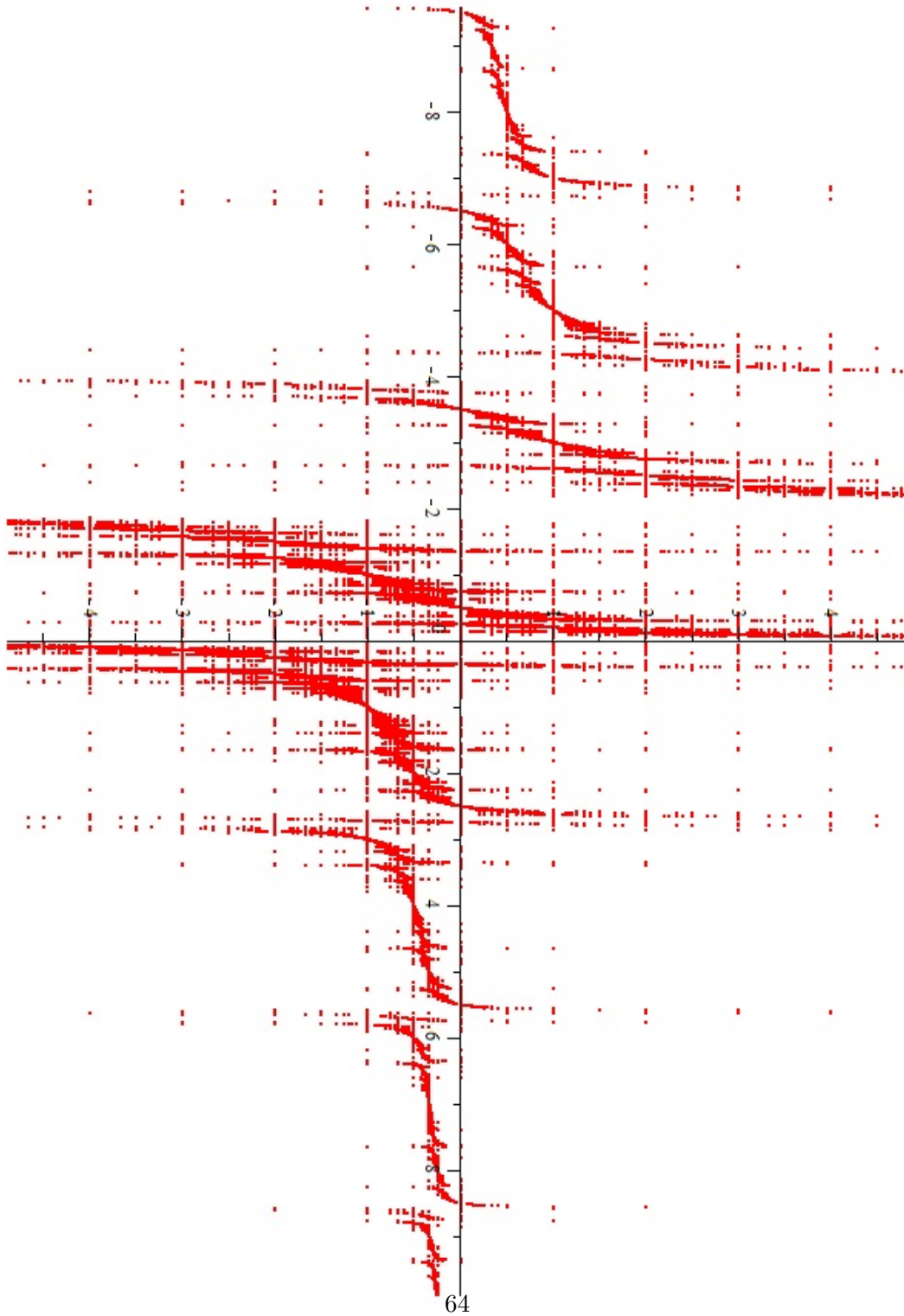
The following orbits of several fractions  $\frac{p}{q}$  under  $\sigma_f$  illustrate several properties mentioned already. They also demonstrate that it is possible for a fraction with odd numerator and even denominator to land on either element of the two-cycle:

$$\begin{array}{ccccccccc} \frac{205}{357} & \mapsto & -\frac{19}{13} & \mapsto & -\frac{5}{3} & \mapsto & -\frac{3}{1} & \mapsto & \frac{1}{1} & \mapsto & -\frac{1}{1} \\ \frac{203}{357} & \mapsto & -\frac{23}{15} & \mapsto & -\frac{7}{3} & \mapsto & \frac{3}{1} & \mapsto & -\frac{1}{1} & & \\ \frac{203}{356} & \mapsto & -\frac{50}{33} & \mapsto & -\frac{13}{6} & \mapsto & \frac{6}{1} & \mapsto & -\frac{1}{2} & \mapsto & \frac{0}{1} \\ \frac{203}{354} & \mapsto & -\frac{28}{19} & \mapsto & -\frac{7}{4} & \mapsto & -\frac{4}{1} & \mapsto & \frac{1}{0} & & \end{array}$$

Next we show that  $\sigma_f$  is surjective and that all fibers are infinite. Recall that  $\alpha$  and  $\beta$  generate  $G$ . Observe that  $\phi$  is a surjective virtual endomorphism since  $\phi(\alpha^{-1}\beta\alpha) = \alpha$  and  $\phi(\beta\alpha\beta^{-1}) = \beta$ . Thus, if  $\frac{p}{q} = \frac{0}{1}.w'$  where  $w' \in G$ , then  $\sigma_f(\frac{1}{0}.w) = \frac{p}{q}$  where  $w$  is chosen so that  $\phi(w) = w'$ . We show that  $\sigma_f$  is infinite-to-one in the case of rational numbers of the form  $\frac{1}{0}.w'$ . Since  $\phi(\beta^2\alpha^2)$  is trivial, one knows from Equation 7 that  $\sigma_f(\frac{0}{1}.(\beta^2\alpha^2)^k) = \frac{1}{0}$  for all  $k \in \mathbb{Z}$ . Since  $\frac{0}{1}.(\beta^2\alpha^2)^k$  are all different rational numbers, the preimage of  $\frac{1}{0}$  is infinite. By surjectivity of  $\phi$ , there is a  $w$  so that  $\phi(w) = w'$  and the infinite set of fractions  $\{\frac{0}{1}.(\beta^2\alpha^2)^k w : k \in \mathbb{Z}\}$  all map to  $\frac{p}{q}$ .

Several useful identities are given below that explain some behavior of the graph of  $\sigma_f$  in Figure 7.1. There are numerous other identities which can be proven similarly.

$$\sigma_f\left(\frac{p}{6np+q}\right) = \sigma_f\left(\frac{p}{q}\right) - 2n$$



64

Figure 16: A portion of the plot of the points  $(\frac{p}{q}, \sigma_f(\frac{p}{q}))$  with  $\max(|p|, |q|) < 1000$



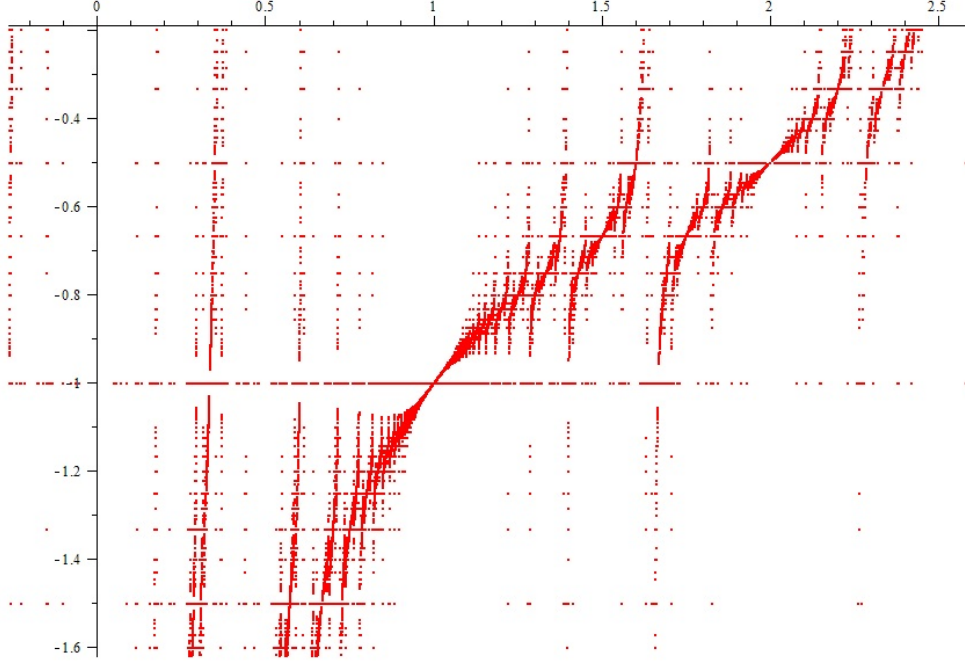


Figure 17: Detail of Figure 7.1

$$\sigma_f\left(\frac{p}{q} + 6n\right) = \frac{1}{\frac{1}{\sigma_f(p/q)} - 2n}$$

To derive the first identity, simply note that Equation 7 can be used to show  $\sigma_f\left(\frac{p}{q} \cdot \alpha^{-3n}\right) = \sigma_f\left(\frac{p}{q}\right) \cdot \beta^{-n}$  for all  $n \in \mathbb{N}$ . The second is proven similarly. The next two identities can be proven using Equation 7 and the fact that  $\phi((\alpha\beta)^n) = (\beta\alpha)^n$  as well as a handful of explicit  $\sigma_f$  computations mentioned before.

$$\sigma_f\left(\frac{n+1}{n}\right) = -\frac{n}{n+1}, n > 0$$

$$\sigma_f\left(\frac{n}{n+1}\right) = \begin{cases} -\frac{n-1}{n-2} & n > 0 \text{ odd} \\ -\frac{n+1}{n} & n > 0 \text{ even} \end{cases}$$

Another useful identity is the following:

$$\sigma_f\left(\left(\frac{p}{q}\right)^{-1}\right) = \left(\sigma_f\left(\frac{p}{q}\right)\right)^{-1}. \quad (9)$$

This is proven by first showing that  $z \mapsto \bar{z}$  sends the curve corresponding to  $\frac{p}{q}$  to the curve corresponding to  $\frac{q}{p}$ . The map  $z \mapsto \bar{z}$  induces an isomorphism

on  $\pi_1(\widehat{\mathbb{C}} \setminus \Theta, 0)$  as follows:

$$\begin{aligned}\alpha &\longmapsto \beta^{-1} \\ \beta &\longmapsto \alpha^{-1}.\end{aligned}$$

Then since  $\frac{p}{q}.\alpha = (\frac{q}{p}.\beta^{-1})^{-1}$  and  $\frac{p}{q}.\beta = (\frac{q}{p}.\alpha^{-1})^{-1}$ , the fact about conjugation is clear. Equation 9 holds since  $f$  commutes with  $z \mapsto \bar{z}$ .

## 7 Slopes of Curves in $\widehat{\mathbb{C}} \setminus P$ when $|P| = 4$

Section 3 presents a way to assign elements of  $\overline{\mathbb{Q}}$  to curves in  $\widehat{\mathbb{C}} \setminus P$  using the Weil-Petersson boundary of Teichmüller space. Another natural way to assign an element of  $\overline{\mathbb{Q}}$  to such a curve is to compute its “slope.” The purpose of this section is to describe this latter assignment, and for a fixed curve, present a formula relating the two different assignments of  $\overline{\mathbb{Q}}$  just mentioned. Usually one employs the term “slope” for lines in  $\mathbb{R}^2$  and closed curves in  $\mathbb{T}^2$ , and this section will show how these slopes have a vital connection to slopes in  $\widehat{\mathbb{C}} \setminus P$ . It is possible to define the notion of slope for the sphere with any four points removed, where note that normalizing by a Möbius transformation, we may assume that the four points have the form  $\{z_0, 1, \omega, \bar{\omega}\}$ . First, the case when  $z_0$  arbitrary is considered, and then the highly symmetric case when  $z_0 = 0$  will be examined.

### 7.1 Slopes in $\widehat{\mathbb{C}} \setminus P$ when $|P| = 4$

To define slope on  $\widehat{\mathbb{C}} \setminus P$  where  $P = \{z_0, 1, \omega, \bar{\omega}\}$ , it is convenient to first arbitrarily fix two minimally intersecting curves which we will declare to have slope  $\frac{0}{1}$  and  $\frac{1}{0}$ . Connect  $z_0$  and  $\omega$  by a simple arc that avoids  $P$ , and the curve which is the boundary of a simply connected neighborhood of this arc is denoted by  $a$ . Then connect  $z_0$  and  $\bar{\omega}$  by a simple arc in  $\widehat{\mathbb{C}} \setminus P$  that doesn’t cross  $a$ . By taking a simply connected neighborhood as before, one produces  $b$ . The curves  $a$  and  $b$  in  $\widehat{\mathbb{C}} \setminus P$  are declared to have slope  $\frac{0}{1}$  and  $\frac{1}{0}$  respectively. One can chose an orientation for these curves by assuming that the point at infinity lies to the right, but it will be evident in the following work that the definition of slope is independent of this choice of orientation.

Up to isomorphism, there exists a canonical double cover  $(T, e_0) \longrightarrow (\widehat{\mathbb{C}}, 0)$  of  $\widehat{\mathbb{C}}$  branched over the four points in  $P$  where  $e_0 \in T$  is the preimage of 0. To determine the topological type of  $T$ , apply the Riemann Hurwitz formula as follows, where  $N$  is the number of critical points:

$$\chi(T) = 2 \cdot \chi(\widehat{\mathbb{C}}) - N = 2(2) - 4 = 0.$$

By the topological classification of surfaces,  $T$  is homeomorphic to the two-dimensional torus  $\mathbb{T}$ , and for the remainder of this section the latter notation is used to denote the double cover. This cover is unique up to isomorphism in the branched sense, and since there is a standard definition of slope in  $\mathbb{T}$  having fixed a basis for homology, it is natural to lift  $a$  and  $b$  under this branched cover to define slope in  $\widehat{\mathbb{C}} \setminus P$ . Denote by  $\tilde{P}$  the set of preimages of  $P = \{z_0, 1, \omega, \bar{\omega}\}$  under the double cover where it is clear that  $|\tilde{P}| = 4$ . Also, denote by  $(\mathbb{C}, 0) \longrightarrow (\mathbb{T}, e_0)$  the universal cover, though an explicit choice of cover will not be fixed until later. We use the symbol  $\simeq$  to indicate that two curves in a surface are homotopic in that surface.

**Lemma 7.1** *The curves  $a$  and  $b$  in  $\widehat{\mathbb{C}} \setminus P$  each lift to pairs of oriented simple closed curves  $\tilde{a}_1, \tilde{a}_2$  and  $\tilde{b}_1, \tilde{b}_2$  in  $\mathbb{T} \setminus \tilde{P}$  where  $\tilde{a}_1 \simeq \tilde{a}_2$  and  $\tilde{b}_1 \simeq \tilde{b}_2$  in  $\mathbb{T}$*

**Proof** Let  $g_1, g_2, g_3, g_4$  be small positively oriented loops about each point in  $P$ , where the four homology classes  $[g_i]$  evidently generate  $H_1(\widehat{\mathbb{C}} \setminus P, \mathbb{Z})$ . In other words,  $H_1(\widehat{\mathbb{C}}, \mathbb{Z}) = \{\sum c_i [g_i] | c_i \in \mathbb{Z}\}$ . A simple closed curve in  $\widehat{\mathbb{C}} \setminus P$  lifts to the double cover if it lies in the kernel of the homomorphism

$$\rho : H_1(\widehat{\mathbb{C}}, \mathbb{Z}) \longrightarrow \mathbb{Z}/2\mathbb{Z}$$

defined by

$$\rho\left(\sum c_i [g_i]\right) = \sum c_i \pmod{2}.$$

Since the curves  $a$  and  $b$  are nonperipheral, they must bound a disc containing two of the loops, so without loss of generality, one can say that  $a$  is homologous to  $\pm(g_1 + g_2)$ . Since

$$\rho(a) = \rho(\pm(g_1 + g_2)) = \pm(1 + 1) \equiv 0$$

it is clear that  $a$  lifts to  $\mathbb{T}$ . A similar argument applies to  $b$ . Since the cover is two-to-one,  $a$  lifts to two disjoint curves  $\tilde{a}_1, \tilde{a}_2$  in  $\mathbb{T}$ , and  $b$  lifts to two disjoint curves  $\tilde{b}_1, \tilde{b}_2$ . Note that  $\tilde{a}_1$  and  $\tilde{b}_1$  intersect minimally in  $\widehat{\mathbb{C}} \setminus P$  in the sense that

$$\min_{a' \simeq \tilde{a}_1, b' \simeq \tilde{b}_1} |a' \cap b'| = 1$$

because

$$\min_{a' \simeq a, b' \simeq b} |a' \cap b'| = 2.$$

So in fact these the curves  $\tilde{a}_i$  are not homotopic to the curves  $\tilde{b}_i$  in  $\mathbb{T}$ .

Finally, we prove that these curves are homotopic in  $\mathbb{T}$ . By definition, the nontrivial deck transformation  $h : \mathbb{T} \rightarrow \mathbb{T}$  must interchange  $\tilde{a}_1$  with

$\tilde{a}_2$  and it must interchange  $\tilde{b}_1$  with  $\tilde{b}_2$ . On the level of the universal cover  $(\mathbb{C}, 0) \rightarrow (\mathbb{T}, e_0)$ , choose the lift of  $h$  that fixes the origin. The only involutive holomorphic deck transformation of the torus cover that fixes the origin is the map  $z \mapsto -z$ . Thus, the induced map on homology is  $h_* : H_1(\mathbb{T}, \mathbb{Z}) \rightarrow H_1(\mathbb{T}, \mathbb{Z})$  given by  $(x, y) \mapsto (-x, -y)$ . But two curves in the torus whose homology classes agree up to sign must be freely homotopic in the torus.  $\square$

We now define precisely the notion of slope in  $\mathbb{T}$ . Since  $\tilde{a}_1$  and  $\tilde{b}_1$  form an ordered basis of  $H_1(\mathbb{T}, \mathbb{Z})$ , the assignment

$$\begin{aligned}\tilde{a}_1 &\mapsto (1, 0) \\ \tilde{b}_1 &\mapsto (0, 1),\end{aligned}$$

gives a natural identification  $H_1(\mathbb{T}, \mathbb{Z}) \cong \mathbb{Z} \oplus \mathbb{Z}$ . Slopes are assigned to homology classes by the map

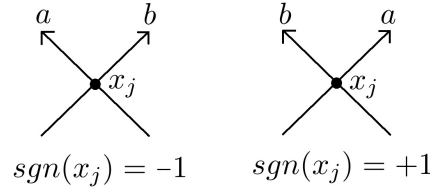
$$(q, p) \mapsto \frac{p}{q}$$

where  $p$  and  $q$  are relatively prime. Define a *curve of slope  $\frac{p}{q}$  in  $\mathbb{T}$*  to be a simple closed curve lying in the homology class corresponding to  $(q, p)$ . Recall that the lift of an essential curve in  $\tilde{\mathbb{C}} \setminus P_f$  is two essential homotopic curves in  $\mathbb{T}$  with opposite orientation by Lemma 7.1. On the level of homology, we may assume these lifts are  $(q, p)$  and  $(-q, -p)$  which both have slope  $\frac{p}{q}$ . Define a *curve of slope  $\frac{p}{q}$  in  $\tilde{\mathbb{C}} \setminus P$*  to be the curve that lifts to a curve of slope  $\frac{p}{q}$  in the torus.

It is a standard fact that the cup product yields a signed intersection form for essential curves in  $\mathbb{T}$ , and this can be used to give another interpretation of slope in  $\mathbb{T}$ . Let  $a$  and  $b$  be two oriented curves in an oriented surface  $X$ . Apply a homotopy so the curves intersect minimally at  $N$  distinct points  $x_1, \dots, x_N$ . Then the *signed intersection number* of  $a$  and  $b$  is defined by  $\iota(a, b) = \sum_{j=1}^N \text{sgn}(x_j)$  where the sign function  $\text{sgn}(x_j)$  is computed using the conventions below.

A straightforward cup product computation shows that the signed intersection number for curves of slope  $\frac{p}{q}$  and  $\frac{r}{s}$  in  $\mathbb{T}$  is the determinant of  $\begin{bmatrix} p & r \\ q & s \end{bmatrix}$ . One can then see that for relatively prime  $p$  and  $q$ , a curve of slope  $\frac{p}{q}$  will have  $p$  signed intersections with  $\tilde{a}_1$  and  $q$  signed intersections with  $\tilde{b}_1$ .

Next we define slope in  $\mathbb{C}$  with respect to the lattice  $\Lambda$ . Note that  $H_1(\mathbb{T}, \mathbb{Z}) \cong \pi_1(\mathbb{T}, e_0)$ , and so the basis formed by  $\tilde{a}_1$  and  $\tilde{b}_1$  act on the universal cover  $(\mathbb{C}, 0) \rightarrow (\mathbb{T}, e_0)$  by translation; explicitly choose the universal



cover so that the translation corresponding to  $a$  is  $z \mapsto z + 1$  and the one corresponding to  $b$  is  $z \mapsto z + \tau$  for some nonreal complex number  $\tau$ . The torus  $\mathbb{T}$  can then be thought of as the quotient  $\mathbb{C}/\Lambda$  where  $\Lambda = \langle 1, \tau \rangle$ . The following defines *the line of slope  $\frac{p}{q}$  in  $(\mathbb{C}, \Lambda)$*  where  $t \in \mathbb{R}$  and  $c_0 \in \mathbb{C}$  is chosen so that the line avoids the lattice  $\Lambda$ :

$$t \mapsto t(p \cdot \tau + q) + c_0.$$

Pushing this curve down to  $\tilde{\mathbb{C}} \setminus P$  and forgetting the orientation on the curve yields a curve of slope  $\frac{p}{q}$  in  $\tilde{\mathbb{C}} \setminus P$  as defined before.

## 7.2 Slopes in $\widehat{\mathbb{C}} \setminus P$ when $P = \{0, 1, \omega, \bar{\omega}\}$

Now apply the methods described above to the highly symmetric case when  $P = P_f$ . The choice of  $\frac{0}{1}$  and  $\frac{1}{0}$  curves in  $\widehat{\mathbb{C}} \setminus P$  are exhibited in Figure 18, and following the steps above, the map  $\pi : \mathbb{C} \rightarrow \widehat{\mathbb{C}}$  is produced. Note that the triangulation of the domain and range of  $\pi$  in the figure provides a convenient combinatorial model of the map. Moreover, because of the symmetry of  $P$ , one can explicitly find a formula for  $\pi$  in terms of the Weierstrass function.

The holomorphic map  $\pi$  is produced by describing an explicit map from  $\mathbb{C}$  to a tetrahedron using the numbering scheme of the triangulation. Then an application of the radial projection followed by the stereographic projection produces the image of  $\pi$  as it is displayed in Figure 18. Specifically, use an isometry to map the triangle in  $\mathbb{C}$  labelled by 3 whose vertices include  $0, 1/2$ , and  $1/4 + \sqrt{3}/4i$  to the top face of the tetrahedron in Figure 6 by:

$$\begin{aligned} 0 &\mapsto B \\ \frac{1}{4} + \frac{\sqrt{3}}{4} \cdot i &\mapsto D \\ \frac{1}{2} &\mapsto C \end{aligned}$$

One can then extend the map over  $\mathbb{C}$  using reflection. Postcomposing this map to the tetrahedron with the radial projection and then the stereographic projection with north pole  $N$  as in Figure 6 yields the map  $\pi$  which is a meromorphic function with double zeros at each point in the lattice  $\Lambda = \langle 1, \tau := e^{2\pi \cdot i/3} \rangle$ . Then on  $\mathbb{C}$ , the function  $\frac{1}{\pi}$  is doubly periodic with respect to  $\Lambda$  and has double poles at each point in  $\Lambda$ . According to an elementary result in the theory of elliptic functions, one might hope to write  $\frac{1}{\pi}$  as a linear combination of the Weierstrass  $\wp$ -function and its derivative. One can see from the statement of Theorem 7.2 that it is not even necessary to use the derivative. Denote by  $\wp_\Lambda$  the Weierstrass function with lattice  $\Lambda$ , i.e.

$$\wp_\Lambda(z) = \frac{1}{z^2} + \sum_{\lambda \in \Lambda} \frac{1}{(z - \lambda)^2} - \frac{1}{\lambda}$$

**Theorem 7.2** *There exists a number  $c \in \mathbb{C}$  such that  $1/\pi(z) = c\wp_\Lambda(z)$ .*

**Proof** The goal is to show that  $\wp_\Lambda(z) \cdot \pi(z)$  is entire, and then the conclusion will follow from an application of Liouville's theorem. First, a brief examination of power series show that  $\wp_\Lambda(z) \cdot \pi(z)$  has no poles at 0:

$$\wp_\Lambda(z) \cdot \pi(z) = (1/z^2 + O(1/z)) \cdot (z^2 \cdot \text{const} + O(z^3)) = \text{const} + O(z)$$

Next, we use the fact that  $\wp_\Lambda(z)$  and  $\pi$  are doubly periodic on  $\Lambda$  to say that  $\wp_\Lambda(z) \cdot \pi$  has no poles on  $\Lambda$ . Furthermore, it is clear that  $\wp_\Lambda(z) \cdot \pi(z)$  has no poles over a whole fundamental parallelogram in  $\Lambda$  for the reason that  $\pi(z)$  is analytic and by definition, the only poles of  $\wp_\Lambda(z)$  lie on  $\Lambda$ . Using the periodicity of  $\wp_\Lambda(z)$  and  $\pi$ , we conclude that  $\wp_\Lambda(z) \cdot \pi$  has no poles on all of  $\mathbb{C}$ .  $\square$

To find the explicit value of  $c$ , note that  $\pi(1/2) = 1$  from an examination of Figure 18. Upon substitution, the equation from Theorem 7.2 becomes  $\frac{1}{\pi(1/2)} = 1 = c \cdot \wp_\Lambda(1/2)$  and so  $c = \frac{1}{\wp_\Lambda(1/2)}$ . Thus we have found an explicit formula for  $\pi$ :

$$\pi(z) = \frac{\wp_\Lambda(1/2)}{\wp_\Lambda(z)}.$$

It will be important to be able to produce a line of slope  $\frac{p}{q}$  in  $\widehat{\mathbb{C}} \setminus P_f$ . Curves of slope  $\frac{1}{0}$  and  $\frac{0}{1}$  in both  $(\mathbb{C}, \Lambda)$  and  $\widehat{\mathbb{C}} \setminus P$  are depicted in Figure 18, and the following lines:

$$t \mapsto t + \frac{\sqrt{3}}{8}i, t \in \mathbb{R}$$

$$t \mapsto t \cdot e^{2\pi \cdot i/3} + \frac{\sqrt{3}}{4}i, t \in \mathbb{R}$$

have slope  $\frac{0}{1}$  and  $\frac{1}{0}$  respectively in  $(\mathbb{C}, \Lambda)$ . Now to draw a line of slope  $\frac{p}{q}$  in  $(\mathbb{C}, \Lambda)$ , choose a generic point  $c_0 \in \mathbb{C}$  and draw the line

$$t \mapsto c_0 + t(p \cdot e^{2\pi \cdot i/3} + q \cdot t), t \in \mathbb{R}$$

Projecting this line to  $\widehat{\mathbb{C}} \setminus P_f$  gives a curve of slope  $\frac{p}{q}$  in  $\widehat{\mathbb{C}} \setminus P_f$ . It can be observed that a curve of slope  $\frac{p}{q}$  in  $\widehat{\mathbb{C}} \setminus P$  lies in the same homotopy class as a curve in  $\widehat{\mathbb{C}} \setminus P$  corresponding to the point  $-\frac{p}{q}$  in the Weil-Petersson boundary.

## 8 The Twisting Problem for $f$

Following the notation of [1] and Section 3, it is useful to think of  $\text{PMCG}(\widehat{\mathbb{C}}, P_f) = \langle T_\alpha, T_\beta \rangle$  as a right action on the class of Thurston maps. For  $f(z) = \frac{3z^2}{2z^3+1}$  and  $g \in \text{PMCG}(\widehat{\mathbb{C}}, P_f)$ , use the notation  $f \cdot g := g \circ f$ . It will not be uncommon for the symbol  $T$  to be suppressed as well. For example, one has

$$f \cdot \alpha\beta = f \cdot T_\alpha T_\beta = T_\beta \circ T_\alpha \circ f.$$

The goal of this section is to solve the twisting problem which is stated as follows:

*What is the Thurston class of  $f \cdot g$  where  $g \in \text{PMCG}(\widehat{\mathbb{C}}, P_f)$ ?*

This question has relevance to the work of Mary Rees on Wittner captures for quadratic pre-periodic polynomials [29]. Such a polynomial is post-composed by a homeomorphism that corresponds to the end result of pushing  $\infty$  along a path into some iterated preimage of the critical point. This creates a new Thurston map, and a different choice of the path corresponds to post-composing the new Thurston map by a Dehn twist.

A discussion of known results about polynomial twisting was made in Section 2.4. Following Bartholdi and Nekrashevych [1], we begin by extending the virtual endomorphism  $\phi$  over the whole mapping class group to a map  $\bar{\phi}$  and then study its dynamical properties.

### 8.1 Limiting behavior of the Extended Virtual Endomorphism

Recall the definition of the virtual endomorphism  $\phi_f : H \rightarrow \pi_1(\widehat{\mathbb{C}} \setminus \Theta)$  made in Section 4 which was extended to a map  $\bar{\phi}$  on the whole mapping class

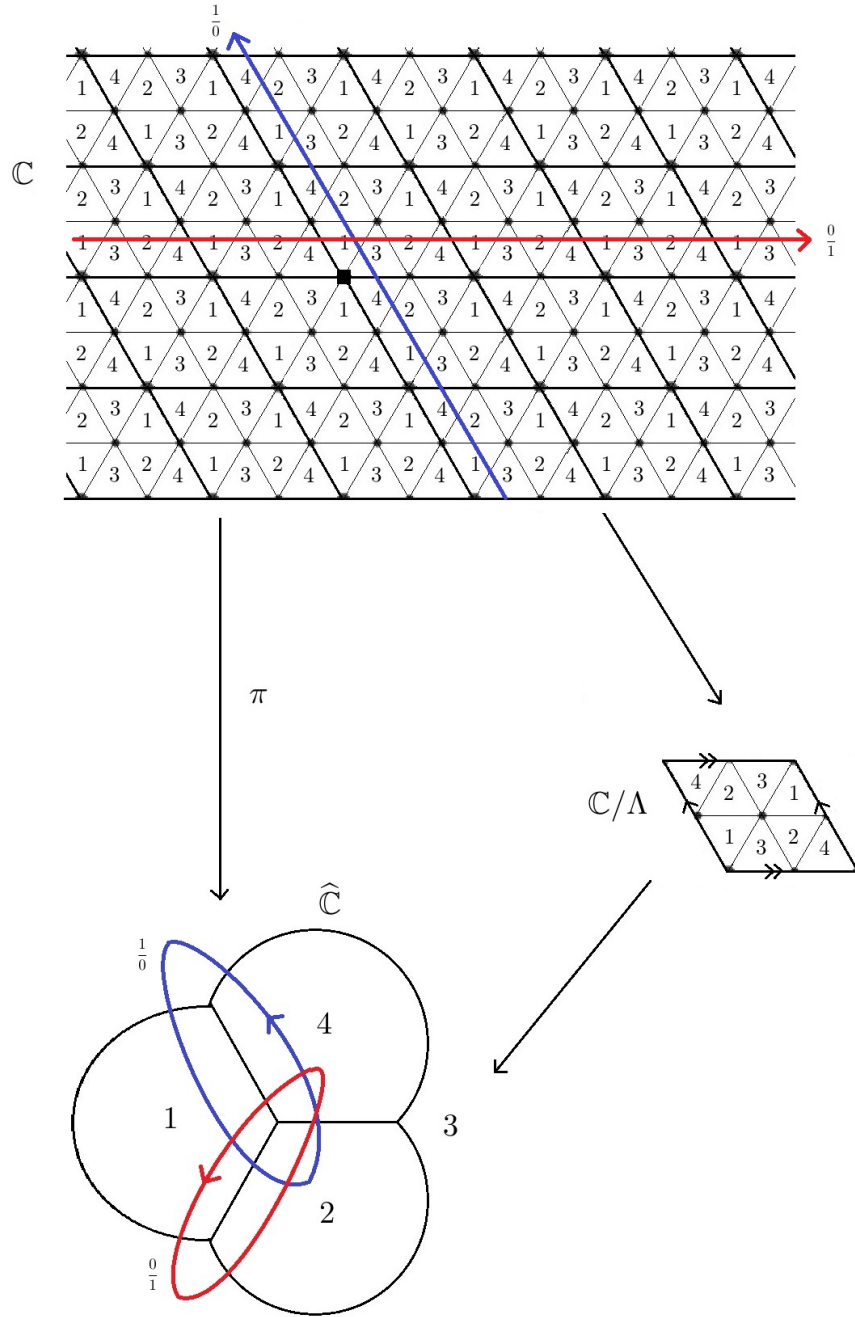


Figure 18: The map  $\pi : (\mathbb{C}, \Lambda) \rightarrow (\widehat{\mathbb{C}}, 0)$  used to compute slopes in  $(\widehat{\mathbb{C}}, P_f)$ . Larger dots indicate points in  $\Lambda$ , with the exception of the origin which is marked by a filled box. The vertices of the small triangles are the half-lattice points of  $\Lambda$ .



group to compute the pullback on curves. In a slightly different way, extend the virtual endomorphism  $\psi : H_f \rightarrow \text{PMCG}(\widehat{\mathbb{C}}, P_f)$  to the whole mapping class group:

$$\bar{\psi} : \text{PMCG}(\widehat{\mathbb{C}}, P_f) \longrightarrow \text{PMCG}(\widehat{\mathbb{C}}, P_f)$$

defined as follows:

$$\bar{\psi}(g) = \begin{cases} \psi(g) & g \in H \\ \alpha\psi(g\alpha^{-1}) & g \in H\alpha \\ \alpha^{-1}\psi(g\alpha) & g \in H\alpha^{-1} \\ \beta^{-1}\psi(g\beta) & g \in H\beta^{-1}. \end{cases}$$

**Lemma 8.1** *The Thurston map  $f \cdot g$  is Thurston equivalent to  $f \cdot \bar{\psi}(g)$ .*

**Proof** The result is proven here when  $g \in H$  and  $g \in H\alpha^{-1}$ , and the others are proven in an analogous way. First suppose that  $g \in H$ . Then

$$g \circ f = f \circ \psi(g).$$

Since  $(f \circ \psi(g))^{\psi(g)} = \psi(g) \circ f$ , one obtains

$$g \circ f \sim \psi(g) \circ f$$

Next suppose that  $g \in H\alpha^{-1}$ .

$$\begin{aligned} f \cdot g &= f \cdot g\alpha\alpha^{-1} \\ &= \psi(g\alpha) \cdot f \cdot \alpha^{-1} \\ &\sim f \cdot \alpha^{-1}\psi(g\alpha) \\ &= f \cdot \bar{\psi}(g) \end{aligned}$$

□

As was the case in [1], an arbitrary element of  $\text{PMCG}(\widehat{\mathbb{C}}, P_f)$  lands in some more easily understood proper subset under iteration of  $\bar{\psi}$ .

**Theorem 8.2** *Let  $g \in \text{PMCG}(\widehat{\mathbb{C}}, P_f)$ . Then there is an  $N$  so that for all  $n > N$ ,  $\bar{\psi}^{\circ n}(g)$  is contained in the following set:*

$$\mathfrak{M} = \{e, \beta, \alpha^{-1}, \alpha^2\beta^{-1}, \alpha^{-1}\beta\alpha^{-1}, \alpha\beta^{-1}, \beta^2\} \cup \{\alpha(\beta\alpha)^k : k \in \mathbb{Z}\}$$

**Proof** Informally, we will speak of  $\mathfrak{M}$  as the “mystery maps.” It is easy to use direct computation to show that  $\overline{\psi}(\mathfrak{M}) \subset \mathfrak{M}$ . It will be shown that for any  $g$  outside of  $\mathfrak{M}$ , some iterate of  $\overline{\psi}$  decreases word length measured with respect to the basis  $\{\alpha, \beta\}$ . The argument is divided into four cases, depending on which coset of  $H$  contains  $g$ , where the goal of each case is to show that  $g$  lands in  $\mathfrak{M}$  under iteration of  $\overline{\psi}$ . The following proof is not comprehensive, but aims to present the key points of the argument.

*Case 1:  $g \in H$ :* Recall from Lemma 5.4 that  $|\overline{\psi}(g)| = |\psi(g)| \leq |g| - 2$  except when  $g = (\alpha\beta)^n$ . Since  $\overline{\psi}((\alpha\beta)^n) = (\beta\alpha)^n$ , one must consider cases depending on the residue of  $n \bmod 3$ .

- If  $n \equiv 0 \pmod{3}$ , then  $\overline{\psi}^2(g) = (\alpha^{-1}\beta^{-1})^{\frac{n}{3}}$  where evidently  $|g| < |\overline{\psi}^2(g)|$  except when  $n = 0$ .
- If  $n \equiv 1 \pmod{3}$ , then  $\overline{\psi}^2(g) = \alpha^{-1}(\alpha^{-1}\beta^{-1})^{\frac{n-1}{3}}\alpha^{-1}$  where evidently  $|g| < |\overline{\psi}^2(g)|$  except when  $n = 1$ .
- If  $n \equiv 2 \pmod{3}$ , then  $\overline{\psi}^2(g) = \beta(\alpha^{-1}\beta^{-1})^{\frac{n-2}{3}}\alpha^{-1}$  where evidently  $|g| < |\overline{\psi}^2(g)|$  except when  $n = -1$ .

But direct computation shows that the three exceptional cases just mentioned where  $g = (\alpha\beta)^n$ ,  $n = -1, 0, 1$  eventually land in  $\mathfrak{M}$ .

*Case 2:  $g \in H\alpha^{-1}$ :* Assume that  $g$  is reduced and therefore corresponds to a path in Figure 12 that starts at vertex 1 and ends at 4 with no backtracking. Divide into two subcases depending on the prefix of this word. First suppose that  $g$  is of the form  $g = hg'$  where  $h \neq (\alpha\beta)^m$  with the additional assumptions that  $g'$  never visits 1 once it leaves initially, and  $|g| = |h| + |g'|$ . By the triangle inequality and then Lemma 5.4,

$$\begin{aligned} |\overline{\psi}(g)| &= |\alpha^{-1}\psi(h)\psi(g'\alpha)| \\ &\leq 1 + |\psi(h)| + |\psi(g'\alpha)| \\ &\leq 1 + |h| - 2 + |g'\alpha| - 2 \\ &\leq |h| + |g'| - 2 \end{aligned}$$

On the other hand, suppose  $g$  has the form  $(\alpha\beta)^m g'$  where  $g'$  never returns to 1 and  $|g| = 2m + |g'|$ . If  $g'$  passes through the edge labeled  $(\beta\alpha, e)$ , one can see immediately from Figure 15 that  $g$  has length decreased by at least two. The following is an exhaustive list of words that start at 1, end at 4, and do not pass through  $(\beta\alpha, e)$ .

- $(\alpha\beta)^m \alpha^{-1} \beta^n$

- $(\alpha\beta)^m \alpha^2 \beta^n$
- $(\alpha\beta)^m \beta^{-1} \alpha \beta^n$

The images of  $(\alpha\beta)^m \alpha^{-1} \beta^n$  under  $\bar{\psi}^2$  are tabulated below where  $\otimes$  denotes the cases where  $\bar{\psi}((\alpha\beta)^m \alpha^{-1} \beta^n) \in H$  which have already been considered in full.

	$m \equiv 0$	$m \equiv 1$	$m \equiv 2$
$n \equiv 0$	$\alpha^{-1}(\alpha\beta)^{m/3} \beta^{n/3}$	$\otimes$	$(\beta\alpha)^{(m+1)/3} \beta^{n+1}$
$n \equiv 1$	$\otimes$	$\alpha^2(\beta\alpha)^{(m-1)/3} \beta^{(n-1)/3}$	$\beta(\alpha\beta)^{(m+1)/3} \beta^n$
$n \equiv 2$	$\alpha(\alpha\beta)^{m/3} \beta^{(n-2)/3}$	$\alpha^{-1}(\alpha\beta)^{(m-1)/3} \beta^{(n+1)/3}$	$\beta(\alpha\beta)^{(m+1)/3} \beta^n$

An examination of this table and some thought about the other possible values of  $m$  and  $n$  leads to the conclusion that the only times when the lengths are not decreased by  $\bar{\psi}^2$  (assuming they don't land in the  $\otimes$  case) are when  $m = 0$  and  $n = 0$ , and when  $m = 0$  and  $n = -1$ . But the images of  $\bar{\psi}$  in both of these cases lie in  $\mathfrak{M}$ . A similar kind of analysis must be conducted for the other two types of words in the bulleted list, and the desired conclusion holds.

*Case 3:  $g \in H\beta$ :* This case is very similar to the previous case, except that now the symbol  $\otimes$  can be used when  $\bar{\psi}(g) \in H \cup H\alpha^{-1}$ . This simplifies computation significantly. Suppose  $g$  has the form  $(\alpha\beta)^m g'$  where  $g'$  ends at 2, never returns to 1 or passes through the edge labeled  $(\beta\alpha, e)$ , and has the form  $|g| = 2m + |g'|$ . The following three kinds of group element are the only ones which meet this criterion, and one can create tables like the ones in Case 2 to come to the desired conclusion.

- $(\alpha\beta)^m \beta \alpha^n$
- $(\alpha\beta)^m \beta^{-2} \alpha^n$
- $(\alpha\beta)^m \alpha \beta^{-1} \alpha^n$

*Case 4:  $g \in H\alpha$ :* This case is more involved than the other three. Words traversing  $(\beta\alpha, e)$  or  $(\alpha^{-1}\beta^{-1}, e)$  obviously decrease length under application of  $\bar{\psi}$ . From now on, therefore, we only examine paths that start at 1 and go to 3 that do not backtrack or pass through the edge labeled  $(\beta\alpha, e)$ . Case 4 will be broken into two subcases depending on whether words avoid “small loops”, namely the two edges in the Schreier graph that have identical initial and terminal vertices. For  $h \in H$ , the following is the list of all words that

start at 1 and end at 3, and do not pass through any small loops or the edge labeled  $(\beta\alpha, e)$ .

- $h\beta^2$  where  $|h\beta^2| = |h| + 2$
- $h\alpha$  where  $|h\alpha| = |h| + 1$
- $h\alpha^{-2}$  where  $|h\alpha^{-2}| = |h| + 2$
- $h\beta^{-1}$  where  $|h\beta^{-1}| = |h| + 1$

The first three items do not require much attention, but the last involves a significant amount of computation.

*Case  $h\beta^2$ :*  $\bar{\psi}(h\beta^2) = \alpha\psi(h)\beta^{-1}$  from which one can see that  $|\bar{\psi}(h\beta^2)| \leq |h\beta^2|$  unless  $h = (\alpha\beta)^n$ . However,  $\bar{\psi}((\alpha\beta)^n\beta^2) = \alpha(\beta\alpha)^n\beta^{-1} \in H\beta$  for all  $n$ . The  $H\beta$  case has been fully considered already.

*Case  $h\alpha$ :*  $\bar{\psi}(h\alpha) = \alpha\psi(h)$ , where as before,  $\bar{\psi}$  is length decreasing except when  $h = (\alpha\beta)^n$ . But  $\bar{\psi}((\alpha\beta)^n\alpha) = \alpha(\beta\alpha)^n \in \mathfrak{M}$ .

*Case  $h\alpha^{-2}$ :*  $\bar{\psi}(h\alpha^{-2}) = \alpha\psi(h)\beta^{-1}$ , which is exactly the output we had in the  $h\beta^2$  case. A similar analysis yields the same conclusion.

*Case  $h\beta^{-1}$ :*  $\bar{\psi}(h\beta^{-1}) = \alpha\psi(h)\alpha^{-1}\beta^{-1}$ , which is different from before, because now we must not only understand the situation when  $h = (\alpha\beta)^n$ , but also the case when  $|\psi(h)| = |h| - 2$ . When  $h = (\alpha\beta)^n$ ,

$$\begin{aligned} \bar{\psi}((\beta^{-1}\alpha^{-1})^m\beta^{-1}) &= \alpha(\alpha^{-1}\beta^{-1})^m\alpha^{-1}\beta^{-1} \\ &= \beta^{-1}(\alpha^{-1}\beta^{-1})^m \end{aligned}$$

which evidently lies in  $\mathfrak{M}$ .

Now suppose that  $|\psi(h)| = |h| - 2$ . We list all such  $h$ , which are simply paths that start and end at vertex 1, pass through the edges labeled  $(\alpha, \beta)$ ,  $(\beta, \alpha)$ , and  $(\beta^{-1}\alpha^{-1}, \alpha^{-1}\beta^{-1})$  arbitrarily many times, but only pass through two other edges. The left column of the following table is an exhaustive list of all possible  $h\beta^{-1}$  where  $|\psi(h)| = |h| - 2$ . The right column

is  $\overline{\psi}(h\beta^{-1})$ .

$$\begin{array}{ll}
(\alpha\beta)^k \beta \alpha^n \beta^{-1} (\alpha\beta)^m \beta^{-1} & \alpha(\beta\alpha)^k \beta^n (\beta\alpha)^m \alpha^{-1} \beta^{-1} \\
(\alpha\beta)^k \beta \alpha^n \beta^2 (\alpha\beta)^m \beta^{-1} & \alpha(\beta\alpha)^k \beta^n \alpha(\beta\alpha)^m \alpha^{-1} \beta^{-1} \\
(\alpha\beta)^k \beta \alpha^n \beta \alpha^{-1} (\alpha\beta)^m \beta^{-1} & \alpha(\beta\alpha)^k \beta^n \beta^{-1} (\beta\alpha)^m \alpha^{-1} \beta^{-1} \\
(\alpha\beta)^k \beta^{-2} \alpha^n \beta \alpha^{-1} (\alpha\beta)^m \beta^{-1} & \alpha(\beta\alpha)^k \alpha^{-1} \beta^n \beta^{-1} (\beta\alpha)^m \alpha^{-1} \beta^{-1} \\
(\alpha\beta)^k \beta^{-2} \alpha^n \beta^2 (\alpha\beta)^m \beta^{-1} & \alpha(\beta\alpha)^k \alpha^{-1} \beta^n \alpha(\beta\alpha)^m \alpha^{-1} \beta^{-1} \\
(\alpha\beta)^k \beta^{-2} \alpha^n \beta^{-1} (\alpha\beta)^m \beta^{-1} & \alpha(\beta\alpha)^k \alpha^{-1} \beta^n (\beta\alpha)^m \alpha^{-1} \beta^{-1} \\
(\alpha\beta)^k \alpha \beta^{-1} \alpha^n \beta \alpha^{-1} (\alpha\beta)^m \beta^{-1} & \alpha(\beta\alpha)^k \beta^n (\beta\alpha)^m \alpha^{-1} \beta^{-1} \\
(\alpha\beta)^k \alpha \beta^{-1} \alpha^n \beta^2 (\alpha\beta)^m \beta^{-1} & \alpha(\beta\alpha)^k \beta \beta^n \alpha(\beta\alpha)^m \alpha^{-1} \beta^{-1} \\
(\alpha\beta)^k \alpha \beta^{-1} \alpha^n \beta^{-1} (\alpha\beta)^m \beta^{-1} & \alpha(\beta\alpha)^k \beta \beta^n (\beta\alpha)^m \alpha^{-1} \beta^{-1} \\
\\
(\alpha\beta)^k \alpha^{-1} \beta^n \alpha (\alpha\beta)^m \beta^{-1} & \alpha(\beta\alpha)^k \alpha^n (\beta\alpha)^m \alpha^{-1} \beta^{-1} \\
(\alpha\beta)^k \alpha^{-1} \beta^n \alpha^{-2} (\alpha\beta)^m \beta^{-1} & \alpha(\beta\alpha)^k \alpha^n \beta^{-1} (\beta\alpha)^m \alpha^{-1} \beta^{-1} \\
(\alpha\beta)^k \alpha^{-1} \beta^n \alpha^{-1} \beta (\alpha\beta)^m \beta^{-1} & \alpha(\beta\alpha)^k \alpha^n \alpha(\beta\alpha)^m \alpha^{-1} \beta^{-1} \\
(\alpha\beta)^k \alpha^2 \beta^n \alpha (\alpha\beta)^m \beta^{-1} & \alpha(\beta\alpha)^k \beta \alpha^n (\beta\alpha)^m \alpha^{-1} \beta^{-1} \\
(\alpha\beta)^k \alpha^2 \beta^n \alpha^{-2} (\alpha\beta)^m \beta^{-1} & \alpha(\beta\alpha)^k \beta \alpha^n \beta^{-1} (\beta\alpha)^m \alpha^{-1} \beta^{-1} \\
(\alpha\beta)^k \alpha^2 \beta^n \alpha^{-1} \beta (\alpha\beta)^m \beta^{-1} & \alpha(\beta\alpha)^k \beta \alpha^n \alpha(\beta\alpha)^m \alpha^{-1} \beta^{-1} \\
(\alpha\beta)^k \beta^{-1} \alpha \beta^n \alpha (\alpha\beta)^m \beta^{-1} & \alpha(\beta\alpha)^k \alpha^{-1} \alpha^n (\beta\alpha)^m \alpha^{-1} \beta^{-1} \\
(\alpha\beta)^k \beta^{-1} \alpha \beta^n \alpha^{-2} (\alpha\beta)^m \beta^{-1} & \alpha(\beta\alpha)^k \alpha^{-1} \alpha^n \beta^{-1} (\beta\alpha)^m \alpha^{-1} \beta^{-1} \\
(\alpha\beta)^k \beta^{-1} \alpha \beta^n \alpha^{-1} \beta (\alpha\beta)^m \beta^{-1} & \alpha(\beta\alpha)^k \alpha^n (\beta\alpha)^m \alpha^{-1} \beta^{-1}
\end{array}$$

In many of the cases above,  $\overline{\psi}$  is not length decreasing so as usual we pass to a second iterate. In every single case, however, the coset containing  $\overline{\psi}(h\beta^{-1})$  is dependent on the value of  $n$  modulo 3, which vastly simplifies computation. Furthermore, for two of the three possible residues of  $n \pmod 3$ ,  $\overline{\psi}(h\beta^{-1})$  falls into a previously analyzed coset on the second iterate. For the remaining values of  $n \pmod 3$  explicit computation is required, but  $\overline{\psi}^2(h\beta^{-1})$  either falls into a previously considered case, obviously has decreased length, or lands in  $\mathfrak{M}$ . This completes the four kinds of path in the bulleted list above, and we move on to the second subcase.

The following is an exhaustive list of all words that begin at 1, end at 3, never return to 1, and pass through the “small loops” described before.

- $h\beta\alpha^n\beta$  where  $|h\beta\alpha^n\beta| = |h| + 2 + |n|$
- $h\beta^{-2}\alpha^n\beta$  where  $|h\beta^{-2}\alpha^n\beta| = |h| + 3 + |n|$
- $h\alpha\beta^{-1}\alpha^n\beta$  where  $|h\alpha\beta^{-1}\alpha^n\beta| = |h| + 3 + |n|$
- $h\alpha^{-1}\beta^n\alpha^{-1}$  where  $|h\alpha^{-1}\beta^n\alpha^{-1}| = |h| + 2 + |n|$
- $h\alpha^2\beta^n\alpha^{-1}$  where  $|h\alpha^2\beta^n\alpha^{-1}| = |h| + 3 + |n|$
- $h\beta^{-1}\alpha\beta^n\alpha^{-1}$  where  $|h\beta^{-1}\alpha\beta^n\alpha^{-1}| = |h| + 3 + |n|$

where it is assumed that  $n \neq 0$  because the case  $n = 0$  has already been considered. Only three cases are presented below, but the other ones can be analyzed similarly.

*Case  $h\beta\alpha^n\beta$ :* One computes that  $\bar{\psi}(h\beta\alpha^n\beta) = \alpha\psi(h)\beta^n\beta^{-1}$ , and for any  $h$  this evidently has decreased length unless  $h = (\alpha\beta)^k$ . We pass to the second iterate:  $\bar{\psi}^2((\alpha\beta)^k\beta\alpha^n\beta) = (\alpha\beta)^k\alpha\beta\alpha\beta^{(n-1)/3}$ . This has decreased length except in the cases when  $n = -2$  and  $n = 1$  which both fall into  $\mathfrak{M}$ .

*Case  $h\beta^{-2}\alpha^n\beta$ :* Since  $\bar{\psi}(h\beta^{-2}\alpha^n\beta) = \alpha\psi(h)\alpha^{-1}\beta^n\beta^{-1}$ , only consider the case when  $h = (\alpha\beta)^k$ . Then  $\bar{\psi}^2(h\beta^{-2}\alpha^n\beta) = \alpha(\beta\alpha)^k\alpha^{-1}\beta^n\beta^{-1}$  from which it is clear that if  $k > 0$  and if  $k < 0$ , there is cancellation that makes the result clear.

*Case  $h\alpha\beta^{-1}\alpha^n\beta$ :* Since  $\bar{\psi}(h\alpha\beta^{-1}\alpha^n\beta) = \alpha\psi(h)\beta^n$ , it is obvious that  $\bar{\psi}$  decreases length after only one iterate.

□

## 8.2 Solution to the Twisting Problem

To solve the twisting problem for  $f$ , we must analyze the “mystery maps” contained in  $\mathfrak{M}$ . First we deal with the one parameter family contained in  $\mathfrak{M}$  with the following claim.

**Lemma 8.3** *Each Thurston map in  $\{f \cdot \alpha(\beta\alpha)^k : k \in \mathbb{Z}\}$  is obstructed, and they are all pairwise Thurston inequivalent*

**Proof** Let  $F = f \cdot \alpha$ , and we will first show that  $F$  is obstructed. Recall that  $\psi(\alpha\beta) = \beta\alpha$  and so  $f \cdot \alpha\beta = \beta\alpha \cdot f$  by definition of the virtual endomorphism  $\psi$ . Recall that  $\gamma^{-1} = \beta\alpha$ , and so

$$\begin{aligned}
\gamma^{-1} \cdot F &= \beta\alpha \cdot f \cdot \alpha \\
&= f \cdot \alpha\beta \cdot \alpha \\
&= f \cdot \alpha \cdot \beta\alpha \\
&= F \cdot \gamma^{-1}.
\end{aligned}$$

The fact that these two maps commute means that  $F$  is obstructed because the core curve of the Dehn twist  $\gamma^{-1}$  is fixed by degree 1 under pullback of  $F$ . Using a similar computation, one can see that  $\gamma^{-1} \cdot (F\gamma^k) = (F\gamma^k) \cdot \gamma^{-1}$  for all  $k$  which shows that each  $F\gamma^k$  is obstructed as required.

Now we show that the elements of the one-parameter family are pairwise inequivalent. Let  $F_n = F \cdot \gamma^{-n}$  and  $F_m = F \cdot \gamma^{-m}$  be two equivalent elements of this one-parameter family. Then there is a homeomorphism  $h$  so that

$$F_m \cdot h = h \cdot F_n. \quad (10)$$

Let  $C_\gamma$  denote the core curve of  $\gamma^{-1}$ , and note that since  $C_\gamma$  is an obstruction for  $F$ , it is evident that  $h(C_\gamma)$  is an obstruction for  $G$ . The previous paragraph showed that  $C_\gamma$  is an obstruction for  $G$  as well; since the components of an obstruction must be non-intersecting, it must be that  $C_\gamma = h(C_\gamma)$ . Since  $h$  is a pure mapping class element that fixes  $C_\gamma$ , it follows that  $h \in \text{Stab}_{\text{PMCG}}(C_\gamma) = \langle \gamma \rangle$  and so  $h = \gamma^k$  for some integer  $k$ . Substituting into (10) one sees that

$$F \cdot \gamma^{-m} \cdot \gamma^k = \gamma^k \cdot F \cdot \gamma^{-n},$$

and then using the fact that  $\gamma$  commutes with  $F$ ,

$$\gamma^{k-m} \cdot F = \gamma^{k-n} \cdot F.$$

The action of the mapping class group on the left is free [1], and so we see that  $m = n$ .  $\square$

This leaves us with a finite number of elements in  $\mathfrak{M}$  to analyze. The fixed points of the correspondence can be found by solving the equation  $X(\alpha) = Y(\alpha)$  to obtain  $\alpha = 1, -1, 0, \frac{1 \pm \sqrt{15}i}{4}$ , and  $\infty$ . The first two points lie in the forbidden locus and can be disregarded. The Möbius map  $M(z) = \frac{1}{z}$  can be used to show that the rational functions  $F_\alpha$  with  $\alpha = 0, \infty$  are conjugate to each other, as are the rational functions corresponding to  $\alpha = \frac{1 + \sqrt{15}i}{4}, \frac{1 - \sqrt{15}i}{4}$ . Recall that for  $\alpha = [a, b] \in \mathbb{P}^1$ ,

$$F_\alpha(z) = \frac{az^3 + 3bz^2 + 2a}{2bz^3 + 3az + b}.$$

When  $\alpha = 0$ ,  $F_\alpha = f$  and has been analyzed extensively already. When  $\alpha = \frac{1 + \sqrt{15}i}{4}$ ,  $F_\alpha$  is a rational map with simple critical points at  $1, \omega, \bar{\omega}$ , and  $\frac{-7 + \sqrt{15}i}{8}$ , all of which lie on the unit circle. The points  $\omega$  and  $\bar{\omega}$  are interchanged by  $F_\alpha$ , and the other two critical points are fixed. Let  $M$  be

the unique Möbius transformation which sends  $(\frac{-7+\sqrt{15}i}{8}, \omega, 1)$  to  $(0, 1, \infty)$ . Then define the rational function  $g$  to be  $M \circ F_\alpha \circ M^{-1}$  where one computes directly that

$$g(z) = \frac{(\sqrt{5}-1)(3+3\sqrt{5}+2z)z^2}{2(1-6z+\sqrt{5})}.$$

All the critical points of  $g$  lie on the real axis, and it is described by the finite subdivision rule in Figure 19 where the two critical points 0 and  $\infty$  are fixed and the other two are exchanged. The map  $g$  respects shading.

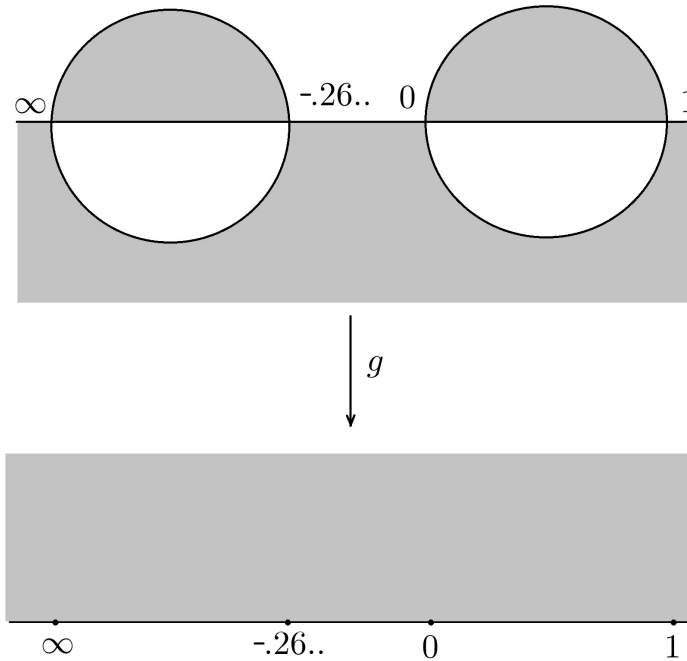


Figure 19: The finite subdivision rule corresponding to  $g$

The map  $g$  has a fixed point lying on the real axis between 0 and 1. This fixed point and its two other preimages are denoted by solid boxes in Figure 20. The paths  $\ell_1$  and  $\ell_2$  connect this basepoint to the two other preimages,



and  $\ell_3$  denotes the constant path at the fixed basepoint. This data along with the lifts of generators in Figure 20 define the wreath recursion.

$$\Phi_g(\alpha) = \langle\langle e, \beta^{-1}\delta^{-1}\gamma^{-1}, e \rangle\rangle(1 \ 2)$$

$$\Phi_g(\beta) = \langle\langle \gamma, e, e \rangle\rangle(1 \ 2)$$

$$\Phi_g(\gamma) = \langle\langle e, \delta\beta, \delta^{-1} \rangle\rangle(2 \ 3)$$

$$\Phi_g(\delta) = \langle\langle e, \delta, e \rangle\rangle(2 \ 3)$$

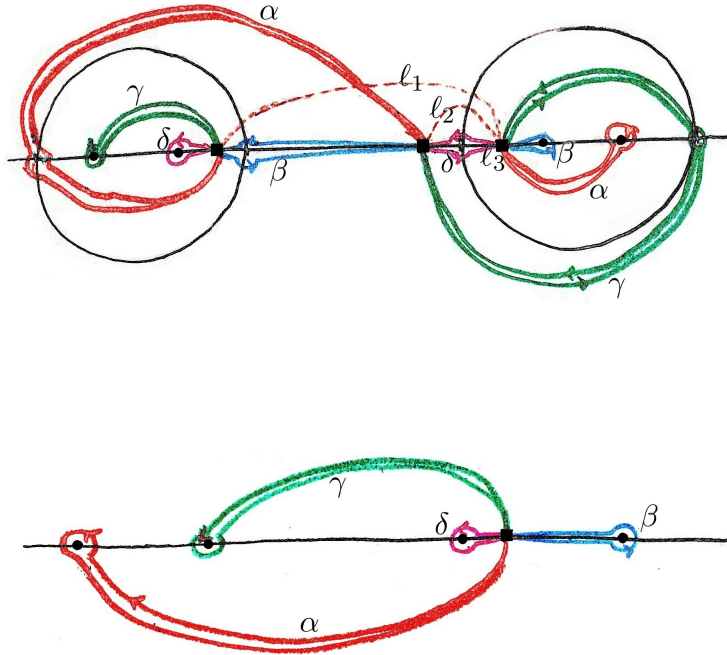


Figure 20: The four generators of  $\pi_1(\widehat{\mathbb{C}} \setminus P_g)$  and their lifts under  $g$

**Lemma 8.4** *For any  $h \in \{e, \beta, \alpha^{-1}, \alpha^2\beta^{-1}, \alpha^{-1}\beta\alpha^{-1}, \alpha\beta^{-1}, \beta^2\}$ , the Thurston map  $f \cdot h$  is unobstructed, and is therefore equivalent to  $f$  or  $g$ .*

**Proof** Note that the two maps  $\alpha^2\beta^{-1}$  and  $\alpha^{-1}\beta\alpha^{-1}$  form a 2-cycle under iteration of  $\bar{\psi}$ , as do  $\alpha\beta^{-1}$  and  $\beta^2$  (the elements  $\beta, \alpha^{-1}$ , and  $e$  are all fixed points for  $\bar{\psi}$ ). It is our goal to show that one map in each of these cycles is not obstructed and so we assume that  $h$  is one of the four maps  $\beta, \alpha^{-1}, \beta^2$ ,

and  $\alpha^2\beta^{-1}$ . If  $f \cdot h$  is obstructed, there must be a curve that pulls back to itself by degree 1. This is a Levy cycle, which is an obstruction to the wreath recursion on the dynamical plane fundamental group being contracting. The four wreath recursions are recorded below, and GAP was used to show that each one is contracting.

$$\begin{aligned}
\Phi_{f.\beta}(\alpha) &= \langle\langle e, e, \beta \rangle\rangle(1 \ 3) & \Phi_{f.\alpha^{-1}}(\alpha) &= \langle\langle e, e, \beta \rangle\rangle(2 \ 3) \\
\Phi_{f.\beta}(\beta) &= \langle\langle e, \delta^{-1}\beta^{-1}, \gamma^{-1} \rangle\rangle(2 \ 3) & \Phi_{f.\alpha^{-1}}(\beta) &= \langle\langle \beta^{-1}, e, \gamma^{-1}\delta^{-1} \rangle\rangle(1 \ 3) \\
\Phi_{f.\beta}(\gamma) &= \langle\langle e, \gamma, e \rangle\rangle(2 \ 3) & \Phi_{f.\alpha^{-1}}(\gamma) &= \langle\langle e, \gamma, e \rangle\rangle(2 \ 3) \\
\Phi_{f.\beta}(\delta) &= \langle\langle \beta^{-1}, e, \beta\delta \rangle\rangle(1 \ 3) & \Phi_{f.\alpha^{-1}}(\delta) &= \langle\langle \delta\beta^{-1}, e, \beta \rangle\rangle(1 \ 3)
\end{aligned}$$

$$\begin{aligned}
\Phi_{f.\alpha^2\beta^{-1}}(\alpha) &= \langle\langle e, e, \delta^{-1}\beta\delta \rangle\rangle(2 \ 3) \\
\Phi_{f.\alpha^2\beta^{-1}}(\beta) &= \langle\langle \beta^{-1}\delta^{-1}\beta\delta\gamma, e, \gamma^{-1}\delta^{-1}\beta^{-1}\delta\gamma^{-1}\delta^{-1} \rangle\rangle(1 \ 3) \\
\Phi_{f.\alpha^2\beta^{-1}}(\gamma) &= \langle\langle e, \gamma, e \rangle\rangle(2 \ 3) \\
\Phi_{f.\alpha^2\beta^{-1}}(\delta) &= \langle\langle \delta\gamma, e, \gamma^{-1}\delta^{-1}\beta^{-1}\delta\beta \rangle\rangle(1 \ 3)
\end{aligned}$$

$$\begin{aligned}
\Phi_{f.\beta^2}(\alpha) &= \langle\langle e, e, \beta \rangle\rangle(1 \ 3) \\
\Phi_{f.\beta^2}(\beta) &= \langle\langle \alpha, e, e \rangle\rangle(1 \ 2) \\
\Phi_{f.\beta^2}(\gamma) &= \langle\langle e, \gamma, e \rangle\rangle(2 \ 3) \\
\Phi_{f.\beta^2}(\delta) &= \langle\langle e, \gamma, \alpha^{-1}\beta^{-1} \rangle\rangle(2 \ 3)
\end{aligned}$$

□

The last step in solving the twisting problem is then to determine which of  $f \cdot \beta$ ,  $f \cdot \alpha^{-1}$ ,  $f \cdot \beta^2$ , and  $f \cdot \alpha^2\beta^{-1}$  are equivalent to  $f$  or  $g$ . Using Thurston rigidity, it is evident that  $f$  and  $g$  are not Thurston equivalent, but combinatorial invariants are needed. For example, one could compute the order of the permutation group acting on a fixed level of the tree of preimages. However, the maps  $f$  and  $g$  both have the same number of elements in their permutation group up to level five, where the permutation groups have an order of approximately  $10^{80}$ . A second attempt was made to distinguish  $f$  and  $g$  using the fact that  $f$  is a mating of two polynomials, and hence must have an element of order  $3^n$  in the level  $n$  permutation group due to the existence of an equator. However,  $g$  also has such elements when  $n \leq 3$ .

The stage is set for another invariant that has never before been used to solve a twisting problem: the dynamical properties of the pullback relation

of  $f$  and  $g$  on curves. Theorem 6.1 states that  $f$  has three elements in its finite global attractor. We use this new invariant to determine the Thurston class of the maps  $f \cdot h$ . Let  $\frac{p}{q}$  denote the curve corresponding to the point  $\frac{p}{q}$  in the Weil-Petersson boundary. Then

$$\sigma_{f \cdot \beta}\left(\frac{p}{q}\right) = \sigma_f\left(B^{-1} \cdot \frac{p}{q}\right)$$

since  $(T_\beta \circ f)^{-1} = f^{-1} \circ T_{\beta^{-1}}$ , and so one computes that  $\sigma_{f \cdot \beta}$  has dynamical behavior

$$\begin{array}{ccc} 0 & \xrightarrow{\quad} & \frac{1}{0} \\ \frac{1}{1} & \xleftarrow{\quad} & 0 \end{array} \qquad \begin{array}{ccc} -\frac{1}{1} & \xrightarrow{\quad} & \frac{1}{1} \\ -\frac{1}{1} & \xleftarrow{\quad} & -\frac{1}{1} \end{array}$$

and so  $f \cdot \beta$  must be equivalent to  $g$ . Using a similar procedure, one can show that the pullback on curves for  $f \cdot \alpha^{-1}$  and  $f \cdot \alpha^2 \beta^{-1}$  contain two distinct two-cycles.

The final map  $f \cdot \beta^2$  has the property that  $\frac{1}{1}$  pulls back to the curve  $\frac{1}{1}$ . The only possible degree for the pullback of any curve under  $f$  (and hence  $f \cdot \beta^2$ ) is 1 or 3 by Lemma 5.3, and it is clear that the degree in this case cannot be 1 since the map  $f \cdot \beta^2$  is not obstructed. Also note that  $\frac{1}{1}$  is mapped to itself in an orientation preserving way because it bounds a disk containing the fixed points 0 and 1. Thus the curve  $\frac{1}{1}$  is an equator for  $f \cdot \beta^2$ , and since there was a unique way to mate the cubic polynomials described in Section 4,  $f \cdot \beta^2$  must be Thurston equivalent to  $f$ .

## 9 Future Work

Though this work has led to greater understanding of the boundary values of Thurston's pullback map and a promising new invariant for Thurston equivalence, there are many questions that go unanswered:

*Does the pullback relation on curves for every rational Thurston map (not a Lattès map) have a finite global attractor?* Such a finiteness result would be invaluable for computing the pullback relation for rational Thurston maps for arbitrary curves. It would make the finite global attractor of the pullback relation a far more feasible invariant for Thurston equivalence, and the implications for the boundary values of the Thurston pullback map would be interesting as well. It could also further the study of mating—a hyperbolic rational Thurston map  $F$  is a mating if and only if there is an equator. Thus, if there are no fixed curves in the finite global attractor, one is assured that  $F$  is not a mating.

In [27], the pullback relation of three quadratics is analyzed—for the rabbit every curve is eventually trivial or lands in a 3-cycle, and for the other two quadratics every curve is eventually trivial. The analytic properties of maps on moduli space in the spirit of Sarah Koch’s work [17] have implications for this problem, as do algebraic properties such as contraction of virtual endomorphisms on word length [1]. The former has been used to show the existence of a finite global attractor, whereas the latter can compute the elements of this attractor explicitly. What made  $f$  particularly interesting was that its virtual endomorphism was not contracting, and the known methods for understanding the analytic properties of the map on moduli space seemed to be inconclusive, yet the finite global attractor was able to be computed using some ad hoc algebra. This suggests that there might be a weaker contraction property for virtual endomorphisms that may be useful, or there may be some analytic properties that need to be discovered.

*For a rational Thurston map  $F$  not equivalent to the Lattès map, is there a bound for the number of elements in the finite global attractor of the pullback on curves in terms of  $|P_F|$  and  $\deg(F)$ ? A further refinement of this question could be to ask if there is a relationship between the mapping properties of the finite global attractor and the mapping properties of  $P_F$ . In every known case, the size of the finite global attractor is less than  $|P_F|$ . Also, the number of cycles of the pullback on curves is always less than the number of cycles in  $P_F$ .*

*Can checking the hypothesis of Thurston’s characterization theorem be reduced to understanding where the pre-images of a finite number of curves lie, and the degree by which they map? In work by Cannon, Floyd, Pilgrim, and Parry [10] in the case of four post-critical points, it is proven that a Euclidean horoball tangent to  $\frac{p}{q}$  in Teichmüller space is mapped by the Thurston’s pullback map associated to a Thurston map  $F$  into a horoball of computable radius tangent to  $\sigma_F(\frac{p}{q})$ . The authors are able to use this result to show that a certain finite subdivision rule is not obstructed, and that its fixed point must lie in the region bounded by some hyperbolic polygon in Teichmüller space. When there are more than four postcritical points, similar results about the mapping properties of horoballs hold, but no explicit examples have been studied. The appeal of these types of result is that from the boundary behavior of the Thurston pullback map allows conclusions to be drawn about the behavior of the Thurston pullback map on large regions of Teichmüller space. Arturo Saens, a student of William Floyd, is currently studying this kind of question when Teichmüller space has dimension one.*

*If some twist of a rational Thurston map is obstructed, does this imply*

that there is a  $\mathbb{Z}$ -parameter family of pairwise inequivalent obstructed maps that can be obtained by twisting? This was the case for  $z^2 + i$  in [1],  $f(z) = \frac{3z^2}{2z^3+1}$  in the work above, and a third example that Jim Belk shared with me. These one-parameter families seem to arise when the map or correspondence on moduli space satisfies certain properties.

## References

- [1] L. Bartholdi and V. Nekrashevych. Thurston equivalence of topological polynomials. *Acta Math.*, (197):1–51, 2006.
- [2] L. Bartholdi and V. Nekrashevych. Iterated monodromy groups of quadratic polynomials, i. *Groups, Geometry, and Dynamics*, 2(3):1–51, 2008.
- [3] I. Bernstein and A. Edmonds. On the construction of branched coverings of low-dimensional manifolds. *Transactions of the American Mathematical Society*, 247:87–, 1979.
- [4] J. Birman. *Braids, Links, and Mapping Class Groups*. Princeton University Press, Princeton, 1974.
- [5] J. Birman and H. Hilden. On isotopies of homeomorphisms of Riemann surfaces. *Annals of Mathematics*, 97(3):424–439, 1973.
- [6] O. Bogopolski. *Introduction to Group Theory*. EMS Textbooks in Mathematics. European Mathematical Society, 2008.
- [7] H. Bruin, A. Kaffl, and D. Schleicher. Existence of quadratic Hubbard trees. *Fund. Math.*, (202):251–279, 2009.
- [8] X. Buff, A. Epstein, S. Koch, and K. Pilgrim. On Thurston’s pullback map. In *Complex dynamics*, pages 561–583. A K Peters, Wellesley, MA, 2009.
- [9] J. W. Cannon, W. J. Floyd, and W. R. Parry. Finite subdivision rules. *Conform. Geom. Dyn.*, 5:153–196 (electronic), 2001.
- [10] J.W. Cannon, W.J. Floyd, K. Pilgrim, and W.R. Parry. Nearly Euclidean Thurston maps and finite subdivision rules. *arXiv:1204.3615v1*.
- [11] M. Crescimanno and W. Taylor. Large N phases of chiral QCD2. *Nuclear Phys.*, (1), 1995.

- [12] A. Douady and J. Hubbard. A proof of Thurston's topological characterization of rational functions. *Acta Math.*, (171):263–297, 1993.
- [13] B. Farb and Margalit D. *A Primer on Mapping Class Groups*, volume 49 of *Princeton Mathematical Series*. Princeton University Press, 2011.
- [14] M. Hirsch. *Differential Topology*. Springer-Verlag, New York, 1976.
- [15] J. Hubbard. *Teichmüller Theory and Applications to Geometry, Topology, and Dynamics*. Matrix Editions, 2006.
- [16] G. Kelsey. Mega-bimodules of topological polynomials: Sub-hyperbolicity and Thurston obstructions. <http://www.math.uiuc.edu/~gkelsey2/files/Papers/GAKThesis.pdf>, 2011.
- [17] S. Koch. Teichmüller theory and critically finite endomorphisms. *Submitted*.
- [18] S. Lang. *Introduction to Modular Forms*, volume 222 of *Grundlehren der mathematischen Wissenschaften*. Springer, 2010.
- [19] A. Lubotzky and D. Segal. *Subgroup Growth*, volume 212 of *Progress in Mathematics*. Birkhäuser Verlag, 2003.
- [20] M. Lyubich. The quadratic family as a qualitatively solvable model of chaos. *Notices of the AMS*, 47(9):1042–1052, 2000.
- [21] G. McCarty. Homeotopy groups. *Transactions of the American Mathematical Society*, 106(2):293–304, 1963.
- [22] C. McMullen. Families of rational maps and iterative root-finding algorithms. *Annals of Mathematics*, 125:467–493, 1987.
- [23] J. Milnor. Pasting together Julia sets: A worked out example of mating. *Experimental Mathematics*, (13:1):55, 2000.
- [24] J. Milnor. On Lattès maps. In *Dynamics on the Riemann Sphere*, pages 9–44. European Mathematical Society, Zürich, Switzerland, 2006.
- [25] V. Nekrashevych. *Self-Similar Groups*, volume 117 of *Mathematical Surveys and Monographs*. American Mathematical Society, 2005.
- [26] V. Nekrashevych. Combinatorics of polynomial iterations. In *Complex Dynamics—Families and Friends*, pages 169–214. A K Peters, Wellesley, MA, 2009.

- [27] K. Pilgrim. An algebraic formulation of Thurston's characterization of rational functions. *To appear, special issue of Annales de la Faculte des Sciences de Toulouse*, 2010.
- [28] L. Quintas. The homotopy groups of the space of homeomorphisms of a multiply punctured surface. *Illinois J. Math.*, 9(4):721–725, 1965.
- [29] M. Rees. A partial description of parameter space of rational maps of degree two: Part i. *Acta mathematica*, 168, 1992.
- [30] N. Selinger. Thurston's pullback map on the augmented Teichmüller space and applications. *Inventiones mathematicae*, pages 1–32, 2011.
- [31] S. Wolpert. The Weil-Petersson metric geometry. In *Handbook of Teichmueller theory, Vol. II*. European Math. Soc., 2009.

Department of Mathematics  
Indiana University  
Bloomington, IN 47405, U.S.A.  
E-mail: rlodge@indiana.edu